



**UNIVERSITY OF TRENTO**  
**Italy**

**International PhD Program in Biomolecular Sciences**  
**Centre for Integrative Biology**  
**XXVII Cycle**

**MOLECULAR EFFECTS**  
**OF THE NAMPT INHIBITOR FK866**  
**ON LEUKEMIA CELLS**

Tutor: Dr. **ALESSANDRO PROVENZANI**  
Advisor: Dr. **VITO GIUSEPPE D'AGOSTINO**  
Centre for Integrative Biology, CIBIO  
Laboratory of Genomic Screening

Ph.D. Thesis of  
**CHIARA ZUCAL**  
Centre for Integrative Biology, CIBIO  
Laboratory of Genomic Screening

Academic year 2014-2015



## ABSTRACT

Aberrant activation of metabolic pathways has emerged as an hallmark of proliferating cancer cells and pharmaceutical approaches targeting cell metabolism hold great potential for cancer treatment. A critical factor in cellular metabolism is nicotinamide adenine dinucleotide (NAD<sup>+</sup>) and cancer cells highly rely on it to face increased metabolic demands and proliferation rates. Intracellular NAD<sup>+</sup> is a key metabolite involved in several cellular processes, acting either as a coenzyme in redox reactions or as a substrate for NAD<sup>+</sup>-degrading enzymes such as poly (ADP-ribose) polymerases (PARPs), CD38, and sirtuins, regulating processes that undergo fundamental changes during malignant transformation. Although NAD<sup>+</sup> can be generated *de novo* from tryptophan precursor, the major route of biosynthesis is through a nicotinamide-salvage process.

Nicotinamide phosphoribosyltransferase (NAMPT) is the rate-limiting enzyme in NAD<sup>+</sup> biosynthesis from nicotinamide in mammalian cells. A number of cancers present an increased expression of NAMPT, and high NAMPT levels have been shown to be essential to support cancer cell growth, survival and EMT transition and to correlate with adverse prognosis.

NAMPT is therefore a key factor regulating tumor cell metabolism and is thus considered a promising anti-cancer target. FK866 is a specific NAMPT inhibitor that lowers NAD<sup>+</sup> concentration in cancer cells, reducing the activity of NAD<sup>+</sup>-dependent enzymes, impacting on ATP production and promoting cell death. NAMPT inhibition was proven to be highly effective in both lymphoid and myeloid-derived hematological malignancies in preclinical studies without affecting healthy cells, such as hematopoietic stem cells. FK866 has completed a phase I trial in oncology with advanced solid tumors. Thrombocytopenia was the dose-limiting toxicity, suggesting that this drug is a good candidate for clinical applications.

We investigated the mechanism of action of FK866 in T-ALL derived cell lines as well as in primary leukemia cells. FK866-induced metabolic stress and NAMPT ablation elicited a strong arrest of protein synthesis as early cell response. FK866 induced activation of the AMP-activated protein kinase

(AMPK), which subsequently drove the inhibition of the mTOR/4EBP1 signaling cascade and of the major initiation factor EIF2A, impairing protein synthesis. Furthermore, FK866-induced stress reduced the levels of the anti-apoptotic protein MCL1 and impacted on the endoplasmic reticulum homeostasis.

In addition, we established and characterized an FK866-resistant model derived from the T-ALL cell line Jurkat. Target-specific acquired resistance has been described after several therapies and can be modeled *in vitro* by growing cells in presence of increasing concentrations of drug. In our resistant cells, FK866 treatment only partially impacted on NAD<sup>+</sup> content, whereas ATP levels were recovered and protein translation was resumed. Notably, during *in vitro* acquisition of drug resistance, mutations in the NAMPT gene have not occurred. Finally, FK866-resistant cells developed cross-resistance to the glucocorticoid dexamethasone.

In the last years, many NAMPT inhibitors have been synthesized and characterized. The obtained results provide new insight into the role of the NAMPT-mediated NAD<sup>+</sup> salvage pathway in cancer cell metabolism and the molecular mechanisms of FK866, which will be useful to formulate specific and effective combinatorial drug therapies.

# INDEX

<b>INTRODUCTION .....</b>	<b>1</b>
<b>1. Metabolism and cancer .....</b>	<b>1</b>
1.1 The hallmarks of cancer: reprogramming energy metabolism .....	1
1.2 The Warburg effect .....	2
<b>2. NAD<sup>+</sup> .....</b>	<b>3</b>
2.1 The NAD <sup>+</sup> metabolome: a key determinant of cancer cell biology .....	3
2.2 The NAD <sup>+</sup> biosynthesis .....	5
<b>3. NAMPT .....</b>	<b>7</b>
3.1 NAMPT in cancer .....	10
<b>4. FK866 .....</b>	<b>12</b>
<b>5. Metabolic checkpoints: AMPK and mTOR .....</b>	<b>16</b>
5.1 LKB1- AMPK .....	17
5.2 mTOR .....	19
<b>6. Cell fate determinants in response to stress: phospho-EIF2A and the UPR .....</b>	<b>21</b>
<b>AIM OF THE THESIS.....</b>	<b>25</b>
<b>METHODS.....</b>	<b>26</b>
<b>RESULTS .....</b>	<b>34</b>
<b>1. Investigating the mechanism of action of FK866.....</b>	<b>34</b>
<b>2. Drug resistance to FK866 .....</b>	<b>53</b>
2.1 Drug resistance to NAMPT inhibitors .....	53
2.2 Development of FK866-resistant Jurkat cell line .....	54
2.2 Characterization of the resistant model: translational control.....	56
2.3 Drug sensitivity and resistance testing (DSRT) .....	57
2.4 Characterization of the resistant model: transcriptional regulation .....	61
<b>DISCUSSION.....</b>	<b>64</b>
<b>REFERENCES.....</b>	<b>70</b>
<b>ORIGINAL AUTHORSHIP .....</b>	<b>86</b>
<b>SIDE PROJECTS.....</b>	<b>87</b>

**ABBREVIATIONS and ACRONYMS**

$\Delta\psi_m$	Mitochondrial transmembrane potential
4EBP1	Eukaryotic translation initiation factor 4E-Binding Protein 1
7AAD	7-AminoActinomycin D
ACC	Acetyl-CoA Carboxylase
AKT	RAC-alpha serine/threonine-protein kinase
AML	Acute Myeloid Leukemia
AMP	Adenosine MonoPhosphate
AMPK	AMP-activated Protein Kinase
ATP	Adenosine TriPhosphate
BCL-2	B-Cell Lymphoma 2
B-CLL	B-cell Chronic Lymphocytic Leukemia
BiP	Glucose-Regulated Protein, 78kDa
CsA	Cyclosporin-A
EIF2A	Eukaryotic translation Initiation Factor 2A
EIF4E	Eukaryotic translation Initiation Factor 4E
EMT	Epithelial-Mesenchymal Transition
eNAMPT	extracellular form of NAMPT
ER	Endoplasmic Reticulum
FAD	Flavin Adenine Dinucleotide
FADH2	Flavin Adenine Dinucleotide dihydrate
HIF1	Hypoxia-Inducible Factor 1
IDO	Indoleamine-2,3,-Dioxygenase
iNAMPT	intracellular form of NAMPT
LDHA	Lactate Dehydrogenase isoform A
LKB1	Liver Kinase B1
MCL1	Myeloid Cell Leukemia 1
MDR	MultiDrug Resistance
MNK	MAP Kinase Interacting Serine/Threonine Kinase
mRNA	messenger Ribonucleid Acid
MTOR	Mammalian Target of Rapamycin
mTORC1	mTOR complex 1
mTORC2	mTOR complex 2
MYC	v-myc avian myelocytomatosis viral oncogene homolog
NA	Nicotinic Acid
NAD <sup>+</sup>	Nicotinamide Adenine Dinucleotide
NADH	Nicotinamide Adenine Dinucleotide Hydrate
NAM	Nicotinamide

NAMPT	Nicotinamide PhosphoribosylTransferase
NAPRT	Nicotinic Acid PhosphoribosylTransferase
NMN	Nicotinamide MonoNucleotide
NMNAT	Nicotinamide/Nicotinic acid MonoNucleotide AdenylylTransferase
NR	Nicotinamide Riboside
NRK	Nicotinamide Riboside Kinase
p70S6K	p70 ribosomal S6 Kinase
PARP	Poly (ADP-Ribose) Polymerase
PBEF	Pre B-cell colony Enhancing Factor
Pgp	P-GlycoProtein
PI	Propidium Iodide
PI3K	PhosphoInositide-3-Kinase
ROS	Reactive Oxygen Species
RT-PCR	Reverse Transcription Polymerase Chain Reaction
SIRT	Sirtuin
T-ALL	T-cell Acute Lymphoblastic Leukemia
TCA	TriCarboxylic Acid
TDO	Tryptophan-2,3,-DiOxygenase
TP53	Tumor Protein p53
TSC2	Tuberous Sclerosis Complex-2
UPR	Unfolded Protein Response



# INTRODUCTION

## 1. Metabolism and cancer

### 1.1 The hallmarks of cancer: reprogramming energy metabolism

In 2000, Robert Weinberg and Douglas Hanahan published in *Cell* a very renowned article titled "The Hallmarks of Cancer", which comprised the description of six biological capabilities acquired during the multistep development of human tumors. In 2011, they updated their list by proposing four new hallmarks. Among these, the first was the capability of major reprogramming of cellular energy metabolism in order to support continuous cell growth and uncontrolled proliferation. Cancer cells replace the metabolic program that operates in the majority of normal tissues inducing alterations in their metabolism, which becomes therefore an attractive target for cancer therapy ([1], **Figure 1**).

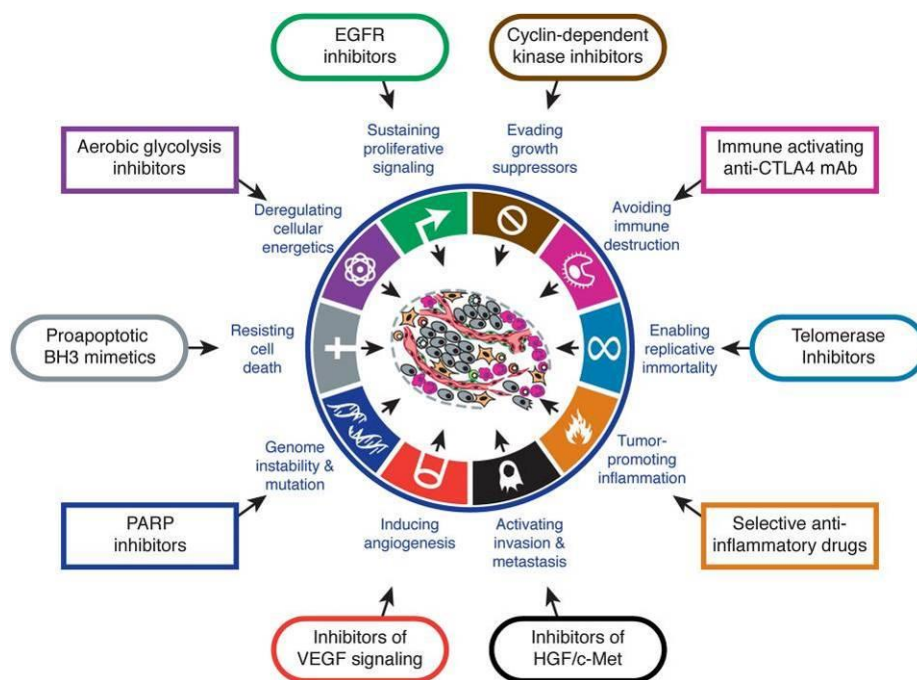


**Figure 1. Therapeutic targeting of the Hallmarks of Cancer**

Illustrative examples of drugs that interfere with the acquired capabilities necessary for tumor growth and progression [1].

## 1.2 The Warburg effect

During the past century, cancer research has focused on the altered cellular metabolism linked to cancer progression. In 1924, Warburg made the first discovery that related tumor biology to metabolism. He observed an anomalous characteristic of cancer cells: even in the presence of oxygen, they can reprogram their glucose metabolism and sustain energy production largely through glycolysis pathway rather than through the tricarboxylic acid (TCA) cycle [2]. This “aerobic glycolysis”, the so called “Warburg effect”, seems to be a general property of highly malignant tumors, regardless of their carcinogenic origin [3].

Under aerobic conditions, most cells process glucose to pyruvate through glycolysis and then completely oxidize most of it to carbon dioxide in the mitochondria. The process generates reduced electron carriers (NADH and  $\text{FADH}_2$ ), reconverted to  $\text{NAD}^+$  and FAD through oxidative phosphorylation, resulting in the production of 34 molecules of ATP *per* oxidation of one glucose molecule [4]. Cancer cells instead switch to the less-efficient ATP generation from aerobic glycolysis. In spite of this, they benefit from the increased glycolysis because it leads to elevated glycolytic intermediates, including those generating amino acids, nucleotides and lipids required for the biosynthesis of macromolecules and organelles and for supporting their high proliferation-rate [5]. The reliance on glycolysis has been recently reported to be promoted by oncogenes (e.g., RAS,MYC), inhibited by tumor suppressors (e.g., TP53), and accentuated under hypoxic conditions by increasing the levels of the HIF1 $\alpha$  and HIF2 $\alpha$  transcription factors, which stimulate the expression of glycolytic transporters and enzymes [6].

In tumor cells, lactate dehydrogenase isoform A (LDHA) preferentially converts accumulating pyruvate to lactate, thereby regenerating  $\text{NAD}^+$  from NADH to maintain glycolysis. The ratio of  $\text{NAD}^+$  to NADH is balanced in favor of  $\text{NAD}^+$  in normal cells, whereas in tumors an increase of NADH relative to  $\text{NAD}^+$  is reported based on the LDHA reaction. The accumulation of lactate implies as well the secretion of the excess, which contributes to an extracellular environment that promotes tumor progression ([7], **Figure 2**).

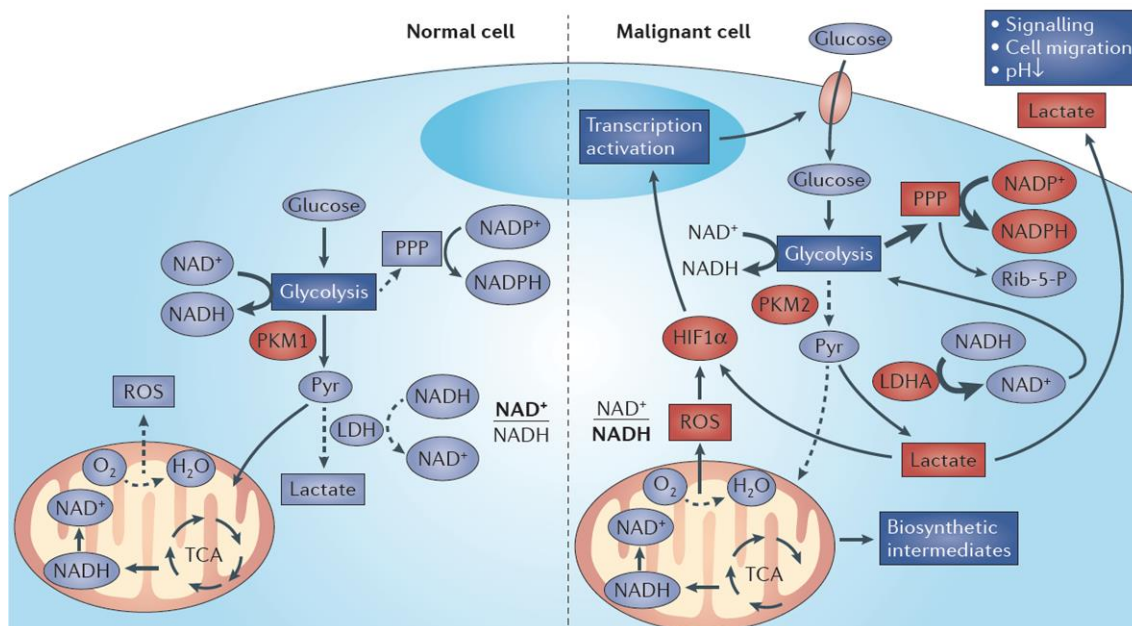


**Figure 2. The Warburg effect**

Comparison of cell metabolism in normal (left side) and malignant cells (right side). In cancer cells, even under normoxic conditions, a high rate of glycolysis and increased glucose uptake is observed, that together with the tumor-specific increase of the less active pyruvate kinase M2 (PKM2) raises the concentrations of glycolytic intermediates. They are mostly diverted into the pentose phosphate pathway (PPP) and NADPH is produced to counteract oxidative stress and to build up macromolecules including the production of ribose-5-phosphate (Rib-5-P) for nucleic acid synthesis [7].

## 2. NAD<sup>+</sup>

### 2.1 The NAD<sup>+</sup> metabolome: a key determinant of cancer cell biology

Since the beginning of the last century, pyridine nucleotides, namely NAD<sup>+</sup> and its phosphorylated form NADP, have been identified as the major redox carriers in all organisms.

In 1904, sir Arthur Harden inferred the existence of a low molecular cofactor or 'cozymase' required for sugar fermentation in yeast. In subsequent years, cozymase was established as a universal factor participating in fermentation, respiration and glycolysis in a variety of organisms. In 1920, Hans von Euler-Chelpin succeeded in its isolation from yeast extracts and determined its chemical composition of a sugar, an adenine and a phosphate. The current function of NAD<sup>+</sup> was established by Otto Warburg in 1936, who discovered its

capability to transfer hydrogen from one molecule to another [8]. As the redox couple  $\text{NAD}^+/\text{NADH}$ ,  $\text{NAD}^+$  plays a crucial role in numerous cellular processes acting primarily as electron-shuttling agent involved in supporting the activity of enzymes that catalyze oxidation-reduction reactions. However, beyond its coenzymatic activity, it has recently been reported to have an unexpectedly wide variety of pivotal roles in cellular functions.  $\text{NAD}^+$  is vital not only for energy transduction, but also as a key component of signaling pathways. Thus, it has emerged as one of the most important link between regulatory and bioenergetic processes and is now regarded as a universal energy and signal-carrying molecule. Signaling pathways that involve  $\text{NAD}^+$  and its phosphorylated form NADP are many and often undergo crucial changes in cancer cells.

$\text{NAD}^+$  serves as substrate for  $\text{NAD}^+$ -dependent enzymes; it is required for three major families of enzymes in mammals: ADP-ribose transferases, including PARPs,  $\text{NAD}^+$ -dependent protein deacetylases (sirtuins) and cyclic ADP (cADP)-ribose synthases (CD38 and CD157) involved in calcium mobilization. Endogenous mono-ADP-ribosylation in higher eukaryotes appears to modulate immune response, cell adhesion, signal and energy metabolism [9].  $\text{NAD}^+$ -dependent enzymes release nicotinamide during their reaction, which needs to be recycled to maintain tissue  $\text{NAD}^+$  levels [10]. Furthermore,  $\text{NAD}^+$ -H regulates the transcriptional corepressor CtBP (carboxyl-terminal binding protein) through binding. CtBP is involved in transcriptional pathways important for development, cell cycle regulation and transformation [11].

$\text{NAD}^+$  can also be converted to NADP and reduced to NADPH, which is necessary for fatty acid synthesis and anti-oxidant defense [12].

$\text{NAD}^+$ -mediated signaling events participate in the regulation of crucial biological processes, including transcription, cell cycle progression, DNA repair, apoptosis, chromatin dynamics regulation, telomerase activity, circadian rhythm, longevity, caloric-restriction response and metabolic regulation. The control of such fundamental events has implications in different pathological conditions and has been linked to cancer development.

Therefore, an increased  $\text{NAD}^+$  demand is present in cancer cells to support their altered  $\text{NAD}^+$ -dependent metabolic and signaling pathways [1].

## 2.2 The NAD<sup>+</sup> biosynthesis

Unlike metabolic redox reactions, which oxidize or reduce NAD<sup>+</sup>-H in a reversible manner, NAD<sup>+</sup>-dependent signaling reactions continuously consume NAD<sup>+</sup> and involve the degradation of the molecule. In fact, the incessant regeneration and maintenance of the cellular NAD<sup>+</sup> pool is challenging and essential to maintain cell proliferation. The necessity of a permanent nucleotide resynthesis through different biosynthetic pathways supports the targeting of NAD<sup>+</sup> metabolism as a new therapeutic concept for cancer treatment [7].

In mammals, NAD<sup>+</sup> can be synthesized either from the “*de novo* pathway” starting from tryptophan or from nicotinamide (NAM), nicotinic acid (NA) and nicotinamide riboside (NR) [13], representing the “salvage pathways” that allow the recycling of metabolites derived from normal cellular catabolism.

Tryptophan’s role as NAD<sup>+</sup> precursor was first suggested by nutritional studies on human pellagra in 1945 [14]. In subsequent years, its crucial role has been confirmed in most living organism, including mammals [15]. The first, rate-limiting step in NAD<sup>+</sup> biosynthesis is the conversion of tryptophan to N-formylkynurenine, catalyzed by either indoleamine 2,3-dioxygenase (IDO) or tryptophan 2,3-dioxygenase (TDO). TDO is the major hepatic enzyme [16], whereas in extrahepatic tissues the cytosolic IDO plays an important role, mostly in lung, small intestine, placenta and in the immune system [17]. A decrease in TDO activity occurs concomitantly with IDO induction in response to inflammatory stimuli (e.g. interferon-gamma), suggesting a coordinate shift in tryptophan degradation from the liver to extrahepatic tissues [18].

N-formylkynurenine is subsequently converted in four individual steps to the unstable  $\alpha$ -amino- $\beta$ -carboxymuconate- $\epsilon$ -semialdehyde (ACMS), which can undergo spontaneous cyclization to quinolinic acid. Quinolinic acid is then converted to nicotinic acid mononucleotide (NAMN) by a quinolinic acid phosphoribosyltransferase (QPRTase) and converges to the Preiss-Handler pathway leading to NAD<sup>+</sup> ([19], **Figure 3**).

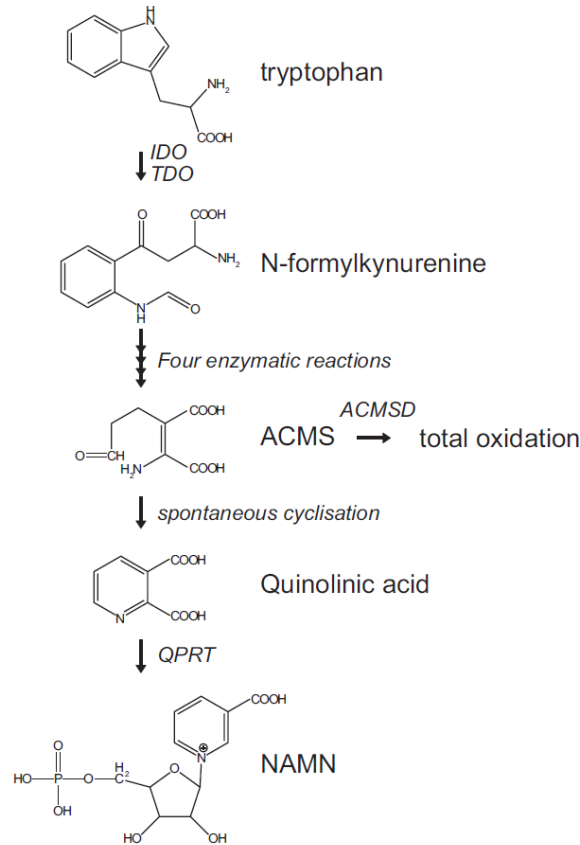


### Figure 3. Mammalian *de novo* NAD<sup>+</sup> pathway

The *de novo* biosynthesis of NAD<sup>+</sup> starts with the conversion of tryptophan to N-formylkynurenine catalyzed by either IDO or TDO, which is subsequently converted to the unstable ACMS. ACMS is then either converted by ACMSD and directed to total oxidation or undergoes nonenzymatic cyclization to quinolinic acid. The final step is comprised of the QPRT-catalyzed formation of NAMN.

IDO, indoleamine 2,3-dioxygenase. TDO, tryptophan 2,3-dioxygenase. ACMS, α-amino-β-carboxymuconate-ε-semialdehyde. ACMSD, ACMS decarboxylase. QPRT, quinolinate phosphoribosyltransferase. NAMN, NA mononucleotide [10].

In spite of this well-known and conserved pathway based on tryptophan catabolism, the main source of NAD<sup>+</sup> in mammals are the salvage pathways, which utilize the niacin-derived molecules NA, NAM and NR as precursors. Nicotinamide rather than nicotinic acid is thought to be the predominant NAD<sup>+</sup> precursor in mammals [20] and quantification of its level in human plasma revealed a fivefold higher concentration with respect to NA levels [21]. Moreover, the cleavage of the ADP-ribose moiety of NAD<sup>+</sup> by numerous NAD<sup>+</sup>-dependent enzymes, such as sirtuins and PARPs, leads to the concomitant release of nicotinamide [10].

Nicotinic acid is converted to NAMN as starting point of the Preiss-Handler pathway converging with the primary NAD<sup>+</sup> biosynthesis from tryptophan [22]. NAD<sup>+</sup> synthesis from nicotinamide in lower organisms, such as bacteria and yeast, implies the enzymatic conversion to NA by nicotinamidase (NDase), followed by integration in the Preiss-Handler pathway. In contrast, mammals convert NAM to NAM mononucleotide (NMN) by NAM phosphoribosyltransferase (NAMPT) enzyme, which catalyzes the rate-limiting step in the mammalian NAD<sup>+</sup> salvage pathway from nicotinamide. NAMPT catalyzes the condensation of nicotinamide with 5-phosphoribosyl-1-pyrophosphate to yield nicotinamide mononucleotide. NMN together with ATP is further converted to NAD<sup>+</sup> by a nicotinamide mononucleotide adenylyltransferase (NMNAT) [23]. Three mammalian genes encoding adenylyltransferases have been recently identified, with a distinct cellular localization (nucleus, cytoplasm, mitochondria), that can use both NMN and NAMN as substrate [24], [25]. Lastly, the third NAD<sup>+</sup> salvage pathway, which was originally known as the only NAD<sup>+</sup> biosynthesis pathway in certain bacteria, is comprised of the phosphorylation of NR to NMN by NR kinase (NRK). The pathway is highly conserved in yeast and human for which two NRK enzymes have been described ([13], **Figure 4**).

### **3. NAMPT**

NAD<sup>+</sup> synthesis by NAMPT is essential for cellular metabolism, energy production, and DNA repair, which are processes deeply impaired during malignant transformation. As NAD<sup>+</sup> is rapidly consumed in cancer cells, due to higher turnover, and converted to nicotinamide, NAMPT is essential for the replenishment of the intracellular NAD<sup>+</sup> pool.

Nicotinamide phosphoribosyltransferase (NAMPT) has been originally identified as a secreted cytokine-like factor named Pre-B-cell colony enhancing factor (PBEF) involved in the maturation of early B-lineage precursor cells [26]. Bacterial and murine homologs of NAMPT were later identified as a cytosolic nicotinamide phosphoribosyltransferase involved in NAD<sup>+</sup> biosynthesis [27].

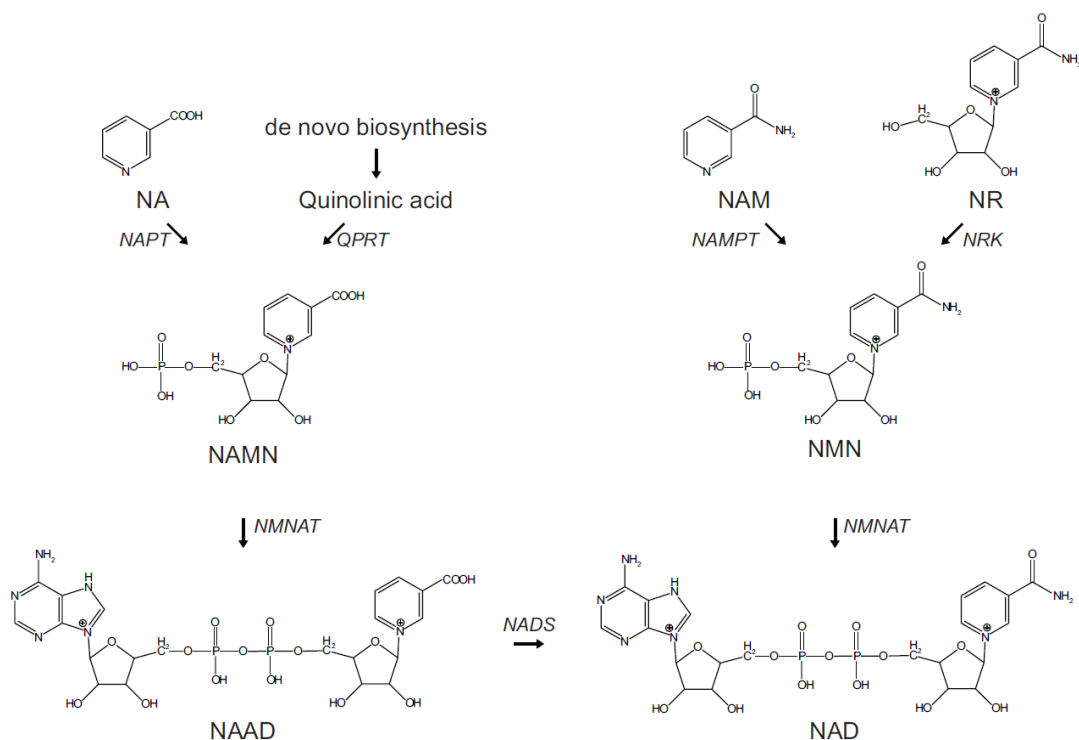


#### Figure 4. Mammalian NAD<sup>+</sup> salvage pathway

Precursors of NAD<sup>+</sup> in the salvage pathway are NA, NAM and NR. The initial step in NAD<sup>+</sup> synthesis from NA, the so-called Preiss-Handler pathway, is catalyzed by NAPT and results in the formation of NAMN, which can also be derived from the *de novo* NAD<sup>+</sup> biosynthesis starting from tryptophan. NAM is converted by NAMPT forming NMN, which is also the product of phosphorylation of NR by NRK. The subsequent conversion of both NAMN and NMN is catalyzed by the same enzyme, NMNAT. In the case of NAMN, this reaction is followed by amidation by NADS, finally producing NAD<sup>+</sup>. NAPT, NA phosphoribosyltransferase. NAMN, NA mononucleotide. NAMPT, NAM phosphoribosyltransferase. NMN, NAM mononucleotide. NRK, NR kinase. NMNAT, NMN adenylyltransferase. NADS, NAD<sup>+</sup> synthase [10].

The crystal structure of the protein revealed its belonging to the dimeric class of type II phosphoribosyltransferases and mutagenesis studies showed that impaired dimerization exhibits attenuated enzymatic activity and that Asp219 is important in defining the substrate specificity [28]. NAMPT can autophosphorylate at H247. This modification increases its affinity for nicotinamide and its enzymatic activity up to 1000-fold [29].

An insulin-mimetic function was also ascribed to NAMPT, which was described to be secreted by visceral fat of humans and directly bind the insulin receptor, recognized as an adipokine and renamed visfatin [30]. However, this paper was retracted due to inability to find evidences to support the actual binding of

NAMPT to the insulin receptor [31]. More recently, NAD<sup>+</sup> biosynthesis mediated by an extracellular form of NAMPT (eNAMPT) was reported to be involved in the secretion of insulin glucose-stimulated in  $\beta$  cells of the pancreas. NAMPT haplodeficiency caused defects in insulin secretion in pancreatic islets *in vivo* and *in vitro* [32].

“NAMPT” has been approved as the official nomenclature of the protein and the gene by both the HUGO Gene Nomenclature Committee (HGNC) and the Mouse Genomic Nomenclature Committee (MGNC).

The human NAMPT gene is located on chromosome 7 and is composed of 11 exons and 10 introns, encoding for a 491 amino acids polypeptide. The coding sequence is highly conserved through evolution and significant sequence homology was reported to be shared among prokaryotes, primitive metazoans and humans [33]. The crucial role of NAMPT in cell physiology is further demonstrated by the fact that the homozygous gene knockout mouse (homozygous for a mutant allele enzymatically deficient) is embryonically lethal [32].

NAMPT is expressed in several human organs, tissues and cells including heart, brain, placenta, lungs, liver, skeletal muscle, kidney and pancreas [26]. NAMPT presents two different forms: intracellular and extracellular (referred as iNAMPT and eNAMPT respectively). iNAMPT localizes at the cytoplasm, nucleus and mitochondria level [34]. Mitochondrial NAMPT in conjunction with the NAD<sup>+</sup>-dependent deacetylase Sirtuin 3 (SIRT3) promotes cell survival following genotoxic stress [35]. NAMPT gene and NAD<sup>+</sup> levels display circadian oscillations and are regulated by the core clock machinery through binding of the circadian transcription factor CLOCK [36]. Sirtuin 1 (SIRT1) is recruited to NAMPT promoter and contributes to its circadian synthesis [37].

Many functions have been associated with NAMPT, among which the major ones are growth factor, cytokine and nicotinamide phosphoribosyltransferase. Its dysregulation has been implicated in the susceptibility and pathogenesis of a number of human diseases such as obesity, non-alcoholic fatty liver disease, type 2 diabetes, aging and cancer. Furthermore, different studies detected an elevated NAMPT expression after stimulation with TNF $\alpha$  [38], IL-6 [39] and under hypoxic conditions [40]. This could motivate the increased level of

NAMPT mRNA reported in states of obesity, insulin resistance in diabetes and inflammation.

In relation to its role as cytokine, NAMPT expression is up-regulated in a variety of acute and chronic inflammatory diseases including sepsis [41], acute lung injury [42], rheumatoid arthritis [43] and myocardial infarction, where it foams cell macrophages within unstable atherosclerotic lesions [44]. NAMPT plays a key role in the persistence of inflammation through its capacity to delay neutrophil apoptosis [41].

### **3.1 NAMPT in cancer**

NAMPT has been indicated as an attractive diagnostic and drug target for cancer therapy by molecular screening, epidemiological survey and pharmacological studies.

NAMPT expression increases in cancer cells, as reported for the first time in primary colorectal cancer with respect to normal control by using suppression subtractive hybridization (6-fold increase) [45].

NAMPT implication in cancer pathogenesis may be explained by several molecular mechanisms. First of all, NAMPT contributes to tumor evasion of apoptosis by synthesizing  $\text{NAD}^+$  in the salvage pathway. The molecule affects cell death through several mechanisms:  $\text{NAD}^+$  mediates cellular energy metabolism, which is a critical factor determining cell death, the  $\text{NADH}/\text{NAD}^+$  ratio affects mitochondrial permeability transition (MPT),  $\text{NAD}^+$  levels mediate the activity of caspase-activated DNA Fragmentation Factor 40 (DFF40), a nuclease primarily responsible for genomic DNA fragmentation during apoptosis,  $\text{NADPH}$  may mediate cell death by its major effects on oxidative stress and  $\text{NAD}^+$ -dependent sirtuins and poly (ADP-ribose) polymerases play a role in apoptosis [46].

Secondly, NAMPT plays a role in new blood vessels formation and angiogenesis, supporting tumor growth. It promotes endothelial angiogenesis *via* activation of mitogen-activated protein kinase ERK-dependent pathway and PI3K/AKT signaling by inducing vascular endothelial growth factor (VEGF) and matrix metalloproteinases (MMP-2, MMP-9) production [47]. The induced

angiogenesis is mediated by the up-regulation of the endothelial fibroblast growth factor-2 (FGF-2), involving ERK 1/2-dependent gene expression [48].

Lastly, several different molecular targets have been identified that promote carcinogenesis following iNAMPT overexpression, including SIRT1, CtBP, and PARP-1. On the other side, a reduced NAMPT expression was found to strongly dysregulate cancer biology signaling pathways in a meta-analysis of genome-wide expression data [49].

Several different human malignant tumors have been demonstrated to overexpress iNAMPT including colorectal [45], ovarian [50], breast [51], gastric [52], prostate [53], well-differentiated thyroid [54] and endometrial carcinomas [55], myeloma [56], melanoma [57], and astrocytomas [58]. Increased iNAMPT expression also occurs in malignant lymphomas, including diffuse large B-cell lymphoma, follicular B-cell lymphoma, Hodgkin's lymphoma, and peripheral T-cell lymphoma [59].

In glioblastoma (GBM) samples, NAMPT was reported to be increased and identified as a potential malignant astrocytoma serum marker and prognostic indicator among GBMs [58]. In breast cancer, NAMPT was demonstrated to up-regulate Notch1 contributing to tumor growth through the activation of the NF- $\kappa$ B pathway [60].

Although most studies document increased levels of iNAMPT between benign and malignant tissues, several others also correlate up-regulated expression with specific changes in tumor behavior. Higher NAMPT expression correlated with deeper tumor invasion and increased growth, metastases and reduced patient survival in gastric cancer, melanoma, endometrial adenocarcinoma and astrocytomas. In prostate cancer, NAMPT over-expression along with SIRT1 increased tumor cells resistance to oxidative stress [53]. In pancreatic cancer, NAMPT inhibition reduced overall metabolic activity and prevented tumor growth, with a responsiveness modulated by expression level of CD38 [61].

Last, several researchers found that iNAMPT expression confers resistance to chemotherapeutic agents, including fluorouracil, doxorubicin, paclitaxel, etoposide, and phenylethyl isothiocyanate [51], [40], [52], [53]. In addition, NAMPT protects cells against genotoxic stress, as reported for the DNA

alkylating agent methylmethane sulfonate (MMS), that is known to hyper-activate PARP-1 [35].

eNAMPT induced the proliferation of the hepatocellular carcinoma HepG2 cell line *in vitro* compared with normal hepatocytes [62] and affected redox adaptive responses promoting tumor proliferation in human malignant melanoma cells [57]. In breast cancer cells, eNAMPT promotes epithelial-to-mesenchymal transition (EMT) through its function as a cytokine secreted into the extracellular environment independent of its enzymatic activity. EMT was mediated by NAMPT ability to activate the TGF $\beta$  signaling pathway *via* increased TGF $\beta$ 1 production [63].

#### **4. FK866**

Targeting NAMPT activity represents a novel therapeutic strategy for human cancers. FK866/ WK175/ APO866/ K22.175 was identified as the first low molecular weight compound capable of inducing apoptosis by a highly specific noncompetitive inhibition of nicotinamide phosphoribosyltransferase. It was discovered through a chemical screening performed in HepG2 (human liver carcinoma cells) to find new antitumor drugs. Interfering with NAMPT, it represents a novel mechanism for induction of tumor cell apoptosis not by cell intoxication but by gradually depletion of NAD<sup>+</sup> which eventually triggers apoptosis [64].

The three dimensional structural analysis of the NAMPT–FK866 complex revealed that FK866 compound binds at the nicotinamide binding site of NAMPT and compete directly with the nicotinamide substrate to inhibit its activity. This structural analysis provided a molecular basis for the inhibition of FK866 on NAMPT and a starting point for the development of new anticancer agents [28], [65].

NAMPT inhibition attenuated glycolysis at the glyceraldehyde 3-phosphate dehydrogenase step by reducing NAD<sup>+</sup> availability to this enzyme. Attenuated glycolysis resulted in ATP depletion and perturbed metabolic pathways and led to reduced serine biosynthesis and tricarboxylic acid cycle and altered pentose phosphate pathway [66].

FK866 has been recently reported to interfere with multiple biochemical pathways, related to tumor glycolysis, guanylate synthesis, pyridine nucleotide pools, and phospholipid metabolism by using  $^1\text{H}$ -decoupled phosphorus ( $^{31}\text{P}$ ) magnetic resonance spectroscopy (MRS). The drug induced an increase in  $^{31}\text{P}$  MRS signals in the phosphomonoester region and a decrease in  $\text{NAD}^+$  levels, pH, and energetic status in a dose-dependent manner. These metabolic changes associated with FK866-induced tumor cell death and enhanced radiation sensitivity in a mouse mammary carcinoma [67].

Although FK866 has been reported to cause selective cancer cell death in a variety of models of solid tumors and hematologic malignancies, the mechanism of cell death is still debated in the literature.

FK866 induced the apoptotic cascade in human leukemia cells (THP-1, a human acute monocytic leukemia cell line), without any DNA-damaging effects. The decreased level of  $\text{NAD}^+$  initiated the apoptotic death signaling pathway leading to disruption of the mitochondrial membrane potential, release of cytochrome c from the mitochondria, activation of caspase 3, cleavage of caspase 3 and PARP, and DNA degradation with the appearance of a sub-G1 cell cycle population [68]. FK866-induced delayed cell death by apoptosis in hepatocarcinoma cells HepG2 was instead not related to a direct inhibition of the mitochondrial respiratory activity, but caused gradual  $\text{NAD}^+$  depletion [64].

In SH-SY5Y neuroblastoma cells, no evidence of apoptosis was assessed by immunoblotting for caspase 3 activation fragment and immunostaining for cytochrome C and AIF (apoptosis inducing factor) translocation, whereas FK866-initiated autophagy was observed with formation of LC3-positive vesicles that had fused with lysosomes [69]. Autophagy was confirmed to be crucial for FK866-induced cell death in neuroblastoma cells, where the drug effects were potentiated by chloroquine and antagonized by 3-methyladenine or by down-regulating autophagy-related protein 7 [70].

FK866 has been shown to have anti-tumor and anti-metastatic activity and a strong anti-angiogenic potency in a murine renal cell carcinoma model (RENCA) [71].

FK866 repressed gastric cancer cell proliferation suppressing cell migration and anchorage-independent growth [52].

FK866 has been demonstrated to be effective in blood cancer cell lines, where it leads to ATP reduction and delayed induction of cell death.

Against hematological malignancies FK866 was proved to have a potent antitumor activity both in a panel of cell lines and primary cells. Most cancer cells (acute myeloid leukemia [AML], acute lymphoblastic leukemia [ALL], mantle cell lymphoma [MCL], chronic lymphocytic leukemia [CLL], and T-cell lymphoma), but not normal hematopoietic progenitor cells, were sensitive to low concentrations of the drug. NAD<sup>+</sup> depletion and ATP decrease led to cell death in a caspase-independent mode, and this was associated with mitochondrial dysfunction and autophagy. Further, *in vivo* administration of FK866 prevented and abrogated tumor growth in animal models of human AML, lymphoblastic lymphoma, and leukemia without significant toxicity to the animals [72]. FK866 anti-tumor activity in hematologic malignancies has been recently confirmed by a preclinical study [73]. A potent synergistic interaction has been reported between FK866 and the apoptosis activator TRAIL (tumor necrosis factor-related apoptosis-inducing ligand) in human leukemia cell lines and in primary B-cell chronic lymphocytic leukemia cells, but not in normal leukocytes, through a mechanism involving autophagy. FK866-induced NAD<sup>+</sup> depletion, mitochondrial transmembrane potential dissipation and massive ATP shortage leading to autophagic cell death were synergistically increased. A convergence of the two death-inducing stimuli at the mitochondrial level was reported, underlying the synergy between TRAIL and FK866, where NAD<sup>+</sup> shortage and activation of the extrinsic apoptotic cascade (caspase-3) *via* TRAIL cooperate to dissipate the  $\Delta\Psi_m$  (mitochondrial transmembrane potential) [74]. In primary CLL (chronic lymphocytic leukemia) cells apoptosis-mediated death was reported by depletion of cellular NAD<sup>+</sup> content, followed by a drop in ATP, loss of MMP (mitochondrial membrane potential), increase in ROS (reactive oxygen species), and induction of apoptotic signaling without up-regulation of the p53-target p21 also in patients with high-risk features, including del17p13.1 [75]. In multiple myeloma (MM) cell lines and patient cells instead, FK866 triggered autophagy but no toxicities were reported with normal donor as well as MM patients PBMCs. A transcriptional-dependent (TFEB) and independent (PI3K/mTORC1) activation of autophagy mediated the cytotoxicity. A significant

anti-MM activity was demonstrated in a xenograft-murine MM model, associated with down-regulation of ERK1/2 phosphorylation and proteolytic cleavage of LC3 ([76], **Figure 5**). Moreover, FK866-induced NAD<sup>+</sup> depletion enhanced the proteasome inhibitor bortezomib-induced anti-myeloma activity and overcame bortezomib resistance. Synergistic anti-MM cell death was associated with activation of caspases (8, 9, 3) and poly (ADP-ribose) polymerase, and down-regulation of the anti-apoptotic protein MCL-1, enhanced intracellular NAD<sup>+</sup> depletion, inhibition of nuclear factor κB signaling and inhibition of angiogenesis [77].

FK866 anti-lymphoma activity was potentiated when used in combination with Rituximab (RTX), an anti-CD20 antibody. Human B-lymphoma induced cell death was increased by drug combination due to enhancement of autophagy, activation of caspase 3 and exacerbation of mitochondrial depolarization. *In vivo*, combined administration in a model of human aggressive lymphoma significantly decreased tumor burden and prolonged survival over single-agent treatment [78].

FK866 was safe and well tolerated in a phase I study that included 24 patients with various advanced solid tumors that were refractory to standard treatments. Thrombocytopenia was the dose-limiting toxicity in this study, suggesting that this drug is a good candidate to transition into clinic. Regrettably, no objective tumor remission was observed, although a few cases of disease stabilization could be recorded [79].

NAMPT inhibitors as monotherapy have so far shown limited antitumor activity and their benefit should be sought in combination treatments with antineoplastic agents, chemotherapy or radiotherapy that might enhance their therapeutic efficacy. One plausible explanation for the failure of NAMPT inhibition as a single agent anti-cancer therapy could be the action of extracellular NAD<sup>+</sup> or extracellular NAD<sup>+</sup> precursors able to prevent FK866-induced cell death.

For example, the NAD<sup>+</sup>-degrading ectoenzyme CD73 reversed cell death induced by NAMPT inhibition through the supply of ectocellular NAD<sup>+</sup> precursors, suggesting the possibility of implementing antitumor therapies based on combined inhibition of NAMPT and CD73 [81].

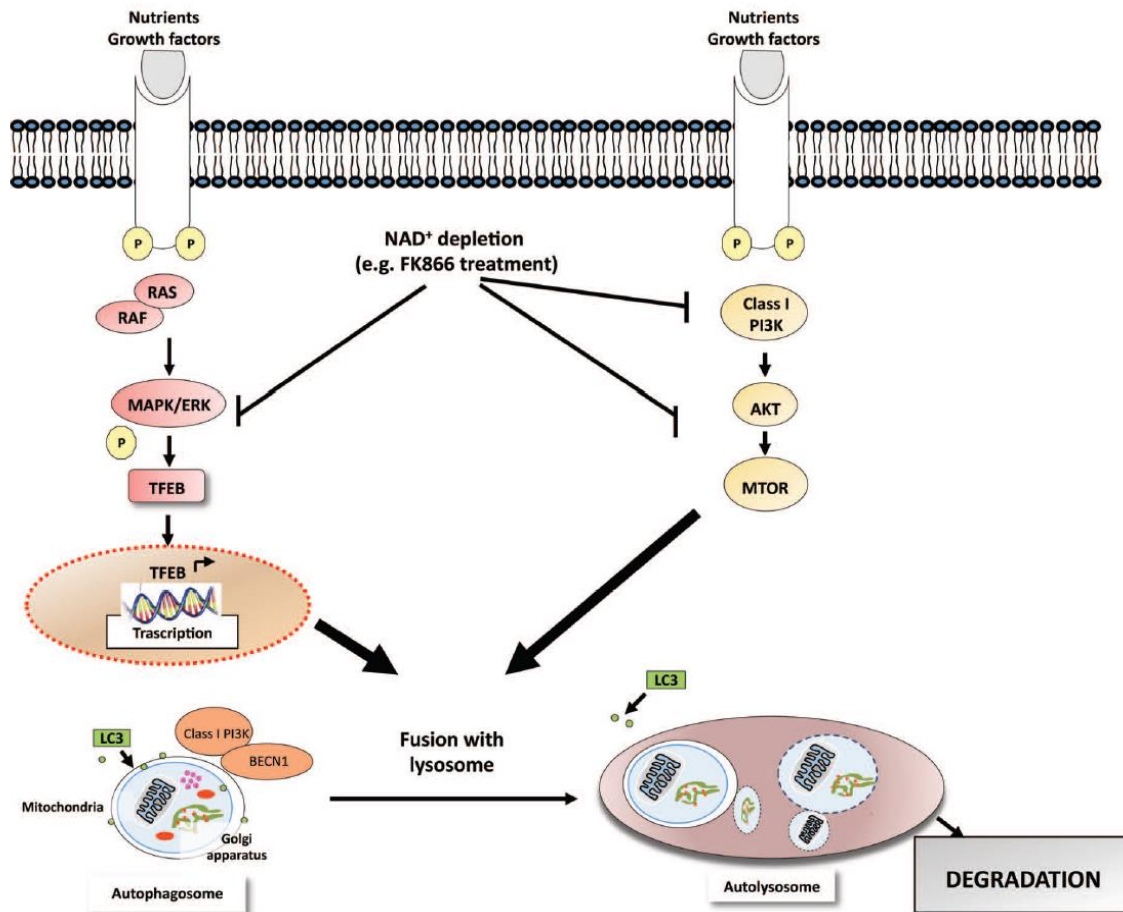


**Figure 5. FK866-induced autophagic cell death of multiple myeloma (MM) cells**

FK866 depletes NAD<sup>+</sup> intracellular stores in MM cells, thereby both blocking MAPKs and inducing translocation of TFEB from the cytoplasm to the nucleus as well as up-regulating autophagy-related genes (transcriptional-dependent mechanism). In parallel, PI3K-mTOR activity is directly inhibited (nontranscriptional-dependent mechanism), further inducing autophagy in MM cells [80].

## 5. Metabolic checkpoints: AMPK and mTOR

The liver kinase B1 (LKB1)/ adenosine mono phosphate activated protein kinase (AMPK)/ tuberous sclerosis complex (TSC)/ mammalian target of rapamycin (mTOR) complex 1 (mTORC1) signaling pathway is central in regulating cellular metabolism and cell growth by integrating information regarding the intracellular energy and oxygen status, the presence of growth factors and nutrient availability. Under circumstances of sufficient energy and nutrient sources, this metabolic pathway stimulates cell growth. In cases of

stress instead, it induces the adjustment of metabolic processes to restore resources in the cell [82].

In a recent study published in 2015, FK866-induced delayed energy stress in hepatocarcinoma cells has been demonstrated to trigger the activation of AMPK and down-regulation of the mTOR signaling which was associated with increased cancer cell death [83].

### **5.1 LKB1- AMPK**

The liver kinase B1 (LKB1, also referred to as serine/threonine kinase 11) is a serine/threonine kinase that is ubiquitously expressed in adult and fetal tissues [84]. The protein lacks a nuclear export domain and in absence of stimulation is therefore retained in the nucleus in its inactive state. Activation of LKB1 is associated with its translocation to the cytoplasm, induced upon binding by the STE20-related adaptor protein  $\alpha$  (STRAD $\alpha$ ) and scaffolding mouse protein 25 (MO25) and the consequent formation of a stable heterotrimeric complex that is actively exported out of the nucleus [85]. Activated LKB1 phosphorylates and activates AMPK (AMP activated protein kinase) in response to energy stress in mammalian cells. Activation induced by AMPK-activating drugs did not occur in cells lacking LKB1 expression. *In vitro* studies demonstrated that LKB1 complexed to STRAD $\alpha$  and MO25 activated AMPK by phosphorylating Thr172 of the  $\alpha$  subunit, and that STRAD $\alpha$  and MO25 subunits enhanced phosphorylation of AMPK by over 100-fold [86].

LKB1-dependent AMPK activation plays a biologically significant role in counteracting apoptosis induced by energy stress [87]. Moreover, LKB1 itself was reported to act as tumor growth suppressor through its cytoplasmic signaling inducing the cyclin-dependent kinase inhibitor p21 in a p53-dependent manner [88].

AMPK is an highly conserved heterotrimeric serine/threonine kinase comprising an  $\alpha$  catalytic subunit and two regulatory subunits ( $\beta$  and  $\gamma$ ). The AMPK cascade is a sensor of cellular energy charge that acts as a 'metabolic master switch' regulating physiological processes related to ATP in order to restore the energy charge in the cell, by suppressing energy-consuming processes such as

glycogen and lipid synthesis on one hand, and enhancing energy-gaining pathways such as glycolysis on the other.

Both catalytic subunit isoforms of AMPK (AMPK $\alpha$ 1 and AMPK $\alpha$ 2) are activated by ATP-depleting processes and metabolic stress such as glucose deprivation, exercise and muscle contraction, ischemia, hypoxia, oxidative stress, osmotic and heat shock and hormones including leptin and adiponectin. The fall of ATP levels and the rise of cellular AMP, due to the reaction catalysed by adenylate kinase, increases the cellular AMP/ATP ratio. This is sensed by AMPK that undergoes a conformational change upon binding of AMP. AMPK can be phosphorylated by LKB1 and, once activated, restores the energetic balance of the cell stimulating ATP production [89].

AMPK $\alpha$  can also be phosphorylated by calcium/calmodulin-dependent protein kinase kinase (CaMKIK), which is triggered through influx of calcium [90].

LKB1/AMPK signaling monitors energy metabolism through regulation of several downstream targets and regulates glucose, lipid and protein metabolism. Activated AMPK inhibits through phosphorylation the metabolic enzymes acetyl-CoA carboxylases (ACC 1 and 2), which promote fatty acid synthesis by production of malonyl-CoA [91]. AMPK was reported to be activated by metformin, the most commonly employed drug for the treatment of type 2 diabetes, resulting in reduction of ACC activity, induction of fatty acid oxidation and suppressed expression of lipogenic enzymes [92].

Inactivation of AMPK has been implicated in tumor progression based on the over-expression of hypoxia-inducible factor-1 $\alpha$  (HIF-1 $\alpha$ ), thereby promoting the Warburg effect by increasing aerobic glycolysis and lactate production [93]. In hepatocellular carcinoma, loss of AMPK promoted carcinogenesis by destabilizing p53 in a SIRT1-dependent manner [94].

One of the downstream effectors of AMPK is the tumor suppressor tuberous sclerosis complex 2 (TSC2), that is activated by phosphorylation (Thr1227 and Ser1345) under energy starvation condition and inhibits mTORC1 complex and mTOR signaling [95]. TSC2 is a GTPase-activating protein (GAP) which inhibits mTOR through inhibition of its activator Rheb, a small Ras family GTPase [96]. TSC2 forms a stable heterodimeric complex with TSC1, which prevents its ubiquitin-mediated degradation and stabilizes its intracellular expression levels

[97]. In contrast to stress-induced activation of TSC1:TSC2 complex, various growth factors and cytokines inhibit the complex by inhibitory phosphorylation of TSC2 through different kinases including PI3K/PKB (also known as AKT), resulting in dissociation of the TSC1:TSC2 complex, followed by its degradation. Moreover, AKT was proved to be a negative regulator of AMPK. AKT activates mTOR through full inhibition of TSC2 and by inhibition of AMPK-mediated activating phosphorylation of TSC2 [98]. Finally, the critical mTOR binding partner raptor (regulatory-associated protein of mTOR) was shown to be a direct substrate of phosphorylation by AMPK, a crucial step required for suppression of mTORC1 activity by energy stress [99].

## 5.2 mTOR

mTOR (mammalian target of rapamycin) is a highly conserved serine/threonine kinase, nutrient-responsive regulator of cell growth and proliferation found in all eukaryotes, active under nutrient-rich conditions in response to glucose, amino acids and growth factors [100]. mTOR is found in two biochemically and functionally distinct signaling complexes: mTORC1 and mTORC2 complex. mTORC1 is nutrient-sensitive, acutely inhibited by the drug rapamycin, and functions as a master regulator of cell growth, angiogenesis, and metabolism. Specifically, this complex is regulated by sensing intracellular as well as extracellular stimuli, such as stress, nutrients, energy, oxygen levels and growth factors. In contrast, mTORC2 is less sensitive to nutrients but more sensitive to growth factors, interacts with RICTOR (rapamycin-insensitive companion of mTOR) and controls actin cytoskeleton [101].

Rheb (Ras homologue enriched in brain) GTPase promotes mTORC1 activity when GTP-bound [102]. The mTORC1 complex consists of mTOR, mLST8/Gbl (mammalian lethal with SEC13 protein 8), raptor (regulatory-associated protein of mTOR) and the recently identified PRAS40 and DEPTOR [103]. Raptor acts as a scaffold to recruit downstream substrates such as the eukaryotic translation initiation factor 4E binding protein 1 (4EBP1) and p70 ribosomal S6 kinase (p70S6K), to the mTORC1 complex.

Upon activation, the mTORC1 controls cell growth by regulating protein translation and cell metabolism through directly phosphorylating and activating p70S6K and through the inhibition of the translation inhibitor 4EBP1 [104]. Phosphorylated 4EBP1 is released from eukaryotic translation initiation factor 4E (EIF4E), which is now free to join the eukaryotic translation initiation factor 4G (EIF4G) and the eukaryotic translation initiation factor 4A (EIF4A) and start cap-dependent protein translation through binding to the 5' cap of mRNAs.

Recently, it has been shown that mTORC1 directly phosphorylates the phosphoprotein MAF1, a key repressor of RNA polymerase III transcription after various stresses, leading to increased protein translation [105]. In addition, activated mTORC1 stimulates angiogenesis by inducing hypoxia-inducible factor 1a (HIF1a), which increases the expression of vascular endothelial growth factor (VEGF) [106]. Furthermore, mTORC1 activity inhibits autophagy *via* phosphorylation of ATG13 and ULK1/2 ([107], **Figure 6**).

NAMPT over-expression reduced mTOR activation during cerebral ischemia where NAMPT promoted neuronal survival through inducing autophagy *via* regulating TSC2-mTOR-p70S6K signaling pathway in a SIRT1-dependent manner [108].

Deregulation of the mTOR signaling pathway is one of the most commonly observed pathological alterations in human cancers. The phosphatidylinositol 3-kinase (PI3K)/AKT kinase cascade signalling pathway plays a crucial role in regulating mTOR and has a cardinal role in cancer cell metabolism promoting cell proliferation, growth and survival. To counteract PI3K, cells contain phosphatase and tensin homologue deleted on chromosome 10 (PTEN). Somatic inactivating mutations in the tumor suppressor gene PTEN are frequently detected in glioblastomas, melanomas, and in prostate and endometrial cancers. Aberrant activation of the PI3K/AKT signaling by genetic alterations in PTEN or AKT result in hyper-activation of mTORC1 signaling and are associated with different types of human cancer [109].

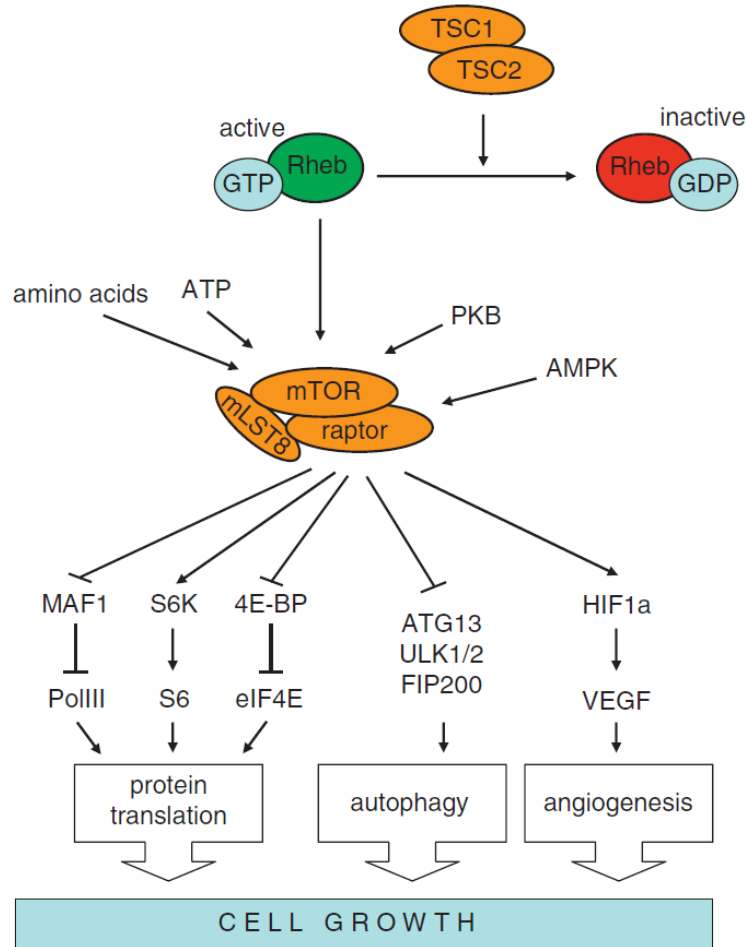


**Figure 6. mTORC1 signaling**

The mTOR complex 1 (mTORC1), consisting of mTOR, raptor and mLST8, controls cell growth mainly through the regulation of protein translation. Activated TSC1:TSC2 complex induces conversion of active GTP-bound Rheb to inactive GDP-bound Rheb. Active Rheb promotes mTORC1 activation, controlling protein translation by activating the ribosomal protein S6 kinase (S6K), inhibiting inhibition eukaryotic initiation factor 4E binding proteins (4E-BP) and the RNA polymerase III (PolIII) repressor MAF1. In addition, mTORC1 induces angiogenesis through induction of hypoxia-inducible factor 1a (HIF1a)-dependent expression of vascular endothelial growth factor (VEGF), and inhibits autophagy by phosphorylating ATG13 and ULK1/2. In addition to TSC-dependent regulation of mTORC1 activity, the complex is directly activated by sufficient levels of energy (ATP) and nutrients (amino acids), as well as through phosphorylation of mTOR by PKB/AKT and of raptor by AMPK [82].

## 6. Cell fate determinants in response to stress: phospho-EIF2A and the UPR

The endoplasmic reticulum (ER) is a multi-functional organelle responsible for many fundamental cellular processes, including calcium storage, lipid biosynthesis and folding and assembly of proteins targeted to a transmembrane or secretory pathway [110]. Different endogenous and exogenous stimuli, such

as pharmacological treatments, viral infections, metabolic demands but also differentiation, may impair, directly or indirectly, the ER functions, possibly resulting in an accumulation of misfolded proteins inside the ER lumen [111]. This might lead to presenting wrongly folded proteins on the cell membrane, affecting the ability of the cell to interact with the extracellular environment and possibly contributing to the insurgence of pathological conditions such as cancer, diabetes and neurodegenerative disorders [112]. In response to this accumulation and in the attempt to maintain cellular homeostasis, the ER activates three different pathways, giving rise to the Unfolded Protein Response (UPR). The first two phases of the counteract are rectifying and consist in decreasing the protein load entering the ER, by globally lowering protein synthesis and translocation into the ER, and strengthening the ER-protein folding machinery, by up-regulating the expression of specific UPR target genes. If these two actions do not succeed in reestablishing cellular homeostasis, a third mechanism, namely cell death, is activated [113].

The UPR is triggered by three transmembrane receptors, PKR-like ER kinase (PERK), inositol-requiring enzyme 1 (IRE1), and activating transcription factor 6 (ATF6), which are all activated by GRP78/BiP, an anti-apoptotic ER chaperone capable of sensing changes in the concentration of unfolded proteins in the ER lumen [114]. GRP78 is physiologically present at high concentrations inside the ER and is found both soluble and constitutively bound to the luminal domain of UPR receptors. As chaperone, it temporarily binds all the proteins entering the ER, promoting the correct folding and remaining attached to misfolded proteins. When the density of unfolded proteins exceeds the ER chaperone and degradation capacity, GRP78 detaches from the UPR receptors, triggering their activation. Beyond acting as a stress sensor and a chaperone, GRP78 regulates calcium homeostasis, translocates newly synthesized polypeptides across the ER membrane and targets misfolded proteins for ER-associated degradation (ERAD) [115], [116]. Among the effects induced by the activation of the UPR, inhibition of general translation is the most conditioning for the cell. It is achieved through the dissociation of GRP78 from the luminal domain of PERK, which promotes its oligomerization and autophosphorylation on the cytosolic domain.

The main effect of the activated form of PERK is the phosphorylation of the  $\alpha$ -subunit of eukaryotic translation initiation factor-2 (EIF2A) at Ser51. EIF-2, a translation initiation factor coupled with GTP in the active form, is involved in the ribosomal selection of the start codon and delivers the starting methionyl-tRNA to the initiating translation machinery. After exerting its function, the GTP complexed-EIF-2 is hydrolyzed to the inactive EIF-2-GDP form and is released from the ribosomal complex. The restoration of the active GTP-bound EIF-2 is performed by the pentameric guanine nucleotide exchange factor EIF2B. Phosphorylation of the  $\alpha$  subunit of EIF-2 at Ser51 leads to the inhibition of EIF-2B activity, reducing guanine nucleotide exchange. This decrease in active form of EIF2 results in a global decrease of translation initiation, consequently lowering the amount of newly synthesized proteins, many of which would be targeted to the ER for secretion and post translational modification [117]. However, EIF2A phosphorylation also promotes the expression of specific genes of which mRNAs are inefficiently processed in absence of stress, like, for example, the transcriptional regulator Activating Transcription Factor 4 (ATF4) enhancing the translation of select mRNAs encoding for proteins that control cell adaptation to stress. Increased levels of ATF4 induce a cascade of transcriptional factors including CHOP/GADD153, contributing to the expression of stress-related genes, important for cellular metabolism, the redox status of the cell and apoptosis ([118], **Figure 7**).

Affecting cell metabolism so deeply, the phosphorylation of EIF2A, and consequently its tandem interaction with ATF4, does not occur only in case of ER stress but is common to responses to different types of stress, such as for example nutrient deprivation and viral infections [111]. On the other hand, phenomena leading to an inhibition of phosphorylation of EIF2A may lead to pathological conditions, as it has been documented in different forms of cancer. In recent years, it has become evident that phosphorylation of the alpha subunit of EIF2 at serine 51(EIF2A-S51P) is an important determinant of cell fate in response to stress playing a role in the balance between cell survival and death.

A family of protein kinases phosphorylate EIF2A in response to different cellular stress conditions. Besides PERK, the family includes the double-stranded RNA

(ds-RNA)-dependent kinase (PKR), the heme-regulated inhibitor kinase (HRI) and the general control non-derepressible-2 (GCN2), which is activated by uncharged tRNA caused by amino acid deficiency. Short-term induction of p-EIF2A has been associated with cell survival whereas long-term induction with cell death [119]–[121].

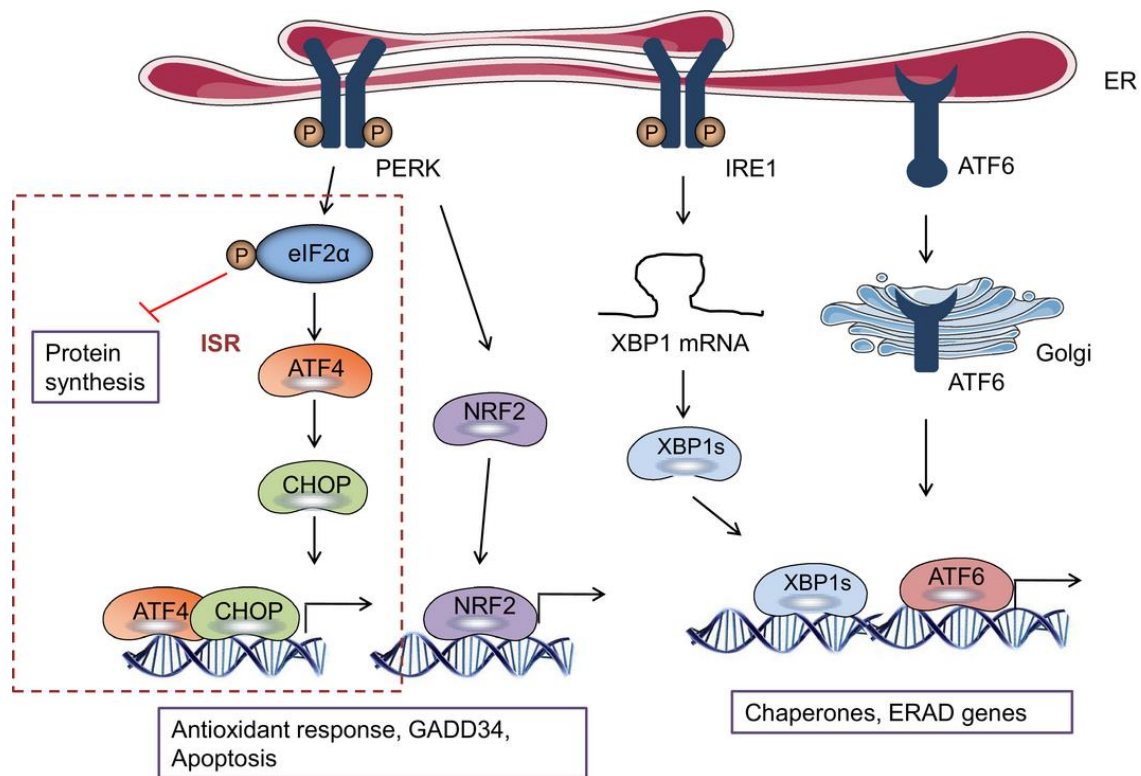


**Figure 7. The unfolded protein response**

Cellular stress conditions disrupt the proper function of the ER and initiates cell stress response. UPR is characterized by the activation of three ER transmembrane effector proteins: PKR-like ER kinase (PERK), inositol requiring enzyme 1 (IRE1) and the activating transcription factor-6 (ATF6). PERK phosphorylates eIF2a attenuating mRNA translation, but inducing the transcription factors ATF4 and CHOP, which will regulate the expression of genes involved in the restoration of the homeostasis and GADD34, an inhibitor of eIF2a, attenuating the response. PERK also phosphorylates and activates the transcription factor NRF2, which induces antioxidant responses. This eIF2a/ATF4/CHOP response is also known as the integrated stress response (ISR). IRE1 is a kinase and an endonuclease that regulates the splicing of the transcription factor XBP1, resulting in the transcription of genes involved in restoring the ER folding capacity. ATF6 is translocated into the Golgi where it is cleaved to release the transcription factor that regulates chaperones expression and ER-associated degradation (ERAD) genes. ATF4, activating transcription factor 4. CHOP, C/EBP-homologous protein. GADD34, protein phosphatase 1 regulatory subunit 15A. NRF2, nuclear factor, erythroid 2 like 2. XBP1, X box-binding protein 1 [122].

## AIM of THE THESIS

My PhD work was funded by the Italian Ministry of Health grant GR-2008-1135635 coordinated by Dr. Alessio Nencioni (University of Genoa) and my research was in the frame of a project aimed at the preclinical evaluation of the NAMPT inhibitor FK866 for the treatment of autoimmunity and lymphoblastic leukemia.

Specific task of the laboratory of Genomic Screening was to perform experiments in T-ALL cell lines (mainly Jurkat cells) and primary T-ALL cells, to assess the effect of FK866 at metabolic and molecular level. Application of gene expression analysis using microarrays aimed at determining changes of key pathways that are influenced by FK866-induced  $\text{NAD}^+$  depletion and identifying the multi-level gene expression regulation exerted by the drug.

We were interested to find differentially expressed genes, in the early phase of cell response to FK866, which can explain the mechanism of cell death induced by the compound.

Our ultimate aim was to define the mechanisms underlying the FK866 resistance phenotype.

Therefore, the aims of my thesis were (1) to investigate the molecular mechanisms of FK866, a specific and potent NAMPT inhibitor, in Jurkat cells; (2) to address the impact of a pharmacological NAMPT inhibition resulting in intracellular  $\text{NAD}^+$  reduction on the energy metabolism and to investigate the pathways activated in response to the insult; and (3) to investigate drug resistance by isolating Jurkat-derived resistant cells and by characterization of the mechanism of resistance.

## METHODS

*The complete description of the Materials and Methods can be found in the manuscripts (see page 88 and 102). The Methods section reported here includes methods used in unpublished experiments or additional details for specific protocols.*

### **Cell lines**

Jurkat human T acute lymphoblastic leukemia (T-ALL) cell line was purchased from the InterLab Cell Line Collection bank (ICLC HTL01002, Genoa, Italy).

MEC.1 human chronic B cell leukemia and OCI/AML3 human acute myeloid leukemia cell lines were purchased from DSMZ (ACC 497 and ACC 582).

Human lung carcinoma A594 (CCL-185) and H460 (HTB-177) cells were purchased from ATCC. These cells were transduced with retroviral vectors encoding either LKB1 cDNA (pBABE-LKB1) or the pBABE control vector.

Cell lines were grown in complete RPMI 1640 (Gibco Life Technologies) supplemented with 10% fetal bovine serum (FBS, Lonza), 2 mM L-glutamine, 100 U/ml penicillin-streptomycin (Lonza) at 37° C under 5% CO<sub>2</sub>.

### **Determination of NAD<sup>+</sup>/NADH and ATP levels**

To determine the content of NAD<sup>+</sup>/NADH cells were harvested after 48 h of treatment and analyzed with NAD<sup>+</sup>/NADH Quantification Kit (BioVision) according to the manufacturer's protocol. Samples were measured using a Tecan Infinite 200 Reader at OD450 nm.

To evaluate the content of intracellular ATP after the treatment, Cell titer Glo Luminescent Cell Viability Assay (Promega) was used following the manufacturer's instructions. Luminescence was measured after 48 h of drug treatment. NAD<sup>+</sup>/NADH and ATP values were normalized to viable cells (Trypan Blue Stain, Lonza).

### **Annexin V/7AAD and PI Flow Cytometry Analysis**

In order to calculate dose-response curve, FITC Annexin V Apoptosis Detection Kit I and 7AAD Staining Solution (BD Pharmingen) were used to stain Jurkat cells treated with FK866 for 48 h, 72 h and 120 h (drug concentration range: 0.1 -100 nM), according to manufacturer's protocol. EC<sub>50</sub> values were determined

by nonlinear regression analysis of viable cells (Prism software v 5.01, GraphPad) by comparison with Mock condition (DMSO). To evaluate cell death, Propidium Iodide Staining Solution from BD Pharmingen was used and analyzed by FACS.

### **Click-iT Labeling Kits**

Click-iT RNA Alexa Fluor 488 Imaging Kit (Invitrogen) was used to quantify by FACS analysis the level of global RNA synthesis. Click-iT RNA assays employ an alkyne-modified nucleoside, EU (5-ethynyl uridine), that is fed to cells and incorporated into nascent RNA. Detection utilizes the chemoselective ligation or "click" reaction between an azide and an alkyne, in which the modified RNA is detected with a corresponding azide-containing dye.

$3 \times 10^6$  Jurkat cells were treated for 45 h with FK866 (or DMSO only in the Mock condition) and incubated for 3 h with 1X EU working solution without removing the drug-containing media. EU detection by FITC signal was performed following manufacturer's protocol after cell fixation and permeabilization. 7AAD Staining Solution (0.25  $\mu$ g/sample) allowed the exclusion of nonviable cells in flow cytometric assay. 3 h of treatment with Actinomycin D (Sigma) 5  $\mu$ M was used as positive control of transcriptional inhibition.

Click-iT AHA Alexa Fluor 488 Protein Synthesis HCS Assay employs an amino acid analog of methionine containing an azido moiety (AHA) that is incorporated into proteins during active protein synthesis detected with an AHA Alexa Fluor 488 alkyne. Cells ( $3 \times 10^6$  cells) were treated for 45 h with FK866, centrifuged and co-incubated for 3 h with Click-iT AHA diluted in L-methionine-free medium (RPMI Medium 1640, Sigma) for a final 50  $\mu$ M concentration and the drug (DMSO for Mock condition). After fixation and permeabilization, AHA was detected by FACS analysis according to manufacturer's instructions. For gating, cells were treated for 3 h with cycloheximide 350  $\mu$ M (Sigma) in order to block translation.

## **Western blotting and sub-cellular fractionation**

After the treatment cells were washed once in PBS and lysed in RIPA lysis buffer (Tris 50 mM pH 7.4, NaCl 150 mM, Igepal CA-630 1%, EDTA 1 mM, Na deoxycholate 0.5%, SDS 0.1%) containing Protease Inhibitor Cocktail (Sigma-Aldrich) for 5 min on ice. After sonication (2 pulses of 7 sec, amplitude 80) and centrifugation at 4°C for 30 min at maximum speed, the supernatants were diluted in SDS-PAGE protein sample buffer and boiled for 5 min. Equal concentration of proteins (quantified with Bradford Reagent, Sigma) was separated on SDS-polyacrylamide gel electrophoresis (SDS-PAGE) and processed following standard procedures. The PVDF membrane (Immobilon-P Membrane, Millipore) signals were detected by chemiluminescence using ECL Western Blotting Detection Reagents (GE Healthcare).

For sub-cellular fractionation, cells were lysed in cold cytosolic lysis buffer (10 mM HEPES pH 7.0, 10 mM KCl, 1 mM EDTA, 0.5% NP-40, 1 mM DTT, and Protease inhibitor cocktail). The supernatant containing cytosolic fraction was collected by centrifugation at 3000 x g for 5 minutes at 4°C. Nuclear pellets were then re-suspended in cold nuclear lysis buffer (10 mM HEPES pH 7.0, 400 mM NaCl, 1 mM EDTA, 25% Glycerol, 1 mM DTT, and Protease inhibitor cocktail). The nuclear extract was harvested by centrifugation at 12000 x g for 15 minutes at 4°C. Then, equal quantities of proteins were separated by electrophoresis on SDS-page gels. Tubulin and nucleolin served as the loading control for the cytosolic and nuclear fraction, respectively.

Desitometric analysis were performed by using the ImageJ software.

## **Polysomal RNA extraction**

For polysomal RNA extraction  $30 \times 10^6$  Jurkat cells/ml were seeded and treated for 48 h. Cells were harvested and treated with cycloheximide (Sigma) for 5 min at 37°C in order to stabilize the polysomes (final concentration 100 µg/ml). After washing cells twice with cold phosphate buffer saline (PBS + cycloheximide 10 µg/ml), 1 ml of lysis buffer was added [10 mM NaCl, 10 mM MgCl<sub>2</sub>, 10 mM Tris-HCl pH 7.5, 1% Triton X-100, 1% sodium deoxycholate, 0.2 U/µl RNase inhibitor (Fermentas), cycloheximide 10 µg/ml and 1 mM dithiothreitol]. Lysates

were transferred to Eppendorf tubes, incubated on ice for 2 min and centrifuged for 5 min at 12000 g at 4°C. The supernatant was loaded directly onto a 15-50% linear sucrose gradient containing 30 mM Tris-HCl pH 7.5, 100 mM NaCl, 10 mM MgCl<sub>2</sub>, and centrifuged at 4°C in a SW41 rotor for 110 min at 180000 g. Subpolysomal and polysomal fractions were collected using a Teledine ISCO gradient maker with automated fraction collector monitoring the absorbance at 254nm. For RNA extraction, the fractions were treated with proteinase K (100 µg/ml) in 1% SDS for 3 h at 37°C. After phenol–chloroform extraction and isopropanol precipitation, the recovered RNA pellets were resuspended in 30 µl of RNase-free water. RNA quality was assessed by the Agilent 2100 Bioanalyzer platform.

RNAs extracted from fractions were pooled for microarray analysis (subpolysomal RNA: fraction 2-7; polysomal RNA: fraction 8-11; total: fraction 2-11).

### **Microarray analyses**

Total, polysomal and subpolysomal RNA were hybridized in quadruplicate on the Agilent Human GE 4x44K v2 Microarray (G2519F-026652) following the manufacturer's protocol. Hybridized microarray slides were scanned with an Agilent DNA Microarray Scanner G2505C. µm resolution with the manufacturer's software (Agilent ScanControl 8.1.3). The scanned TIFF images were analyzed numerically and background corrected using the Agilent Feature Extraction Software version 10.7.7.1 according to the Agilent standard protocol GE1\_107\_Sep09.

The output of Feature Extraction was analyzed with the R software environment for statistical computing (<http://www.r-project.org/>) and the Bioconductor library of biostatistical packages (<http://www.bioconductor.org/>). Low signal Agilent probes, distinguished by a repeated “not detected” flag across the majority of the arrays in every condition, were filtered out from the analysis. Signal intensities across arrays were normalized with the quantile normalization algorithm.

Polysomal RNA and total RNA DEGs were determined adopting a double threshold based on 1) the magnitude of the change (log<sub>2</sub> fold change >1 and <-

1 for induced and repressed genes, respectively); 2) the statistical significance of the change, measured with a moderated t-test (p-value <0.05) implemented in the Bioconductor Limma package.

Translational efficiency (TE) was calculated as the ratio between polysomal and sub-polysomal signals. Genes with significant differences in TE after the treatment with FK866 were selected adopting a double threshold based on 1) the magnitude of the change in TE (log<sub>2</sub> change of TE >1 and <-1 for genes with increased and decreased TE, respectively); 2) the statistical significance of the polysomal fold change, measured with a moderated t-test (p-value <0.05) implemented in the Bioconductor Limma package.

Translatome DEGs were analyzed with the Ingenuity Pathway Analysis (IPA), using the “Canonical Pathways” analysis (<http://www.ingenuity.com/>). Enrichment was tested with the Fisher exact test. The significance of over-representation is determined at a 0.05 p-value threshold.

Total RNA extracted from resistant cells was hybridized in quadruplicate on the Agilent Human GE 4x44K v2 Microarray (G2519F-026652) and compared with total RNA from parental cells. After quantile normalization and removal of low signals, differentially expressed genes were selected according to a double threshold on log<sub>2</sub> FC (absolute value > 0.75) and moderated t-test p-value (<0.05) calculated with the Limma package. The DAVID resource was used for functional annotation enrichment analysis of the resulting lists of DEGs, using annotations from Gene Ontology (<http://www.thegeneontology.org>), KEGG (<http://www.genome.jp/kegg/>), PFAM (<http://pfam.sanger.ac.uk/>). The significance of over-representation was determined using a p-value threshold of 0.05. Gene Ontology terms with more than 500 associated genes were filtered out for being too general.

### **Real-time PCR**

For Real-time PCR, 1µg of total, polysomal and subpolysomal RNA was DNase-treated and cDNA was synthesized using RevertAid First Strand cDNA Synthesis Kit (Fermentas), following the manufacturer’s recommendation. Real-time PCR reactions were carried out using the KAPA PROBE or SYBR FAST

Universal qPCR Kit on a CFX96 Real-Time PCR Detection System (BioRad). Relative mRNA quantification was obtained with the  $\Delta C_t$  method, taking into account the efficiency of cDNA synthesis by the quantification of the ACTB housekeeping gene from the same cDNA. TaqMan probes for Gene Expression Assays were obtained from Applied and used for quantification of NAMPT (Hs00237184\_m1) normalized to the levels of ACTB (Hs99999903\_m1). Primers' sequences used for SYBR Green Real-time PCR are reported as follows:

Gene	Primer Forward	Primer Reverse
ACTB	CTGGAACGGTGAAGGTGACA	AGGGACTTCCTGTAACAATGCA
HSP90AA1	CTGCTTATTTGGTTGCTGAG	CCCATAGGTTACCTGTGTCTG
MYSM1	ACAGCCAGGAAGTGGTGAAA	CCAAGGTCCAAGGAATAAGGC
PRKAA1/AMPK	ACCAAGGTGTAAGGAAAGCA	ACAACCTTCCATTCATAATCCA
STK11/LKB1	GAGCTGATGTCGGTGGGTATG	CACCTTGCCGTAAGAGCCT
BiP/Grp78	TGTTCAACCAATTATCAGCAAATC	TTCTGCTGTATCCTCTTCACCAGT

### Sequencing

We checked for presence of mutations in the NAMPT gene by sequencing its coding sequence in resistant and parental cells. NAMPT gene was amplified by using specific primers designed on the coding region including the ATG and the stop codon (highlighted in bold in the primer sequence). Sequencing was performed by an external sequencing service (BMR-Genomics, Padova, Italy). To sequence the whole coding region, an additional primer pair was designed (NAMPT-seq).

Gene	Primer Forward	Primer Reverse
NAMPT	AG <b>ATGA</b> ATCCTGCGGCAGAA	<b>CCTA</b> ATGATGTGCTGCTTCC
NAMPT-seq	TTATGGAACGAAAGATCCTG	CAAAAGCATCTTTTTCATGGTC

## **Lentiviral transductions**

Lentiviral vector stocks were produced by co-transfection in 293T cells (ATCC CRL-11268) of the packaging plasmid pCMV-deltaR8.91, the VSV-envelope coding plasmid pMD2.G (kind gift of Didier Trono, EPFL, Lausanne) and the transfer vectors. 48 h post transfection vector containing supernatants were collected and viral titers were determined using a qPCR based RT-assay [123]. Half a million Jurkat cells were transduced using a total of 2-4 RTUs of viral vectors. To maximize the transduction efficiency cells were centrifuged at 25°C for 2 h at 1600 g in the presence of vectors and then incubated overnight at 37°C before changing medium. After a recovery period of approximately 48 h cells were seeded and treated as needed.

## **Drug sensitivity and resistance testing (DSRT)**

The DSRT platform is based on an oncology compound collection that covers the active substances from the majority of U.S. Food and Drug Administration/European Medicines Agency (FDA/EMA)–approved anticancer drugs ( $n = 123$ ), as well as emerging investigational and preclinical compounds ( $n = 64$ ) covering a wide range of molecular targets [124]. The compounds were obtained from the National Cancer Institute Drug Testing Program (NCI DTP) and commercial chemical vendors: Active Biochem, Axon Medchem, Cayman Chemical Company, ChemieTek, Enzo Life Sciences, LC Laboratories, Santa Cruz Biotechnology, Selleck, Sequoia Research Products, Sigma-Aldrich, and Tocris Biosciences.

Compounds were dissolved in 100% dimethylsulfoxide (DMSO) and dispensed on tissue culture–treated 384-well plates, plated in five different concentrations in 10-fold dilutions covering a 10000-fold concentration range (e.g., 1–10000 nmol/L), using an acoustic liquid handling device (Echo 550 from Labcyte Inc.). The predrugged plates were kept in pressurized StoragePods (Roylan Developments Ltd.) under inert nitrogen gas until needed. During the screening, compounds were initially dissolved with 5  $\mu$ L of medium while shaking for 30 minutes. Twenty microliters of single-cell suspension (4000 cells) were then

transferred to each well using a Multi Drop Combi (Thermo Scientific) peristaltic dispenser. After 72 h cell viability was measured using CellTiter-Glo luminescent assay (Promega) with a PHERAstar FS (BMG Labtech) plate reader. The data were normalized to negative control (DMSO only) and positive control wells (containing 100  $\mu\text{mol/L}$  benzethonium chloride, effectively killing all cells). For each drug tested a dose-response curve was generated. Drug responses were compared across the samples by calculation of the Drug sensitivity scoring (DSS), using the method described by Yadav B *et al.* [125].

### **Drug combination analysis**

Combination index (CI) was calculated using CompuSyn software V1.0 by the method of Chou and Talalay [126]. Strong synergistic effect has been considered if  $\text{CI} < 0.1$ .

### **Statistical analysis**

Experiments were performed in biological triplicates. T-test was used to calculate final p-values, without assuming variances to be equal (Welch's t-test). P-value  $< 0.05$  was considered statistically significant.

# RESULTS

## 1. Investigating the mechanism of action of FK866

*This section presents an extended summary of the results included in the accompanying manuscripts. For clarity some of the Figures of the manuscripts are also reproduced here. Unpublished data supporting the results will be included.*

*Results in the thesis body reflect my personal contribution to the work.*

*With respect to the first paper (page 88, Zucal C et al.), I was not involved in microarray analysis (performed by TT) and in preparing pLKO.1 transfer vectors for LKB1 silencing by cloning annealed oligos coding for shRNAs (AC). VDA was involved in the polysomal RNA extraction and in flow-cytometric analysis. I did all the other experiments described here and in the paper.*

*With respect to the second one (page 102, Cagnetta A et al), this section presents my personal contribution in the results included in the accompanying manuscript. Specifically, I was involved in the investigation of ER-stress related markers in leukemia cell lines (MEC.1 and OCI/AML3).*

The primary aim of my thesis was to investigate the molecular mechanisms of the specific NAMPT inhibitor FK866 in Jurkat cells, addressing the impact of a pharmacological inhibition resulting in intracellular NAD<sup>+</sup> reduction on the energy metabolism and investigating the pathways activated in response to the insult.

In order to characterize the effects of FK866 on Jurkat cells in the early phases of cell response to stress, a pre-toxic dose of the drug was determined.

Cell viability was quantified through Annexin V/7AAD staining after 48, 72 and 120 hours of FK866 treatment, resulting in a complete cell death in the latter case. As shown in **Figure 8a**, the drug did not highly impact on cell viability at 48 hours, as both the Annexin V and 7AAD positive populations at this time point were low for the tested doses. Calculated EC<sub>50</sub> at 48 hours was 5 nM, dose that was afterwards used in all the performed experiments. In addition, 100 nM concentration of FK866 was chosen since, failing to substantially compromise Jurkat cell viability at 48 hours but providing a stronger NAMPT inhibition, allowed us to study cell signaling in the absence of an ongoing apoptotic response (**Figure 8a**). The absence of caspase 3 and 7 activation further confirmed that apoptosis was not started yet (**Figure 8b**).

On the contrary, the metabolic effect of NAMPT inhibition, namely NAD<sup>+</sup> and ATP intracellular decrease, was clearly present with the selected doses at 48 hours (**Figure 8c**).

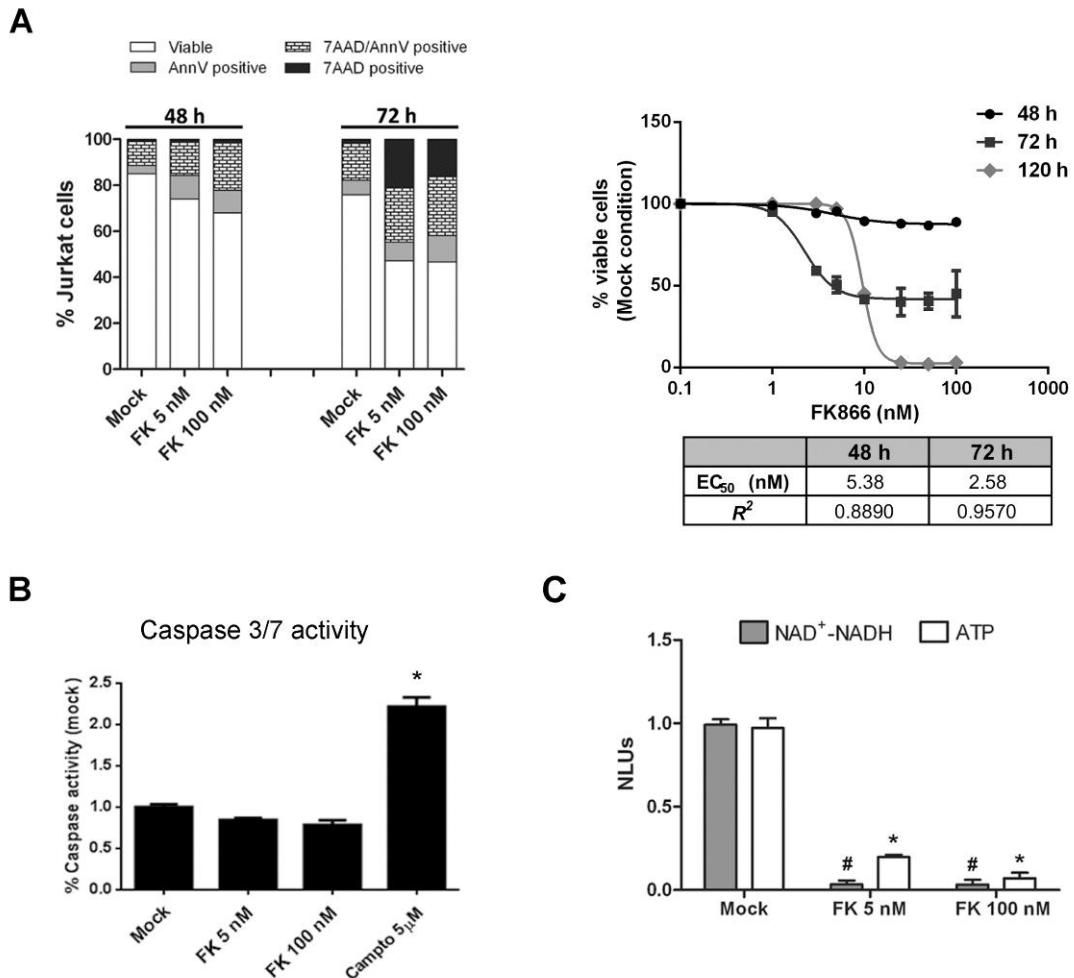


**Figure 8. FK866 induces cell death and metabolic stress in Jurkat cells**

**A**, Flow-cytometric quantification of cell viability at 48, 72 and 120 h performed with AnnexinV and 7AAD staining. Mock, 5 nM FK866 and 100 nM FK866 are shown as representative samples (left panel). **B**, Caspase 3/7 activity was measured in Jurkat cells treated with FK866 for 48 h. Alternatively, cells were exposed to 5  $\mu$ M of Camptothecin for 4 h as a positive control. **C**, Jurkat cells were treated with FK866 for 48 h. Thereafter, intracellular NAD<sup>+</sup>(H) and ATP levels were evaluated in comparison with control cells. RLUs were normalized to number of viable cells. B-C mean $\pm$ SD of three experiments, \* and # indicates p-value <0.05.

In order to better characterize the global effects of NAD<sup>+</sup> depletion inside the cell, we evaluated the rate of transcription and translation upon treatment. We applied a technique based on Click-it reaction, which allows quantification of the ongoing RNA and protein synthesis. Regarding the first, the percentage of incorporation of the uridine-analog EU in the treated samples did not reveal a

highly compromised level of transcription (**Figure 9a**). In contrast, the translational rate, detected by AHA (L-azidohomoalaine), was strongly affected by FK866 (**Figure 9b**).

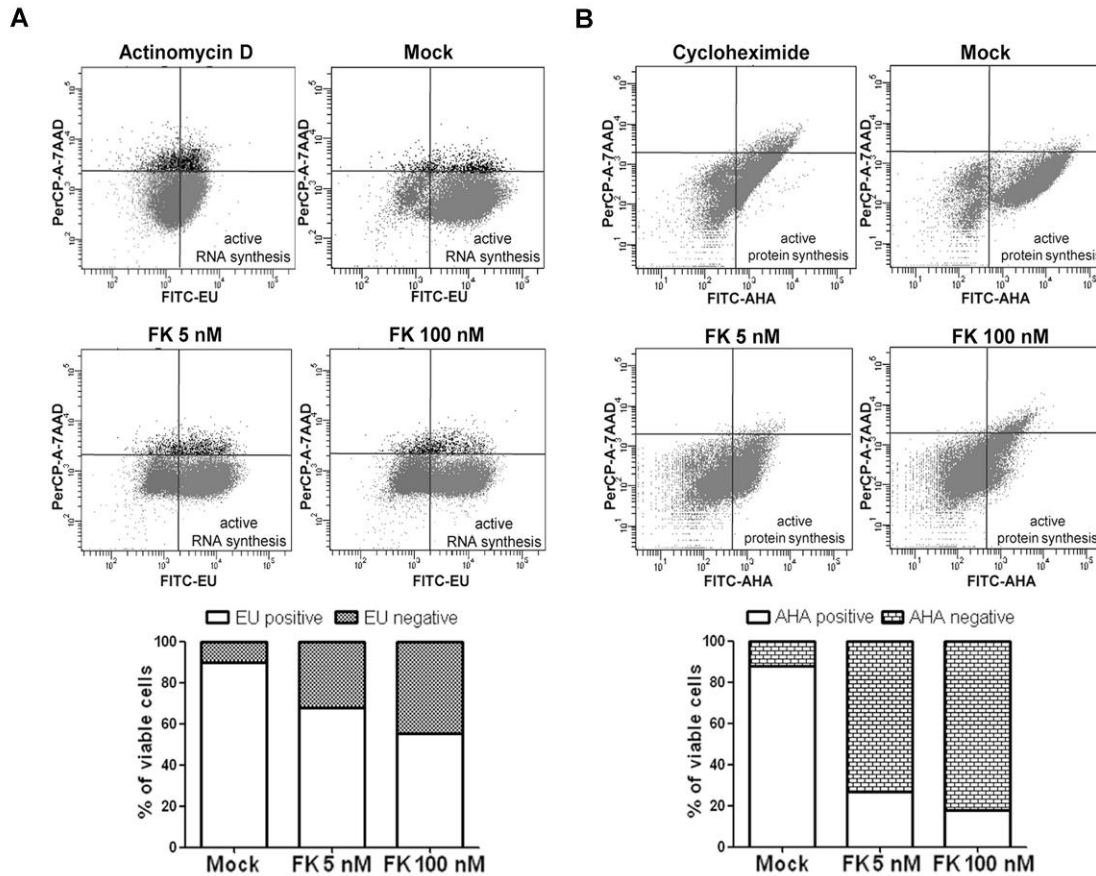


**Figure 9. Macromolecular synthesis is inhibited by FK866**

**A**, RNA synthesis was determined by monitoring EU incorporation with Click-it chemistry after 48 h of treatment with FK866 or 5  $\mu$ M Actinomycin D, an RNA synthesis blocking agent (3 h). The histogram quantifies the dose-dependent transcription inhibition induced by FK866 in the viable cell population. **B**, Protein synthesis was monitored by AHA incorporation after 48 h of treatment with FK866 or 350  $\mu$ M Cycloheximide, a protein synthesis inhibitor (3 h). The histogram quantifies FK866 induced protein synthesis arrest in the viable cell population.

To assess if this translational inhibition was specific for defined classes of genes underlying the cell response to FK866, we performed polysomal mRNA profiles and gene expression analyses on total mRNA levels and on polysome-associated mRNAs. The analysis allowed a ‘bidimensional’ transcriptomic approach, namely a genome-wide measure not only of the level of cellular mRNAs but also of the degree of their engagement in the translation machinery at polysomes.

We observed a marked but not complete depletion of the polysomal mRNAs fractions with respect to the sub-polysomal fractions (representative of mRNPs and mRNAs bound to ribosomal subunits or un-translating monosomes) in Jurkat cells after a 48 hours treatment with 5 nM of FK866, highlighting the interference with the mRNA translation process (**Figure 10a**).

We used single color microarray hybridization to compare total, sub-polysomal and polysomal mRNAs. After data preprocessing, normalization and quality check (**Supplementary Table S1**), 569 differentially expressed genes (DEGs) were detected in total mRNA and 1267 in polysomal mRNA fractions (**Supplementary Table S2**). After comparison of the two lists of DEGs, the expression of 338 genes showed to change in the same direction amongst the two pools (homodirectional DEGs), reflecting a significant concordance between total and polysomal RNA expression (Spearman correlation of 0.76). Noticeably, no DEGs showed opposite regulation and 918 DEGs (73% of all transcriptome) presented significant changes only at the polysomal level, whereas 227 DEGs (40% of transcriptome) changed significantly only in total RNA (**Figure 10b**).

Therefore, we concluded that FK866 had a strong effect in shifting specific mRNAs into polysomes (translatome level) in order to cope with the NAD<sup>+</sup> shortage-induced metabolic stress.

Successively, we measured the Translational Efficiency (TE) of each gene, defined as the ratio between polysomal and sub-polysomal RNA signals. This parameter allows to exclude genes whose expression in the polysome-associated mRNA pool relies on a very strong (or very weak) transcription and to select genes reflecting a proper functional relocation upon treatment [127]. Distribution of genes with significant differences in TE after treatment with FK866 is shown in **Figure 10c**. Among candidate genes positively regulated at the translational level in response to FK866 (**Supplementary Table S3**), MYSM1, HSP90AA1, and PRKAA1 (AMPK) were also validated by qRT-PCR and confirmed to be significantly up-regulated in the polysomal mRNA fraction (**Figure 10d**).

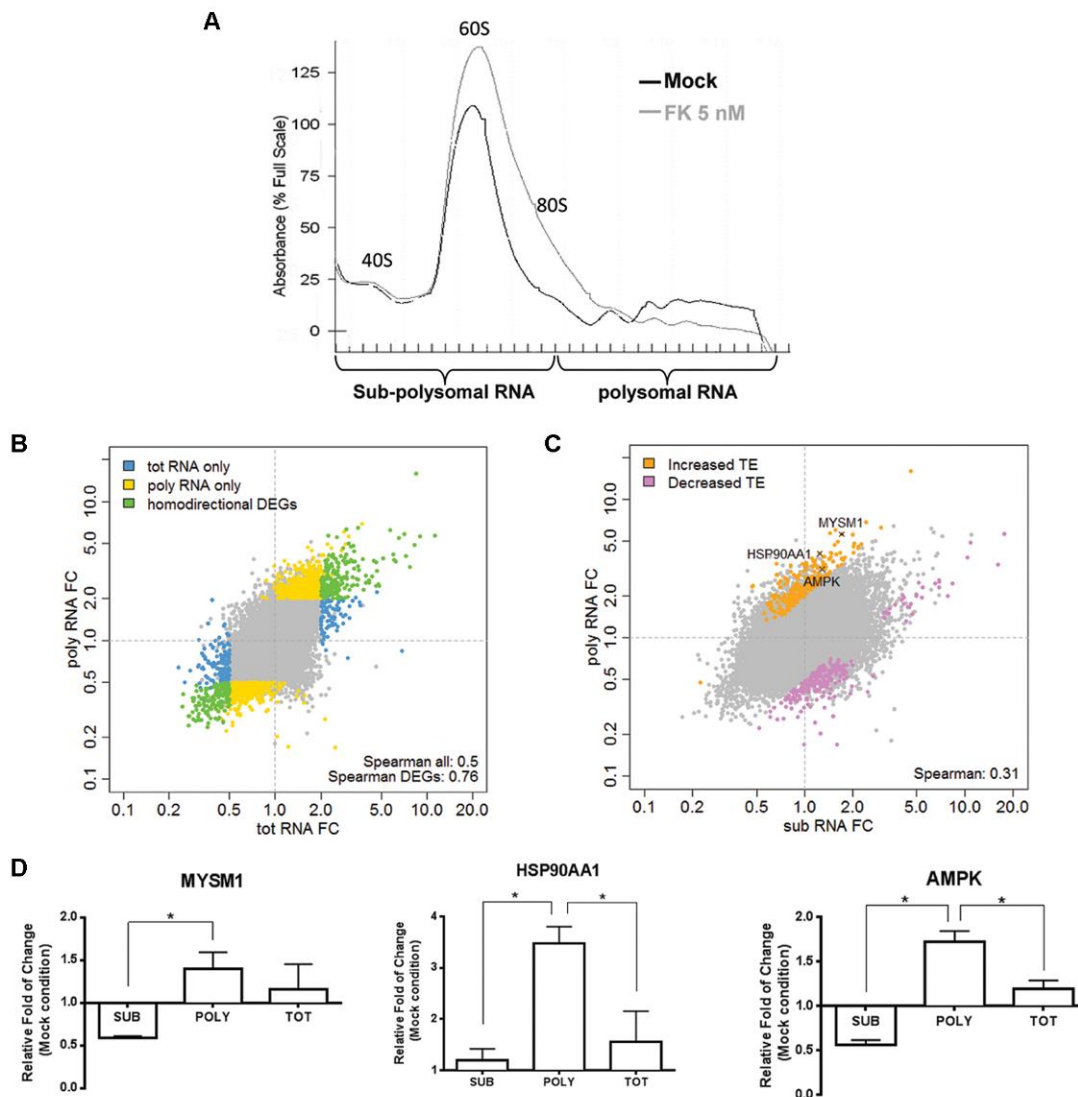


**Figure 10. Multi-level RNA regulation in response to FK866 treatment**

**A**, Representative profile of RNA fractionation of Jurkat cells treated with DMSO or 5 nM FK866 for 48 h, obtained after centrifugation of cytoplasmic lysates on sucrose gradient. Fractions 2 to 7 correspond to sub-polysomal RNA, while fractions 8 through 11 to polysomal RNA. Polysomal profiling was performed four times. Total, sub-polysomal, and polysomal mRNAs extracted from 5 nM FK866-treated and control Jurkat cells were subjected to single color microarray hybridization. **B**, Scatterplot showing genome-wide transcriptional and translational response to FK866 treatment. Transcriptome (total) and translome (polysomal) variations are mildly correlated (0.5 Spearman value), DEGs are more correlated (0.76 Spearman value). Different classes of DEGs are highlighted according to the legend. **C**, Scatterplot showing the genome-wide subpolysomal and polysomal response to FK866 treatment. Genes with statistically significant variations in translational efficiency (TE), characterized by an increased or decreased access to the translating compartment of the cells, are highlighted. **D**, qPCR validation for three candidate genes with significant increases in translational efficiency. Statistical significance was calculated with t-test (\* indicates p-value <0.05).

To find key mRNA targets whose translation is essential and strongly promoted to survive to FK866-induced stress, we performed an over-representation analysis of the signaling pathways of the entire set of genes regulated at polysomal level by using Ingenuity Pathway Analysis software (IPA).

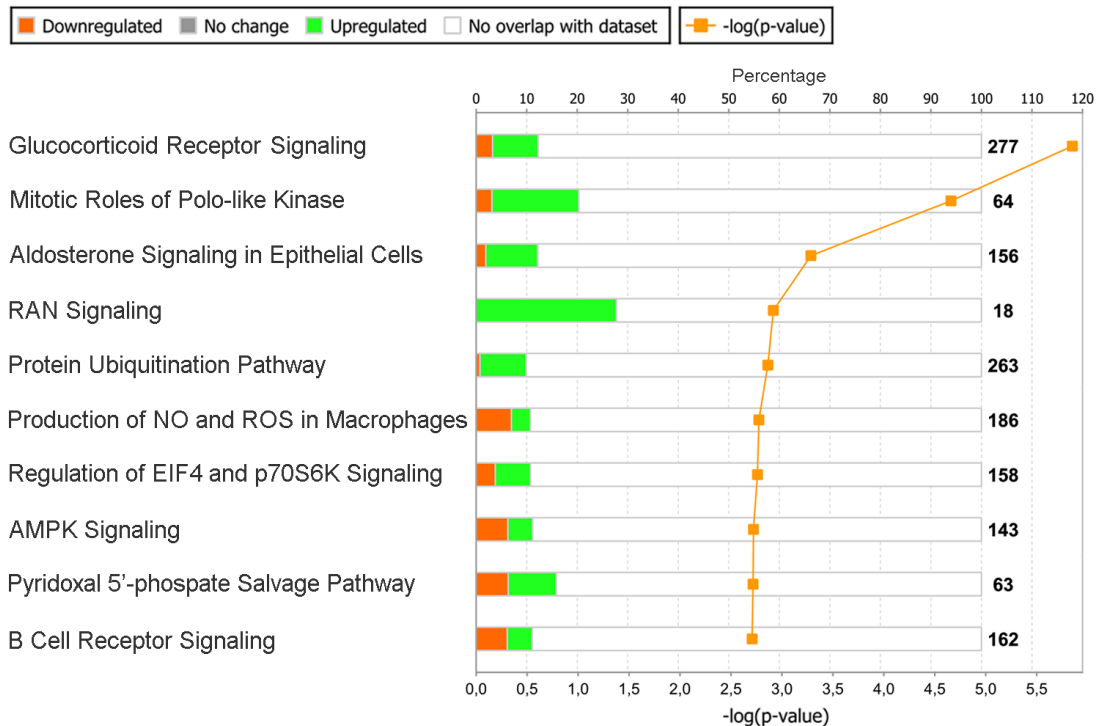


**Figure 11. IPA of the translome following FK866 treatment**

Significantly enriched pathways among translome (polysomal) DEGs, detected by Ingenuity “Classical Pathway Analysis”. Bars display the percentage of down-regulated and up-regulated DEGs contributing to the enrichment of each pathway.

The Glucocorticoid Receptor (GR) Signaling pathway was the top ranked theme and the significant enrichment ( $p=1.42E-06$ ) was caused by the over-representation of 34 differentially regulated genes out of the 277 belonging to this ontology. Analyzing the components of the GR Signaling pathway, we found different factors with regulated polysomal loading that might be possible drug targets. Among them, we found heat shock protein HSP90, signaling kinases as JAKs and MAPKs, the AMP dependent protein kinase PRKAA1 (AMPK) and, interestingly, the NR3C1 (Glucocorticoid Receptor) gene.

In the first ten significantly over-represented pathways, many themes suggested a modulation of the ubiquitination process (druggable protein gene PSMD1) and the production of reactive oxygen species by the interferon

gamma signaling pathway (druggable protein gene IFNGR1). Notably, the modulation of many eukaryotic initiation factors (EIF2A, EIF2B, EIF3C, EIF4A2, EIF4G2, EIF4G3) strongly suggested a role for pathways related to the translation process and connected to the regulation of EIF4E and p70S6K signaling. Finally, the AMPK signaling was identified as a top hit, driven by the presence of the HSP90 and PRKAA1 (AMPK) genes (**Figure 11** and **Supplementary Table S4**).

Taken all the results together, since global translation was observed to be deeply inhibited in the “Click-it” experiment and members of translational control pathways were found to be affected in the IPA analysis, we focused on the investigation of possible impact of FK866 on master regulators of translation. In particular, we mainly explored factors involved in the initiation phase of cap-dependent translation, which is considered the limiting step of translation strictly regulated in the cell. Multiple associated proteins, each designated as EIFs (eukaryotic initiation factors), are required to assemble a translationally competent 80S ribosome, which is recruited in the cytoplasm by the 5' cap structure of the mRNAs.

Specifically, mRNAs are bound by EIF4F, consisting of the EIF4E subunit that binds to the cap, the helicase EIF4A, and scaffolding protein EIF4G. During conditions of low nutrient availability, EIF4E can be sequestered by the EIF4E-binding protein (4EBP1), thus limiting assembly of the EIF4F complex. mTORC1 signaling enhances protein synthesis by phosphorylating 4EBP1, preventing its binding to EIF4E.

The next step of translation involves the recruitment of a 43S preinitiation complex (PIC) composed of the 40S ribosomal subunit bound to EIF3, EIF1, EIF1A, EIF5, and the EIF2-GTP-Met-tRNA<sup>i</sup> ternary complex. Therefore, the initiation factor EIF2A plays an important role in the initiation phase of translation. Its phosphorylated form at serine 51 decreases global protein synthesis [128].

We evaluated the impact on protein translation by detecting the phosphorylation status of mTOR, its target 4EBP1, and EIF2A.

In T-ALL cells, FK866 inhibited mTOR signaling resulting in de-phosphorylation of 4EBP1 in a dose-dependent manner. Furthermore, EIF2A was

phosphorylated upon treatment, indicating an impairment in the initiation phase of translation (**Figure 12**).

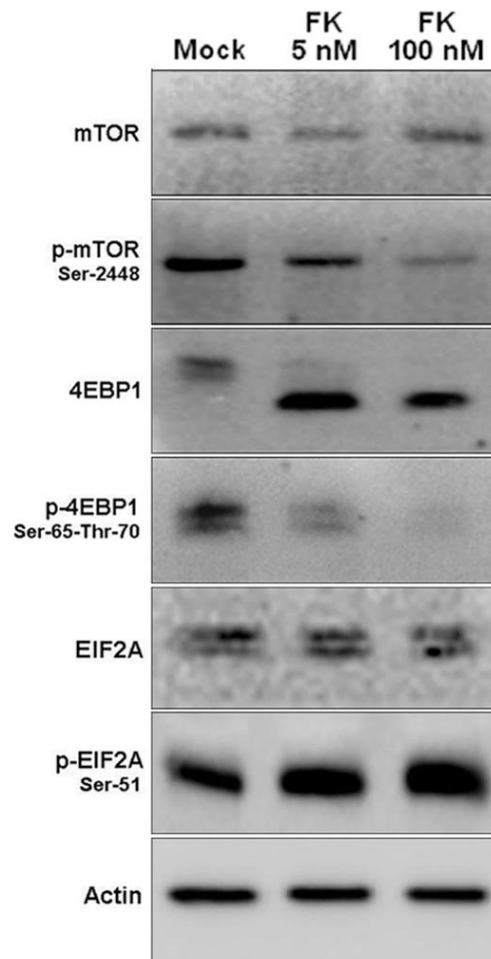


**Figure 12. FK866 blocks translation through mTOR/4EBP1 and EIF2A**

Jurkat cells were treated for 48 h with FK866 and levels of the indicated proteins were detected by immunoblotting. The panel represents one experiment out of at least three biological replicates.  $\beta$ -actin was used as loading control.

AMPK is a cellular energy sensor and a metabolic checkpoint, promptly activated in response to energetic stress. In particular, the kinase inhibits energy-consuming pathways when the intracellular ATP content is low. Among several regulated pathways, AMPK impacts on mTOR signaling affecting protein metabolism. Based on the metabolic impact of FK866, resulting in  $\text{NAD}^+$  and ATP depletion, we investigated the possible role of AMPK in responding to the drug-induced stress.

We demonstrated AMPK activation upon FK866 in Jurkat cells, by detecting the increase in its phosphorylated form at threonine 172 and the inhibition of its

target ACC (Acetyl-CoA carboxylase). Its activity was also involved in the response to FK866 in T-ALL patient's derived samples. Importantly, in drug-responsive primary cells, we reported both the activation of AMPK and the inhibition of EIF2A (**Figure 13**).

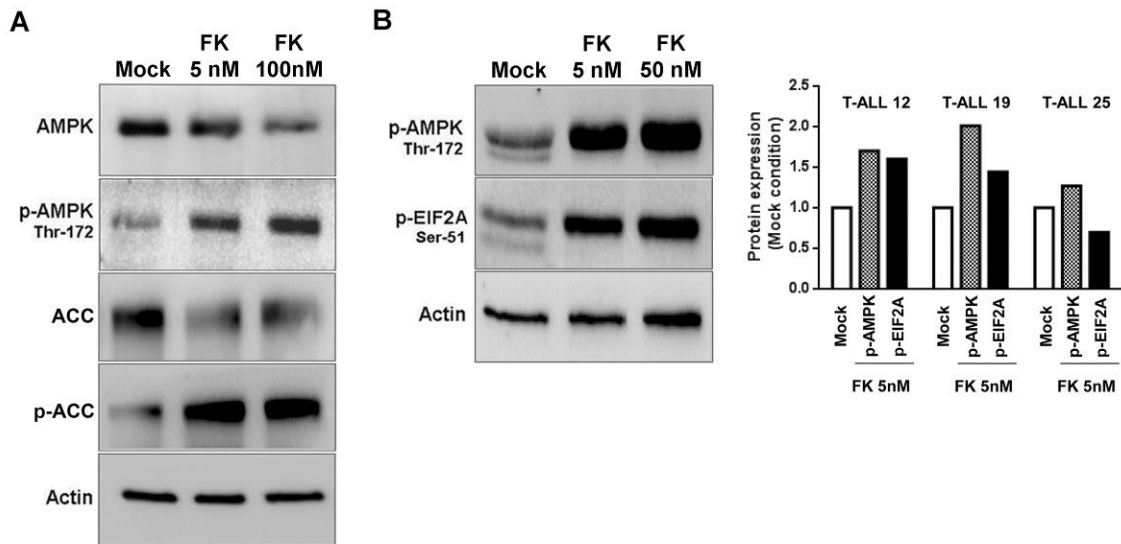


**Figure 13. FK866 activates AMPK**

**A**, Western blot analysis of the indicated proteins after 48 h treatment. One representative experiment out of three biological replicates. **B**, WB of PD T-ALL 12 as representative of T-ALL xenografts samples. Cells were treated with FK866 for 48 h. Histogram shows the densitometric analysis of p-AMPK and p-EIF2A in the three T-ALL xenografts (PD T-ALL 12, 19 and 25).

In order to link the observed inhibition of protein translation with the activation of a cell death program related to  $\text{NAD}^+$  depletion, we evaluated the effect of FK866 on the BCL-2 family of apoptosis regulator proteins. In particular, we checked the level of expression of B-cell lymphoma 2 (BCL-2), which is considered an important anti-apoptotic factor and was not affected by the treatment. By contrast, we observed a strong down-regulation of MCL1 (Induced myeloid leukemia cell differentiation protein). FK866 induced MCL1 down-regulation was dependent on proteasome activation as demonstrated by the rescue of its expression level by co-treatment with the proteasome inhibitor MG132 (**Figure 14**).

Previous studies have shown that inhibition of the mTOR/4EBP1 pathway lead to a reduction in the levels of this anti-apoptotic protein, with important implications for chemosensitivity in leukemia cells [129]. Moreover, stress-

induced phosphorylation of EIF2A was reported to be both essential and sufficient for the translational repression of MCL1 protein [130]. Notably, down-regulation of MCL1 through inhibition of translation has also been shown to occur as a consequence of AMPK activation in tumor cells [131].

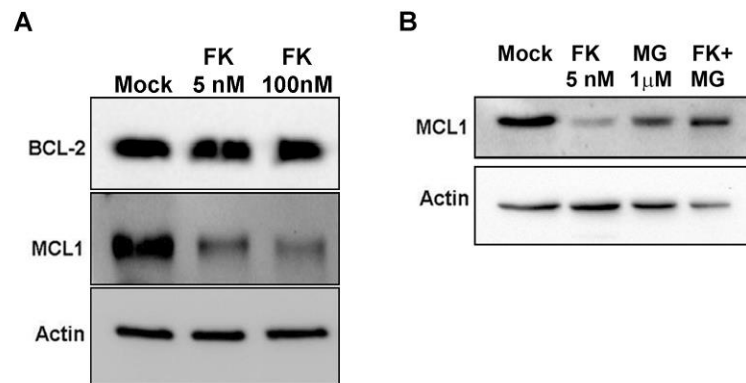


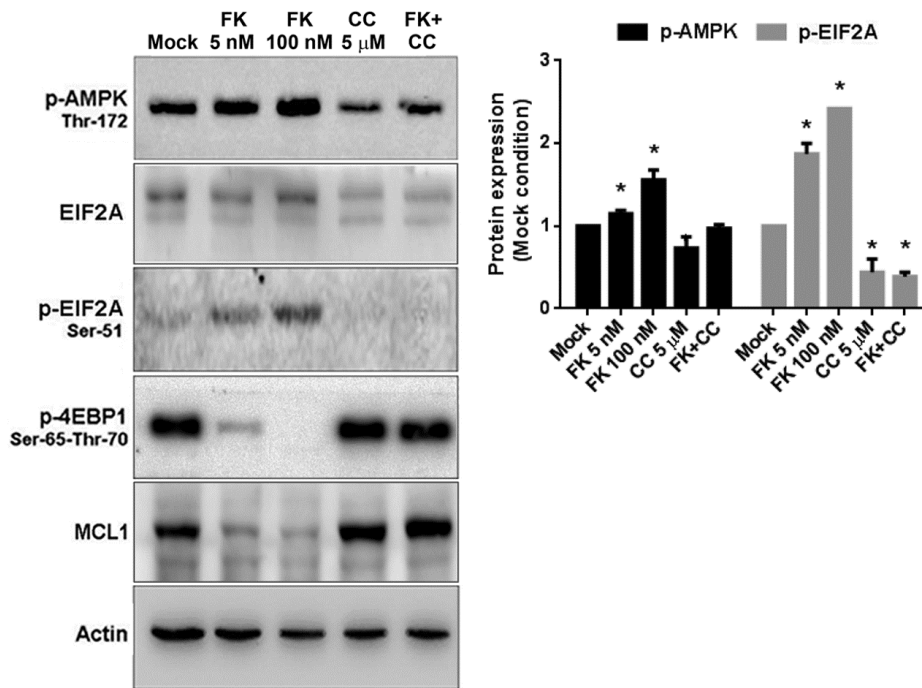
**Figure 14. FK866 down-regulates MCL1**

**A**, WB analysis of the anti-apoptotic proteins BCL-2 and MCL1 after 48 h of FK866 treatment. **B**, WB analysis of MCL1 in Jurkat cells treated with FK866 for 48 h and with the proteasome inhibitor MG132 (MG) 1  $\mu$ M for 24 h. MG132 was added after 24 h of FK866 treatment. A and B represent one experiment out of three biological replicates.

Taken together, these data indicate that AMPK might play a crucial role in the FK866-induced inhibition of translation and in cell fate determination through the modulation of an important member of the BCL-2 family of anti-apoptotic factors.

To verify AMPK implication in the observed protein synthesis inhibition and in the down-regulation of MCL1 level, we modulated its activity by using its inhibitor Compound C (CC). Co-treatment with FK866 and CC blocked AMPK activation and abolished EIF2A phosphorylation and 4EBP1 dephosphorylation. Therefore, interference with AMPK activation impacted on the translational block induced by FK866. Consequently, MCL1 level was rescued in the FK866-treated sample in which AMPK was blocked by Compound C (**Figure 15a**). The link between AMPK and the inhibition of translation *via* EIF2A phosphorylation at serine 51 in response to FK866 treatment was further confirmed by silencing both the alpha1 and the alpha2 catalytic isoforms of the kinase (**Figure 15b**).

**A**



**B**

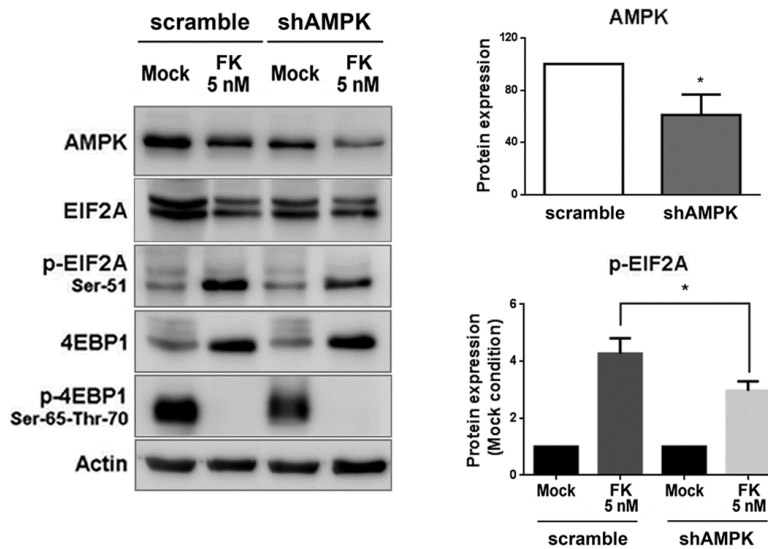


**Figure 15. AMPK is involved in FK866-induced translational inhibition**

**A**, Jurkat cells were treated with or without FK866 at the indicated doses in presence or absence of 5 μM Compound C for 48 h. Thereafter, cells were lysed and protein levels were revealed by immunoblotting. Histogram shows the densitometric analysis of p-AMPK and p-EIF2A. **B**, Cells were transduced with lentiviral particles containing scramble or shAMPK (targeting the α1 and the α2 subunit) and treated for 48 h with or without 5 nM FK866. WB analysis indicated 40% of AMPK silencing (p-value<0.05) and densitometric analysis shows the significant decrease of p-EIF2A in shAMPK Jurkat cells (p-value<0.03). A and B, mean and SD of a biological triplicate.

To sum up this first part of the results, FK866 was shown to be effective in blocking NAMPT activity in Jurkat cells and led to a decrease in NAD<sup>+</sup> and ATP cellular content. The induced stress activated the energetic sensor AMPK which in turn blocked protein synthesis and impacted above all on the initiation factor EIF2A, which readily responded to the metabolic insult.

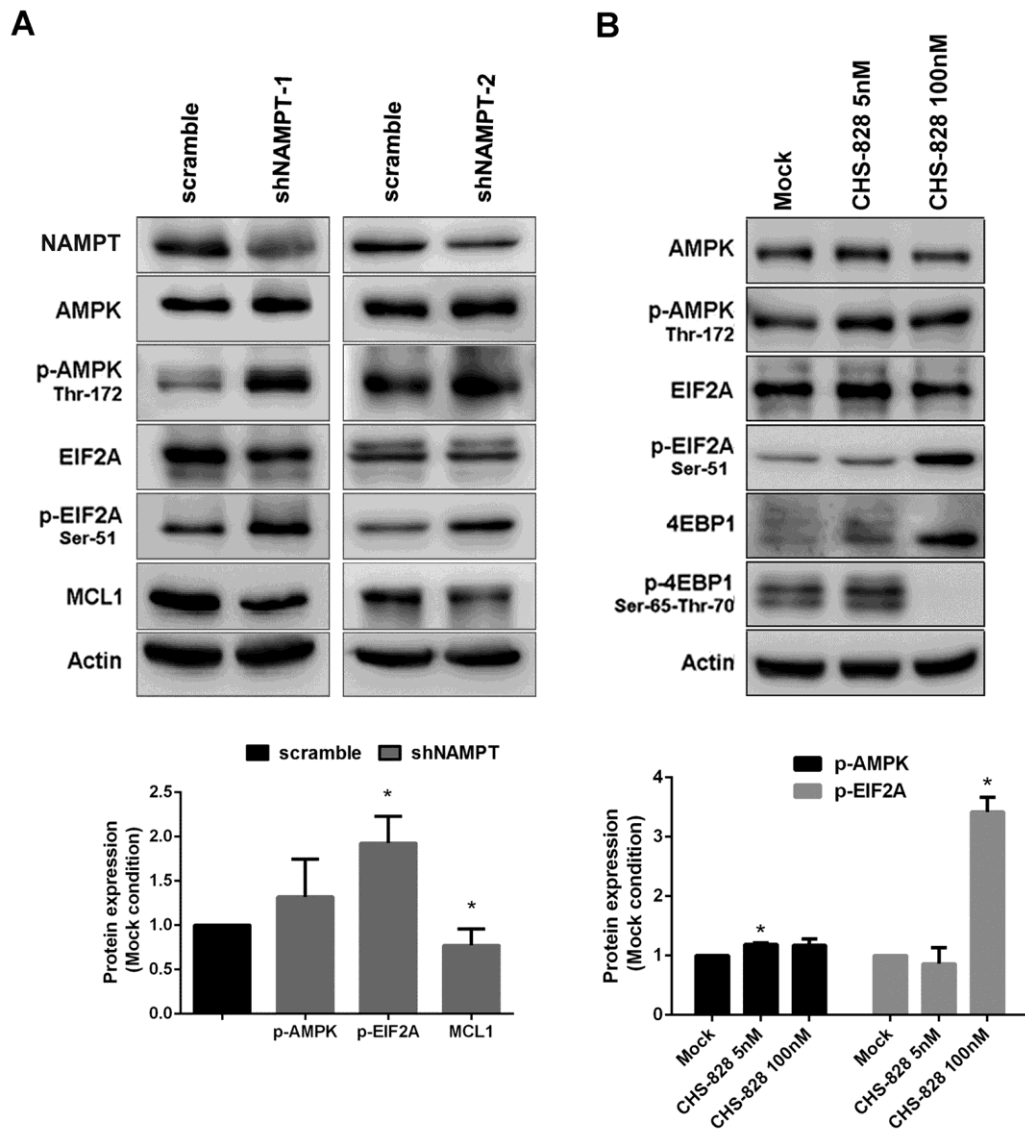


**Figure 16. NAMPT inhibition and genetic ablation induce translational arrest**

**A**, Jurkat cells were transduced with lentiviral particles expressing two NAMPT-silencing shRNAs (shNAMPT-1 and -2), resulting in 50% of NAMPT silencing ( $p < 0.001$ ). WB analysis of proteins compared to scramble condition together with densitometric analysis of the bands. **B**, Jurkat cells were treated for 48 h with CHS-828. The levels of total and phosphorylated proteins were evaluated by WB. Histogram shows the densitometric analysis. A and B, mean $\pm$ SD of a biological triplicate. (\* indicates  $p$ -value  $< 0.05$ ).

The close relationship between  $\text{NAD}^+$  depletion based on blocking its biosynthesis from nicotinamide due to NAMPT inhibition and the aforementioned molecular effects was proved by genetic ablation of the enzyme-coding gene. In NAMPT silenced Jurkat cells we observed again the activation of AMPK, the inhibition of EIF2A and the decreased level of expression of MCL1 (**Figure 16a**). Further support of the link between NAMPT inhibition and protein synthesis arrest came from experiments with CHS-828, a NAMPT inhibitor structurally different from FK866. Testing pre-toxic doses of the drug we reported an impaired translation, highlighted by the phosphorylation status of 4EBP1 and EIF2A (**Figure 16b**).

Thus, cells were reported to cope with the energetic stress connected to NAMPT inhibition and consequent  $\text{NAD}^+$  decrease by blocking energy-consuming pathways, primarily protein synthesis. In our model, AMPK played a major role in tuning the molecular response.

To test our hypothesis, we evaluated the effect on cell viability of impairing AMPK ability to sense metabolic fluctuations. This was performed by modulating the level of its upstream activator LKB1 (liver kinase B1). Jurkat cells were silenced for LKB1 by using two different short hairpin RNAs (shRNAs) expression vectors against its coding sequence. Silenced cells were more sensitive to FK866, proving that activation of AMPK mediated by LKB1 was protective against the metabolic stress (**Figure 17a**). The reliance on LKB1-AMPK pathway to resist the stress was further clarified through the use of two LKB1-deficient lung carcinoma cell lines, A549 and H460. We assessed cell viability after FK866 treatment, comparing cells stably expressing LKB1 due to retroviral vectors with those expressing the empty vector. Cells with a functional LKB1 were significantly more resistant to FK866. Furthermore, only these cells exhibited AMPK activation and EIF2A inactivation after treatment, linking the molecular mechanism which leads to protein translation arrest with cell survival (**Figure 17b**).

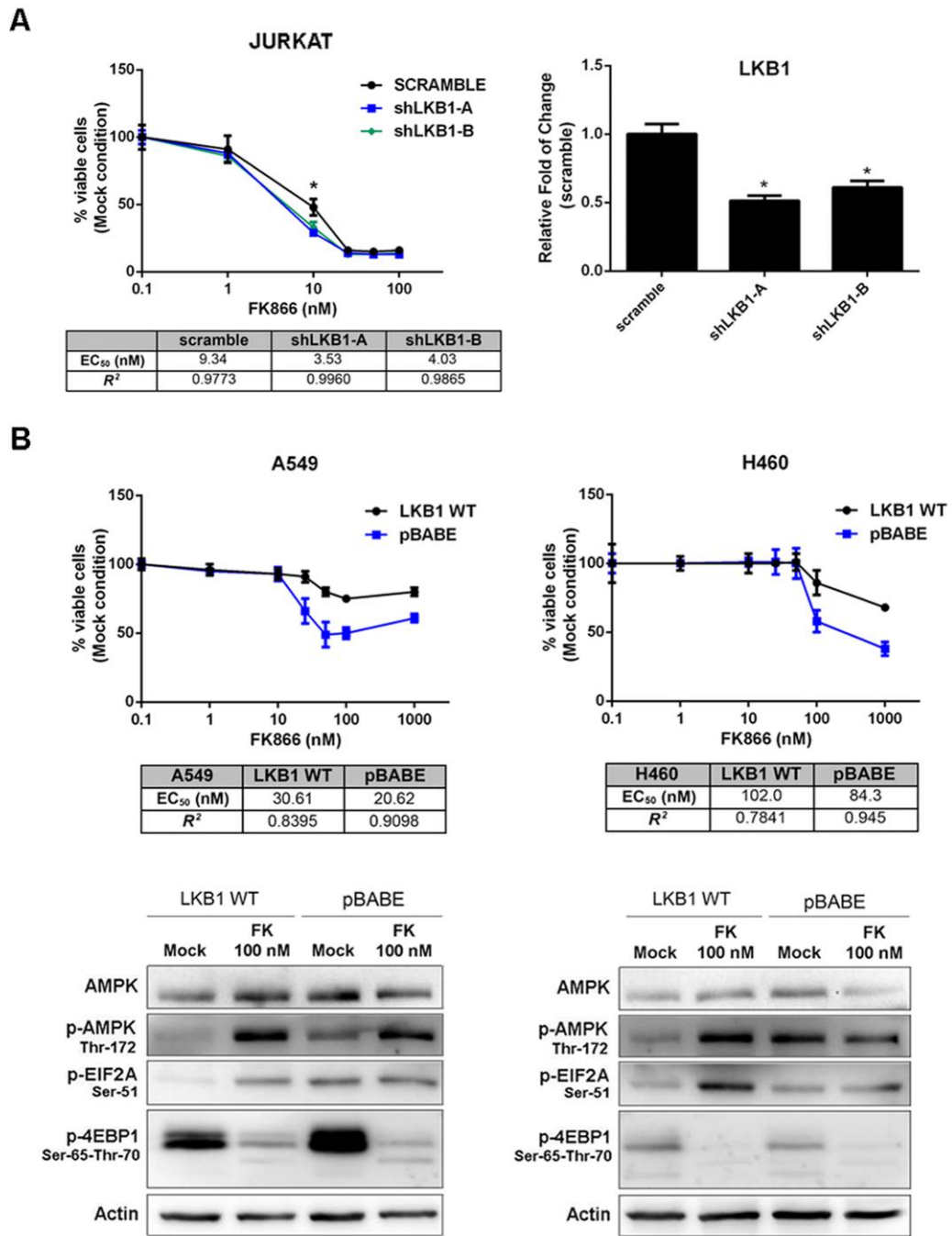


**Figure 17. LKB1 activates AMPK protecting cell from FK866-induced metabolic stress**

**A**, Jurkat cells were transduced for 72 h with shRNAs expressing the control sequence (scramble) or two LKB1-silencing shRNAs (shLKB1-A and -B) and then treated with FK866 for 48 h. Viability was measured by MTT assay in comparison with Mock (DMSO) condition (left). Expression level of LKB1 mRNA, evaluated through qPCR in Jurkat cells after 120 h of lentiviral transduction (right). **B**, A549 and H460 cells expressing LKB1 (LKB1 WT) or an empty vector (pBABE) were treated with FK866 for 48 h and cell viability was evaluated by MTT assay (upper part). WB analysis of A549 and H460 cells treated or not (Mock) with 100 nM FK866 for 48 h (lower part). A and B, mean and SD of a biological triplicate (\*, p-value<0.05).

In our model of cell response to stress, both AMPK and EIF2A play crucial roles in sensing metabolic alterations and readily respond to them to ensure cell survival. Importantly, we demonstrated for the first time that EIF2A inhibition was a specific hallmark of FK866, strictly related to its mechanism of action. We tested the effect of some traditional chemotherapeutic agents such as doxorubicin, dexamethasone, cisplatin and the mTOR inhibitor rapamycin on protein synthesis inhibition, by evaluating the phosphorylation status of EIF2A and 4EBP1. By comparing sub-lethal doses of the drugs, we reported that among all FK866 was the only compound effective on both EIF2A inhibition and 4EBP1 activation (**Figure 18a**). EIF2A acted as an early master regulator of cell fate in response to NAMPT inhibition, as suggested by its inhibitory phosphorylation at serine 51 after FK866 treatment.

To investigate the role of EIF2A inhibition with respect to cell viability, we compared FK866-treated cells expressing the wild type protein, a nonphosphorylatable mutant (S51A) and a phosphomimetic mutant (S51D). Cells expressing the nonphosphorylatable mutant exhibited a stronger cell death response, indicating that the phosphorylation of EIF2A is protective against the induced metabolic stress (**Figure 18b**). For this reason, we investigated more deeply EIF2A-dependent processes, which acquire fundamental relevance in explaining the mechanism of action of NAMPT inhibitors. Among them, we checked for the activation of the unfolded protein response (UPR) and specifically we evaluated the level of BiP, a chaperone protein and a master regulator for ER stress able to control the activation of UPR signaling. After FK866 treatment mRNA level of BiP gene was increased (**Figure 18c**).

In conclusion, we reported that leukemia cells activated a specific molecular response to contrast NAD<sup>+</sup>-depletion *via* NAMPT inhibition. Major players of the response are AMPK, which inhibits protein translation, and EIF2A that is involved in the determination of cell fate and strictly related to the stress response.

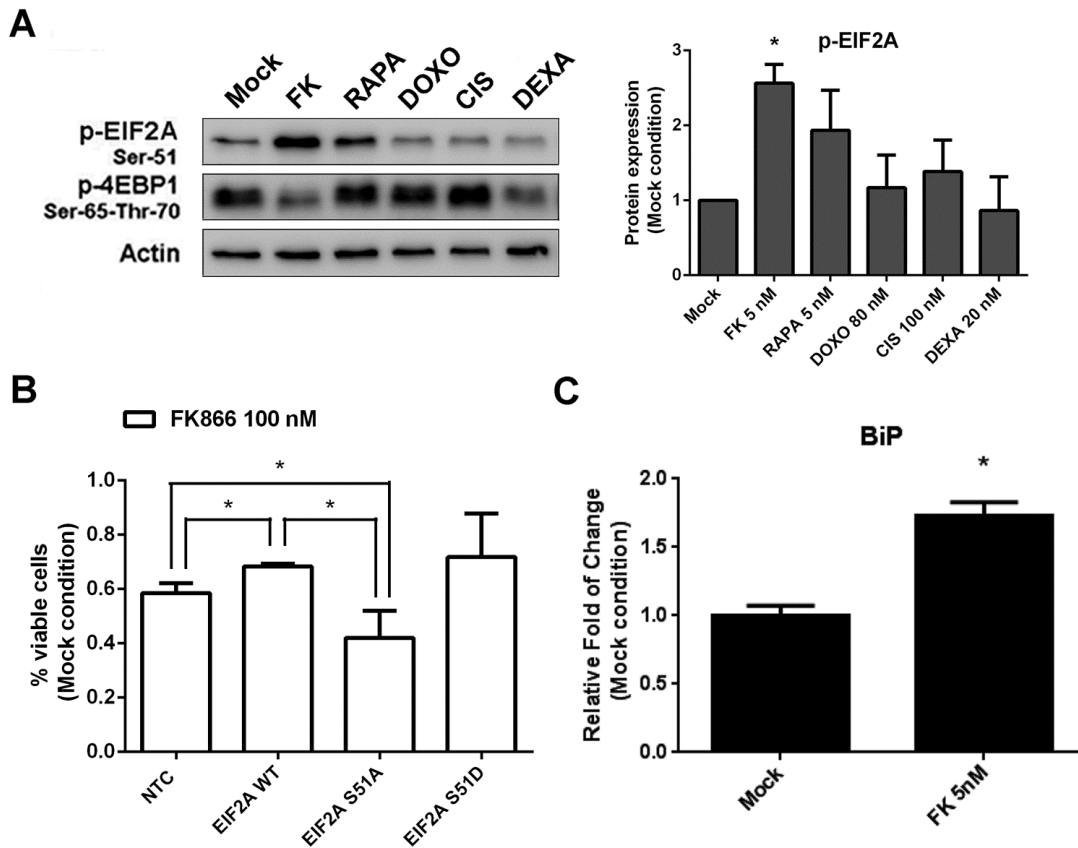


**Figure 18. EIF2A inhibition by FK866 results in protective effects against stress**  
**A**, Jurkat cells were treated for 48 h with FK866, Rapamycin (RAPA), Doxorubicin (DOXO), Cisplatin (CIS) and Dexamethasone (DEXA). The level of p-EIF2A and p-4EBP1 was evaluated. Histogram shows the densitometric analysis of p-EIF2A (\*indicates p-value <0.05). **B**, A549 cells viability after 48 h of treatment with FK866 100 nM in un-transfected (NTC) cells and transfected with EIF2A wild type, EIF2A-S51A, EIF2A-S51D (p-value<0.05). **C**, Expression level of BiP mRNA evaluated in Jurkat cells after 48 h of treatment with FK866 5 nM (\*, p-value<0.0005). A-C, mean and SD of a biological triplicate.

Importantly, we further confirmed a key role for ER stress in the mechanism of action of FK866 and for the activation of UPR in response to the metabolic stress induced by NAMPT inhibition by testing the drug in combination with efflux pump inhibitors.

Indeed, FK866 was frequently reported to exhibit limited cytotoxicity against primary leukemia cells. Therefore, its applicability as a single agent is limited. Common cause of treatment failure is the insurgence of multidrug resistance (MDR), which is strictly related to over-expression of membrane transport proteins. Among them, P-glycoprotein 1 (Pgp, encoded by MDR-1/ABCB1

gene) is one of the key factors involved in extruding drugs across the plasma membrane thus reducing their intracellular concentration and their efficacy [132]. High level of PgP has been frequently observed in hematological malignancies and the expression correlated with poor clinical outcome in Acute Myeloid Leukemia [133]. Therefore, PgP inhibitors represent an attractive approach for cancer treatment. Natural and synthetic identified inhibitors include calcium channel blockers (verapamil and nifedipine), indole alkaloids (reserpine), steroids (progesterone and tamoxifen), the immunosuppressive agents cyclosporin A (CsA), and rapamycin and the second-generation Pgp inhibitor PSC-833 (valspodar).

In our work, we tested the combination of FK866 and PgP inhibitors in leukemia cells, in order to provide a biological rationale for exploiting this approach in the treatment of hematological malignancies.

Firstly, we demonstrated that PgP inhibitors such as CsA and verapamil synergistically potentiated FK866-induced cytotoxicity in leukemia cells, whereas normal CD34<sup>+</sup> hematopoietic progenitor cells and healthy leukocytes were not affected. FK866 was demonstrated to be a PgP substrate, which decreased the drug intracellular concentration. Testing metabolic effects of the combination of FK866 and PgP inhibitors, we reported the exacerbation of cell demise induced by NAMPT inhibition. Drug combination enhanced NAD<sup>+</sup> depletion, ATP shortage and induced  $\Delta\Psi_m$  dissipation (mitochondrial transmembrane potential).

The mechanism underlying the interaction between FK866 and PgP inhibitors, which sensitized leukemia cells to NAMPT inhibition, was further investigated. Interestingly, we reported the involvement of ER stress and UPR in this synergy, confirming that FK866 negatively affects endoplasmic reticulum (ER) physiology.

ER stress inhibition with the chemical chaperone 4-phenyl butyric acid (4-BPA) significantly reduced the cytotoxic effects of FK866, CsA, and of the two combined agents in OCI/AML3 and MEC.1 cells, as well as in primary B-CLL cells (**Figure 19a**).

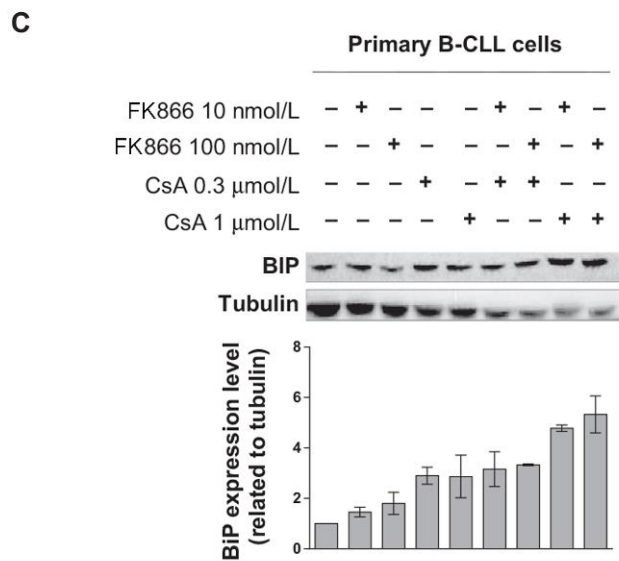
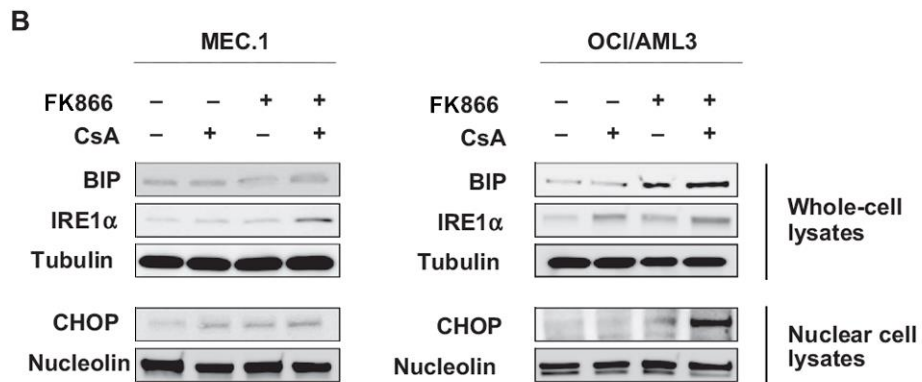
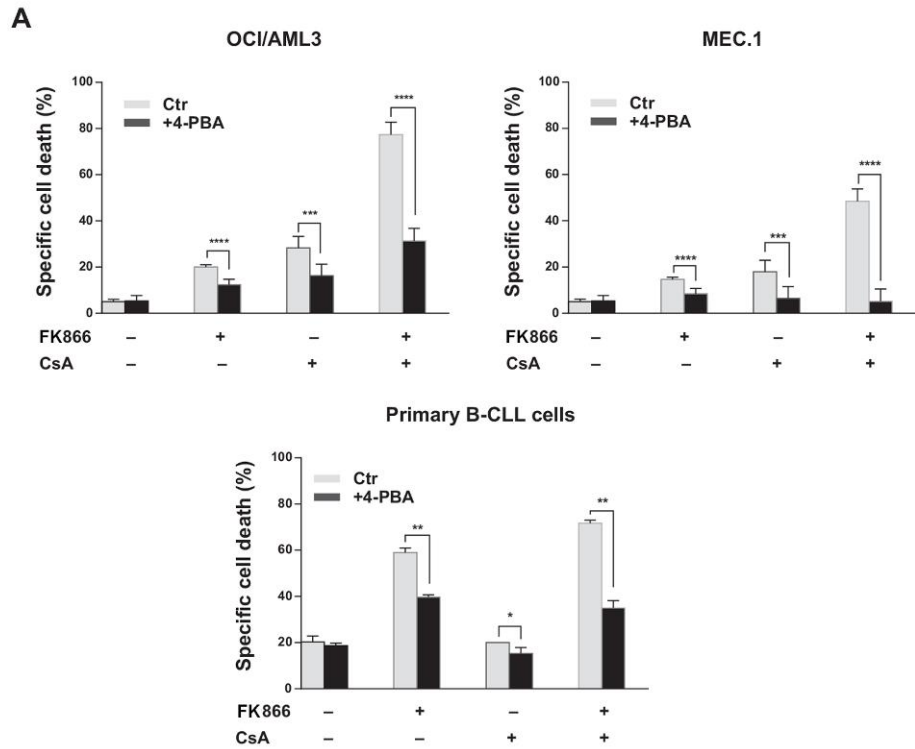


**Figure 19. CsA plus FK866 antileukemic effect is mediated by ER stress–dependent UPR signaling**

**A**, OCI/AML3, MEC.1 or primary B-CLL cells were preincubated for 2 h with or without 4-phenyl butyric acid (4-BPA). Thereafter, leukemia cells were treated with FK866 (3 nmol/L) for 48 h; CsA (1  $\mu$ mol/L) was then added for additional 48 h followed by cell death analysis using PI staining and FACS analysis. Data represent mean and SD of triplicate samples (\*,  $p < 0.01$ ; \*\*,  $p < 0.002$ ; \*\*\*,  $p < 0.0002$ ; \*\*\*\*,  $p < 0.0001$ ). **B**, OCI/AML3 or MEC.1 cells were pretreated with or without FK866 (3 nmol/L) for 24 h, and then CsA (1  $\mu$ mol/L) was added for additional 24 h. WB analysis of cellular fractions was performed using anti-BIP, anti-IRE1 $\alpha$ , anti-CHOP and anti-tubulin or anti-nucleolin antibodies as fraction specific loading controls. **C**, B-CLL primary cells were treated with FK866 (10–100 nmol/L), CsA (0.3–1  $\mu$ mol/L), or combined therapy for 48 h. Cell lysates were subjected to Western blot analysis, using anti-BIP and anti-tubulin antibodies. Blots shown are representative of three independent experiments and histogram shows the densitometric analysis (mean $\pm$ SD).

Moreover, by investigating ER stress related markers we observed an increase of IRE1 $\alpha$ , C/EBP-homologous protein (CHOP) and BIP levels. In cells that were cotreated with FK866 and CsA increase was much stronger as compared with the single-agent treatments (**Figure 19b**). A marked increase in the master regulator of the UPR BIP was also detected in primary B-CLL cells treated with FK866 and CsA (**Figure 19c**).

These findings confirmed a key role for ER stress in the mechanism of action of FK866 and indicated a novel role for UPR in mediating the antitumor activity of FK866 in combination with Pgp inhibitors in leukemia cells.

## 2. Drug resistance to FK866

Insurgence of drug resistance during chemotherapy is a common occurrence and is a major cause of cancer relapse and consequent failure of therapy. It can occur as either *de novo* or acquired resistance following therapy. For several targeted therapies the development of target-specific drug resistance has been described.

### 2.1 Drug resistance to NAMPT inhibitors

Regarding NAMPT inhibitors, pharmacoresistance was reported in HCT-116 colon cancer cell line for GMX1778. A resistant clone presenting an acquired drug resistance was derived through serial selection with increasing sublethal concentrations of the drug. Sequencing of the NAMPT gene in the GMX1778-resistant cell line revealed a single point mutation of amino acid 217, which is located near the active site of NAMPT, from glycine to arginine (G217R). The mutation resulted in an IC<sub>50</sub> value 2500-fold higher than the one calculated in parental cells and was not directly related to changes in NAMPT expression levels. Over-expression of mutated NAMPT (G217R) in HEK-293-T cells increased intracellular NAD<sup>+</sup> levels by 80%, inducing resistance to GMX1778 cytotoxicity [134].

Additionally, mutations in the NAMPT gene (mapped to H191R, D93del and Q388R) conferring drug resistance to other NAMPT inhibitors, including FK866 and CHS-828, were reported in resistant cell lines developed from HCT-116 and in NYH, human small cell lung carcinoma cell line. Specifically, these mutations structurally modified the inhibitor-binding pocket (G217R and H191R), dumping drug efficacy. The resistant cell lines showed tumorigenicity in xenograft mouse models and *in vivo* resistance [135].

More recently, six mutations in the NAMPT gene have been reported in GNE-618 resistant cells derived from RD (rhabdosarcoma), MiaPaCa-2 (pancreatic cancer) and NCIH460 (non-small cell lung cancer) cell lines. In addition to the previously identified G217R and D93del mutations, G217A, G217V, S165F and S165Y were reported as novel. Resistant cell lines were observed to be 10 to 1000-fold less sensitive to the NAMPT inhibitor GNE-618 with respect to

parental ones. However, no cross resistance to GMX1778 and FK866 was detected, suggesting a molecule specific NAMPT resistance.

Interestingly, tumor xenografts established from NCI-H460 cells presenting the S165Y mutation were resistant to high doses of GNE-618 [136].

To date, tumor cell resistance to NAMPT inhibitors has been ascribed to point mutations either proximal or distal to the enzyme substrate binding sites and a reactivation or over-expression of alternative NAD<sup>+</sup> biosynthesis pathways has never been reported.

## 2.2 Development of FK866-resistant Jurkat cell line

The development of drug-resistant cancer cell lines is an helpful approach for investigating the mechanisms of cytotoxicity and resistance to antitumor agents. Acquired resistance can be studied by inducing resistance *in vitro* growing cells in the presence of increasing concentrations of drug.

We have developed FK866-resistant models from Jurkat cells, by using a stepwise increase in treatment dose [137]. The surviving daughter resistant cells were then compared to the parental sensitive cells assessing cell viability and defining EC<sub>50</sub>. Calculated EC<sub>50</sub> after 48 hours of treatment with FK866 was 9.8 μM for the resistant cells, whereas an EC<sub>50</sub> of 5.4 nM could be estimated for parental ones (2000-fold lower). Moreover, resistant cells were also insensitive to long-term (5-day) treatment with 500 nM of FK866 (**Figure 20a**).

In FK866-resistant cells, the levels of intracellular NAD<sup>+</sup> and ATP were estimated after treatment in comparison with the parental cells, in order to assess the efficacy of the drug and to evaluate the induced metabolic stress. NAD<sup>+</sup> levels in the resistant cells were measured as 50% of the untreated sample in the parental cell line. On the contrary, however, FK866 treatment did not heavily impact on NAD<sup>+</sup> content in the resistant model (**Figure 20b**). With respect to ATP, intracellular levels were comparable to the untreated sample in the parental cells and completely recovered also upon treatment with FK866 (**Figure 20c**).

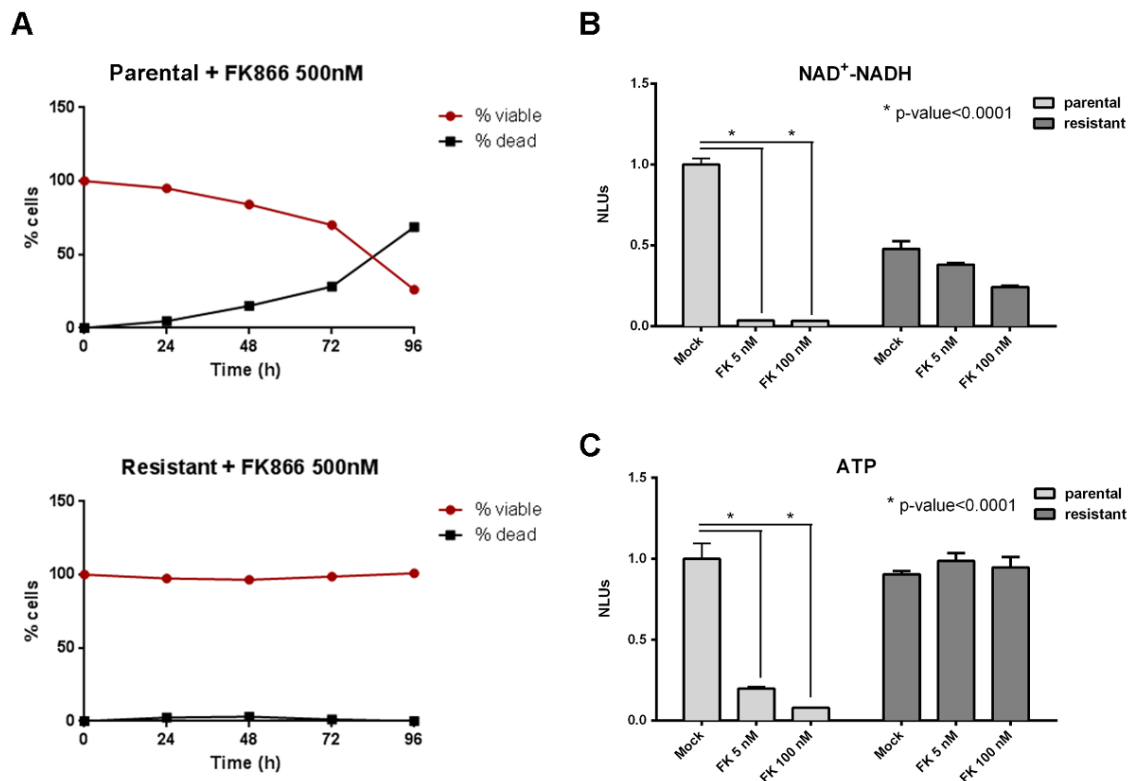


**Figure 20. Isolation and metabolic characterization of FK866-resistant cells**

**A**, Evaluation of Jurkat cells viability in parental and resistant cells during long-term treatment with FK866. Calculation is based on Trypan blue exclusion of dead cells. **B** and **C**, NAD<sup>+</sup>-NADH and ATP intracellular levels were measured in parental and resistant Jurkat cells after drug treatment. Values are normalized to untreated parental cells (Mock). Mean and SD of three independent experiments (\*, p-value<0.0001).

As already mentioned, in reported examples from the literature FK866 resistance is due to mutations of NAMPT gene dumping drug efficacy.

In our case, exclusion of mutations in NAMPT gene was performed by sequencing its coding region in resistant and parental cells. Interestingly, Jurkat cells have thus developed different mechanism to elicit FK866 pharmacoresistance.

Importantly, we observed that NAMPT gene expression was significantly down-regulated by 50% in the resistant model (**Figure 21a**). Moreover, the acquired mechanism of resistance mutation-independent conferred cross-resistance to another NAMPT inhibitor, CHS-828 (**Figure 21b**).

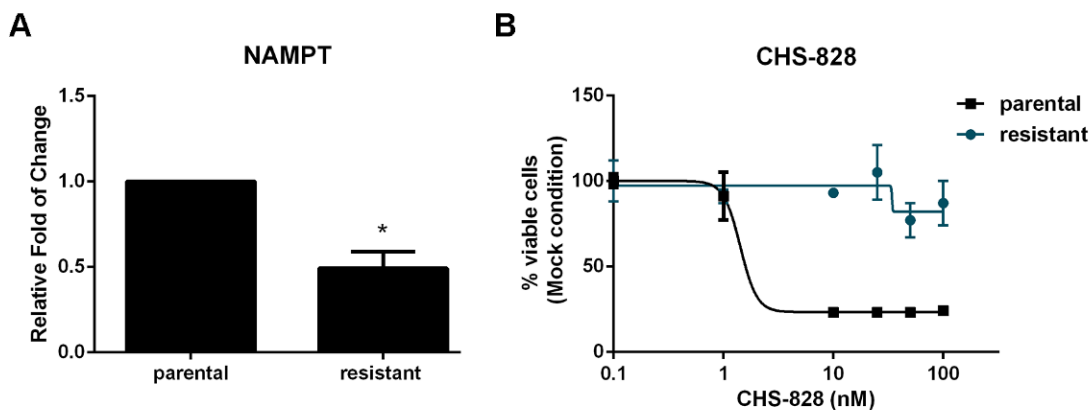


**Figure 21. NAMPT mRNA level in resistant cells and cross-resistance to CHS-828**

**A**, Basal expression level of NAMPT revealing a 50% decrease in FK866-resistant cells compared with parental cells. Mean and SD of three independent experiments (\*, p-value<0.0001). **B**, Viability assessment through MTT assay of parental and FK866-resistant cells in response to a 48 h CHS-828 treatment.

## 2.2 Characterization of the resistant model: translational control

In order to elucidate the stress response of our resistant model in response to FK866, we checked markers of translational arrest that represents the early response in the parental cells. In Jurkat parental cells we identified a general arrest of translation after FK866 treatment, which involves the activation of AMPK probably due to the decrease in ATP intracellular content. In the resistant model drug treatment did not activate AMPK and no inhibition of translation mediated by mTOR/4EBP1 or EIF2A was reported (**Figure 22a**).

The status of phosphorylation of these key pathways involved in translation was a clear indication that protein synthesis resumed, as revealed also by detection of AHA incorporation in the nascent proteins after FK866 treatment of resistant cells (**Figure 22b**).

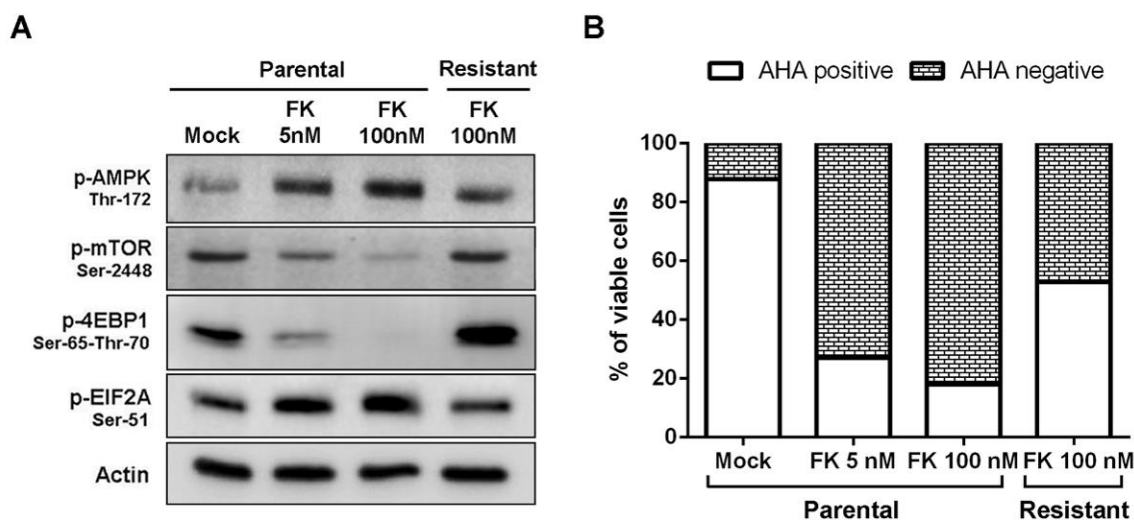


**Figure 22. Protein translation resumed in resistant cells**

**A**, Western Blot analysis of parental and resistant cells after treatment with FK866 for 48 h. Representative panel of three independent experiments **B**, Protein synthesis was monitored in parental and resistant Jurkat cells by AHA incorporation after 48 h of treatment with FK866. The histogram quantifies protein synthesis in the viable cell population.

### 2.3 Drug sensitivity and resistance testing (DSRT)

Isolated FK866-resistant Jurkat cells are in summary able to recover  $\text{NAD}^+$  and ATP levels and to restart translation and are insensitive to drug treatment. However, acquired resistance could confer sensitivity to other drugs and we searched for new drug vulnerabilities and druggable targets through an high-throughput screening.

For this purpose, I spent a period abroad in Helsinki at FIMM (Institute for Molecular Medicine Finland) in the Laboratory of Individualized Systems Medicine under the supervision of Olli Kallioniemi.

During my visit I performed high throughput drug sensitivity and resistance testing (DSRT) with FK866-resistant Jurkat cell line models that we have established. In particular, I tested parental cells in comparison with 3 different FK866-resistant models previously derived by treating Jurkat cells with increasing doses of the drug: 10, 40 and 100 nM FK866 resistant.

The DSRT platform is based on an oncology compound collection, that covers the active substances from the majority of FDA/EMA–approved anticancer drugs ( $n = 123$ ), as well as emerging investigational and preclinical compounds ( $n = 64$ ) covering a wide range of molecular targets (**Supplementary Table**

**S5).** Briefly, drugs were pre-plated in 384-well plates in five different concentrations in a 10 000-fold concentration range, where Jurkat cells were added and then incubated for 72 h. After measuring cell viability, dose-response curves were generated on the basis of the viability readouts and drug responses were compared across the samples by calculation of the Drug sensitivity scoring (DSS), (see methods and [125] for details).

Parental cells were screened and compared with FK866-resistant models in order to identify new drug vulnerabilities and co-resistance. DSRT aimed at discovery of drugs able to kill resistant cells and identification of co-resistance.

Different concentrations of Jurkat parental cells and the 3 resistant models were initially seeded in 384-well plate to determine the number that ensures each sample to be in growth phase at the end of the assay. Cell viability was assessed after 72 hours and by generated growth curves we selected the optimal seeding density, which was determined as 4000 cells/well (**Figure 23a**). DSRT was then performed on parental and resistant cells. Following the drug testing experiment, we assessed the quality of the screening by measuring Z' factors and strictly standardized mean differences (SSMD). Z' values lied between 0.5 and 1, indicating that the screening performance was good. Curve fitting algorithm was thereafter applied and DSS was calculated.

X-Y plots (**Figure 23b**) represent the correlation of the DSRT results of Jurkat parental and resistant 10 nM, 40 nM and 100 nM. DSS of FK866 decreased in the 3 models as expected (**Figure 23c**). Plots illustrate that resistant cells gained sensitivity to Bryostatins 1 among more than 300 compounds tested, a protein kinase C (PKC) activator.

Resistant 10 nM lost sensitivity to danusertib, an Aurora kinase inhibitor, whereas resistant 40 and 100 nM acquired resistance to the synthetic glucocorticoids (GCs) dexamethasone and methylprednisolone (**Figure 23c**).

Because of the low number of identified cross-resistant drugs, we can possibly exclude insurgence of multidrug resistance (MDR) in the FK866-resistant model.

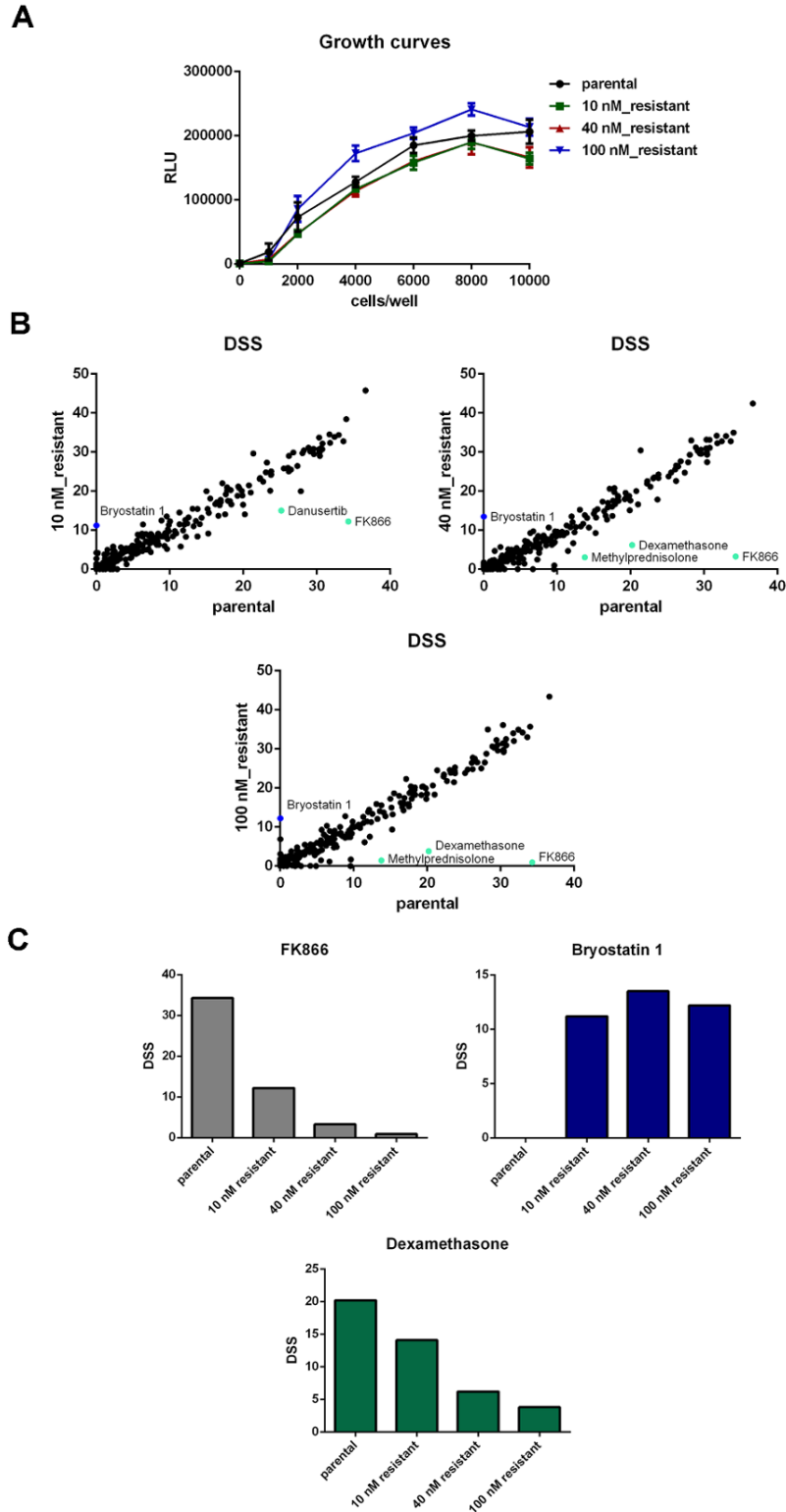


**Figure 23. Growth curves and drug sensitivity scoring (DSS) of resistant cells**

**A**, Growth curves of Jurkat parental and FK866-resistant models. Cells were seeded in 384-well plate and cell viability was measured after 72 hours using CellTiter Glo. **B**, Correlation of the DSRT results of Jurkat parental and resistant 10 nM, 40 nM and 100 nM. Drugs for which the DSS decreased greater than 10 from parental cells are marked in green, drugs for which the DSS increased greater than 10 in resistant cells are marked in blue. **C**, DSS (Drug Sensitivity Scoring) of FK866, Bryostatin 1 and Dexamethasone in the 4 screened samples.

The identified co-resistance to dexamethasone and methylprednisolone are of particular interest because these drugs are immunomodulatory reagents, related to GR (Glucocorticoid Receptor) and glucocorticoid resistance is a major driver of therapeutic failure in T cell acute lymphoblastic leukemia (T-ALL). Notably, induced myeloid leukemia cell differentiation protein MCL-1 over-expression was involved in conferring resistance to glucocorticoids in ALL cells. Over-expression of MCL1 sequestered the BH3-only protein BIM and thus rendered cells unable to activate the pro apoptotic signaling and resistant to GC-induced apoptosis [138]. In addition, inhibition of translation through the mTOR/4EBP1 pathway was reported to reduce the levels of the anti-apoptotic protein MCL1 [129].

In Jurkat cells we identified a translational arrest and reported a decrease in the level of expression of MCL1 (**Figure 14**). Our FK866-resistant model was able to restart translation and treated cells expressed MCL1 at the level of the untreated control (**Figure 24a**). Based on this, we hypothesized that dexamethasone cross-resistance could be strictly related to the observed levels of the anti-apoptotic protein MCL1, as already reported in ALL cells, and could depend on the re-activation of mTOR signaling.

Finally, in contrast to the identified cross-resistance to dexamethasone in resistant models, Jurkat parental cells were sensitive to the drug with a calculated  $EC_{50}$  of 50 nM at 48 hours.

From genome-wide gene expression analyses we observed that the GR signaling pathway was affected by FK866 administration (**Figure 11**), therefore we investigated how FK866 could possibly affect GR-regulated homeostasis.

We evaluated whether FK866 could increase the activity of dexamethasone in Jurkat cells and exacerbate its apoptotic function. In fact, dexamethasone is a well-known activator of the Glucocorticoid Receptor and an inducer of T-ALL cells death [139].

By exposing Jurkat cells to single or combined equipotent concentrations of FK866 and dexamethasone (nanomolar ratio 1:5), we observed that combined drug treatment resulted in a strong synergistic interaction causing cell death (**Figure 24b**) with a Combination Index (CI) value of 0.00270 for cytotoxicity on 50% of cells, as estimated by the Chou and Talalay statistics [126].

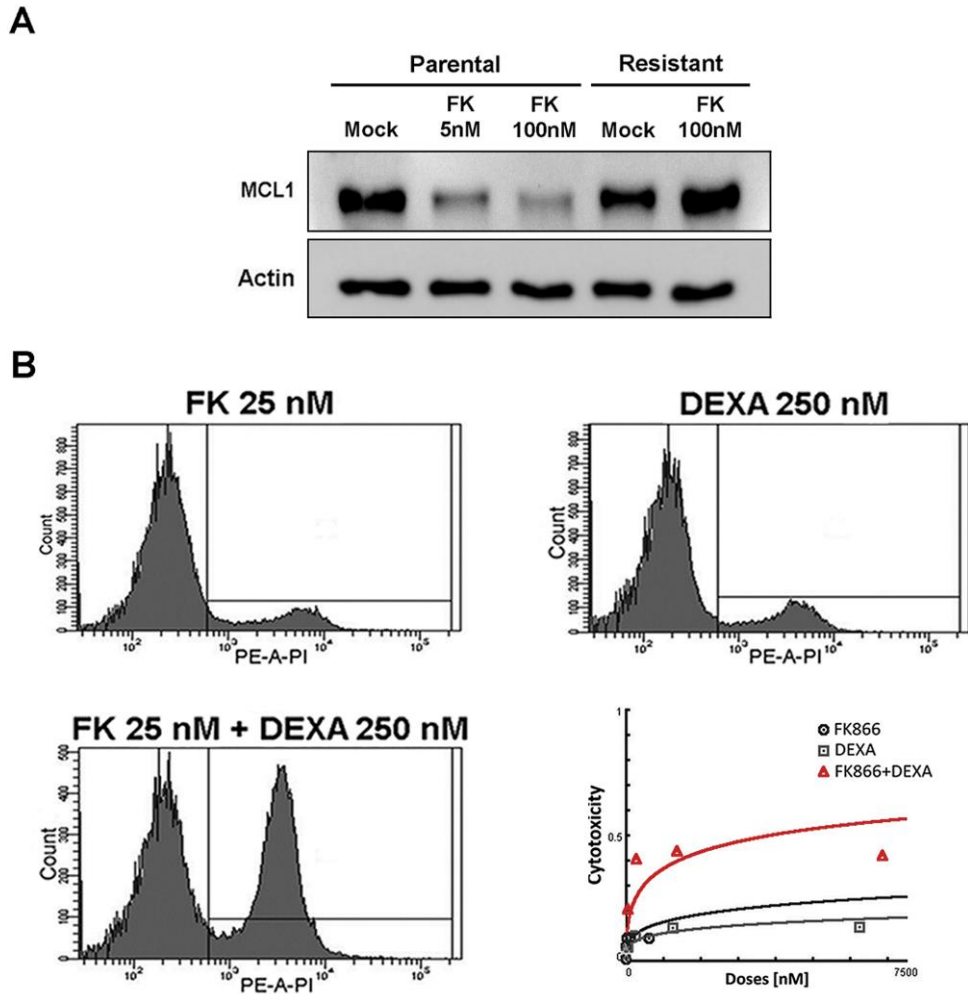


**Figure 24. FK866 shows a strong synergistic interaction with Dexamethasone**

**A**, Western Blot analysis of MCL-1 levels in parental and resistant cells after a 48 h treatment with FK866. Representative panel of three independent biological replicates. **B**, Jurkat cells were treated for 48 h, alone or in drug combination, with equipotent doses of FK866 and Dexamethasone and viability was determined by PI staining and flow-cytometry. Dose-response curves were analyzed by CompuSyn software V1.0 following the Chou and Talalay statistics. The combination showed a significant synergistic interaction with a CI value of 0.00270 for cytotoxicity on 50% of cells.

#### 2.4 Characterization of the resistant model: transcriptional regulation

Genetic and epigenetic changes, resulting in gene expression reprogramming, play a major role in allowing adaptation to the presence of anticancer drugs. Modifications might occur at DNA or RNA level.

We performed gene expression microarray analysis on RNA extracted from resistant and parental cells treated or not with the drug. Comparing the number of DEGs, FK866 treatment induced little variations on resistant cells at

transcriptional level. DEGs in parental cells were 4 times more. Interestingly, the expression level of thousands of genes were different in resistant cells with respect to parental (**Figure 25a**).

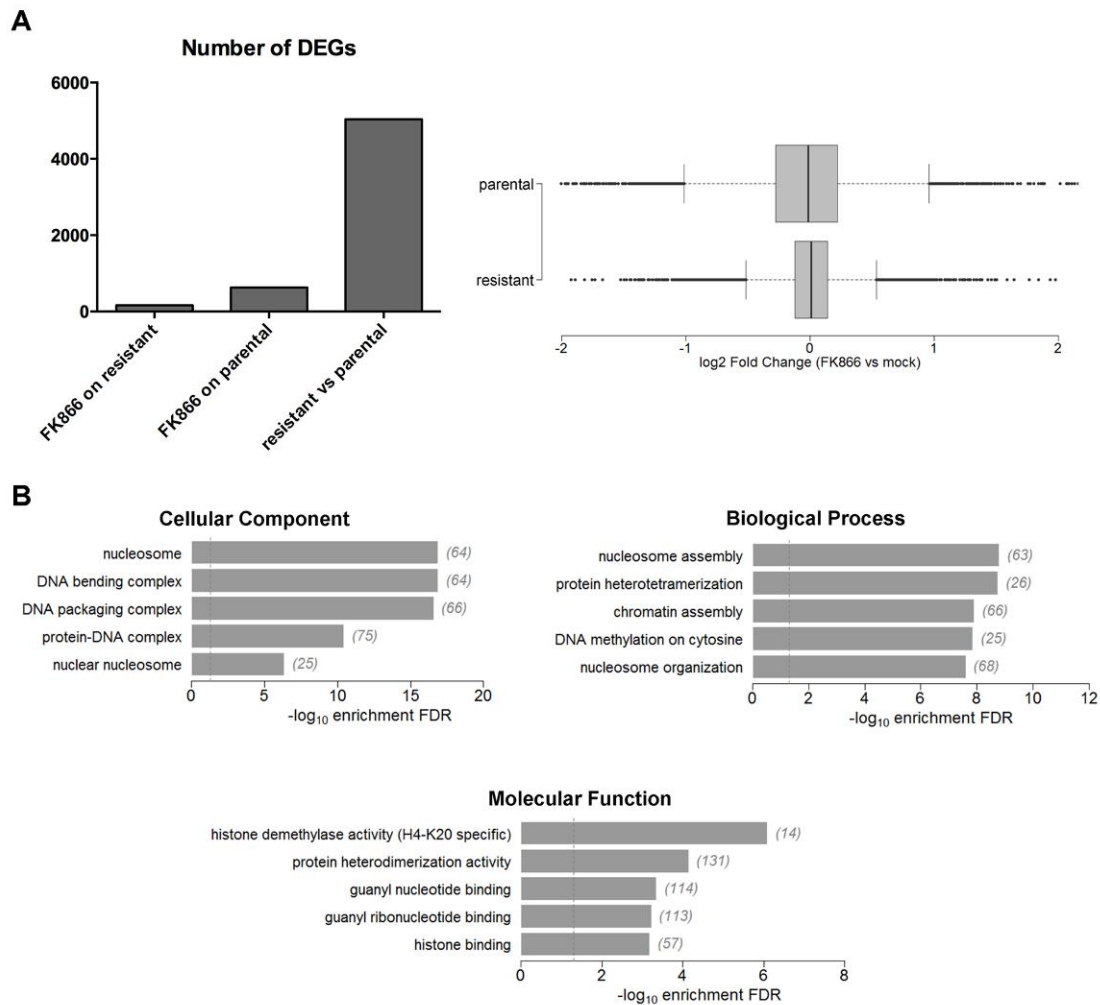


**Figure 25. Gene expression analysis in FK866-treated resistant cells**

**A**, Histogram shows the number of differentially expressed genes selected according to a double threshold on log<sub>2</sub> FC (absolute value > 0.75) and moderated t-test p-value (<0.05). On the right, box whisker plots of pairwise gene expression comparisons, based on log<sub>2</sub> Fold changes. Comparing the sparseness of the distributions, variations induced by FK866 on resistant cells have less magnitude than variations induced by FK866 on normal cells. **B**, Barplots displaying the top 5 enriched Gene Ontology terms for the resistant versus parental comparison. Enrichments are scored according to Fisher Benjamini-Hochberg corrected p-value, displayed in the x axis. Enrichment significance threshold is displayed as a vertical dashed line. The number of DEGs associated to each term is specified next to the corresponding bar, between round brackets.

Among these 5000 genes differentially expressed (DEGs) in parental vs resistant cells, we performed bioinformatics analyses (Gene Ontology) that in

the future will be crossed with their biological function in order to select targets for validation (by real-time PCR, Western blotting). Top 5 enriched Gene Ontology terms related to the comparison between parental and resistant cells highlighted a possible correlation between FK866-resistance and nuclear DNA organization, particularly influencing the nucleosome assembly. Notably, an enriched term in the molecular function ontology referred to histone demethylation. Taking together, these data suggest that resistance to FK866 might involve a different global transcriptional regulation, allowing cells to survive the metabolic stress (**Figure 25b**).

Interestingly, in FK866-resistant models Indoleamine 2,3-dioxygenase (IDO1) gene expression was found to be up-regulated (abs log<sub>2</sub> FC >3). IDO1 is the first and rate-limiting enzyme of tryptophan catabolism through kynurenine pathway, which might support an alternative NAMPT-independent pathway of NAD<sup>+</sup> synthesis.

## DISCUSSION

Alterations in NAD<sup>+</sup> levels have a powerful metabolic impact on cells, especially on cancer cells. During malignant transformation in fact their cellular metabolism undergoes multiple molecular and metabolic adaptations to support aberrant cell growth and survival, resulting in a significantly higher energy demand and NAD<sup>+</sup> turnover that sustain rapid proliferation, relative genomic instability, continuous DNA repair, increased aerobic glycolysis and increased activity of NAD<sup>+</sup>-dependent enzymes. NAD<sup>+</sup> is therefore a key metabolite required as redox co-factor and as substrate for NAD<sup>+</sup>-dependent enzymes, such as poly (ADP-ribose) polymerases (PARPs), ADP-ribosyl cyclases/CD38 and sirtuins, which continuously consume NAD<sup>+</sup> and release nicotinamide.

In mammals, the nicotinamide phosphoribosyltransferase NAMPT is a main regulator of the intracellular NAD<sup>+</sup> pool, constantly recycling NAD<sup>+</sup> from nicotinamide [27]. Because of its relevance in NAD<sup>+</sup> maintenance, it is often over-expressed in tumor cells.

In hematological malignancies, higher NAMPT expression levels were reported in a wide range of cell lines and patient samples [75], [76], [140], [141]. An array-based comparative genomic hybridization analysis of a dataset of hematological cancer cells (derived from the Cancer Cell Line Encyclopedia database, [142]) showed focal amplification of the NAMPT locus (mapping on 7q22.3) and NAMPT transcript levels were found to correlate with the DNA copy number. Moreover, high NAMPT expression in hematologic malignancies was significantly associated with poor overall survival and adverse prognosis [143].

Thus, altogether, these data support the notion that NAMPT plays an important role in the pathophysiology of hematologic malignancies and that it represents an attractive therapeutic target.

Notably, NAMPT inhibitors FK866 and CHS-828 (or GMX1777, a pro-drug of GMX1778) showed potent antitumor activity in several preclinical models of solid and hematologic cancers [64], [134], [144] because NAMPT inhibition led to ATP shortage and to consequent cell death [64]. Moreover, NAMPT inhibition was found to increase the efficacy of standard chemotherapeutics: histone

deacetylase inhibitors [145], tumor necrosis factor-related apoptosis-inducing ligand [140], and poly(ADP-ribose) polymerase inhibitors [146].

Regrettably, clinical trials applying NAMPT inhibitors as monotherapy have so far been less promising. The main forms of reported toxicity for FK866 and CHS-828 were thrombocytopenia, gastrointestinal symptoms (especially for CHS-828), and lymphopenia (for FK866) but no objective tumor remission was observed, although a few cases of disease stabilization could be recorded with FK866 [79], [147]. Understanding cellular mechanisms of response to FK866 can help the development of new analogues that exhibit less toxicity and more efficacy. In our study, we reported an activation of a signaling network in which the AMPK-EIF2A axis was responsible for the early cellular response to FK866-induced metabolic stress. AMPK was activated in response to NAD<sup>+</sup> and ATP depletion and impaired mTOR signaling resulting in protein synthesis arrest, which had a protective role conferring temporary resistance to the FK866-induced energetic stress. We reported that activation of LKB1/AMPK pathway was protective against FK866, suggesting the utilization of this drug as a metabolism-based cancer therapeutic to selectively target LKB1-deficient tumors (sporadic lung, cervical, and endometrial cancers often carry LKB1 deficiency), which are unable to sense energetic stresses and activate mechanisms to restore energy homeostasis [148]. In an experimental condition preceding cell death characterized by high energetic demand, EIF2A acted as an early master regulator of cell fate, blocking anabolic processes and, at the same time, modulating cell death and adaptive pathways. Related to this, we also reported a reduction in the levels of the anti-apoptotic protein MCL1, which has been clearly associated with enhanced lethality in Jurkat cells and could provide a molecular explanation for the anti-leukemic activity of NAMPT inhibitors [149].

According to this observation and with the aim to potentiate FK866 efficacy, we evaluated Cyclosporine-A induced inhibition of P-glycoprotein 1 (Pgp), a key factor mediating multidrug resistance, in combination with FK866. The results indicated that Pgp inhibition increased the cytotoxic effects of FK866 in leukemia cells, not affecting healthy leukocytes and hematopoietic progenitor cells, specifically by increasing the intracellular concentration of the drug and

thereby exacerbating ATP shortage and endoplasmic reticulum stress, which was reported to be a specific response to FK866-induced stress [143].

The relevance of FK866 antileukemic activity in combined therapy was also assessed by using NAD<sup>+</sup>-dependent histone deacetylases (sirtuins) inhibitors alone and in combination with traditional HDAC (NAD<sup>+</sup>-independent deacetylases) inhibitors, in primary leukemia cells and cell lines. Sirtuin inhibitors and FK866 synergistically enhanced HDAC inhibitor activity in leukemia cells and induced the up-regulation of Bax, a pro-apoptotic Bcl2 family-member whose translocation to mitochondria is normally prevented by SIRT1 [145].

One possible explanation for the failure of NAMPT inhibition as an anti-cancer therapy could be the fact that supply of extracellular NAD<sup>+</sup> or extracellular NAD<sup>+</sup> precursors, including nicotinic acid, nicotinamide mononucleotide (NMN) and nicotinamide riboside (NR), can prevent the induced cell death by overcoming blockade of NAD<sup>+</sup> biosynthesis from nicotinamide. The ectoenzyme CD38 degrades NMN and generates nicotinamide (NAM), which can cross the plasma membrane and sustain NAMPT-dependent NAD<sup>+</sup> [150]. Recently, the ectoenzyme CD73 has also been demonstrated to contribute to NAD<sup>+</sup> synthesis by dephosphorylating NMN to produce NR, which crosses the plasma membrane [151]. Both CD38 and CD73 might therefore be involved in modulating cell susceptibility to FK866 and NAMPT inhibition. Specifically, it was demonstrated that CD73 enabled the utilization of extracellular NMN as a precursor for intracellular NAD<sup>+</sup> biosynthesis in human cells and reversed the FK866-induced cell death bypassing NAMPT inhibition. This work highlighted the possibility of implementing antitumor therapies based on combined inhibition of NAMPT and CD73 holding promise for treatments aimed at inhibiting NAD<sup>+</sup> pathways starting from NAM or NMN [81]. High level of CD73 has been observed in several types of cancer and tumor microenvironment contains factors modulating its expression, which is currently believed to promote cancer cell survival and associated with poor prognosis and metastasis [152].

On the contrary, higher expression of CD38, which degrades NAD<sup>+</sup> and NMN to nicotinamide, impaired the efficacy of NAD<sup>+</sup> and NMN-mediated rescue from

FK866-induced cell death because NAM utilization in these cells is blocked by NAMPT inhibition. Thus, CD38 expression by tumor cells could account for their inability to overcome NAMPT inhibition, when they are supplemented with NAM-containing precursors. Interestingly, preclinical and clinical studies revealed a sensitivity of normal lymphocytes to FK866, as inferred from the observed lymphopenia in response to this drug [79] that might be related to the high CD38 expression in lymphocytes [153].

In order to potentiate the efficacy of NAMPT inhibitors, work has been done to define predictive biomarkers of drug sensitivity that may be used for clinical testing. In a panel of 25 tumor cell lines an inverse correlation between NAMPT mRNA expression levels and GMX1778 cytotoxicity was reported [134]. These results were also confirmed at the protein level in three non-small-cell lung carcinoma (NSCLC) cell lines less sensitive to GMX1778, which expressed relatively higher levels of NAMPT when compared to a sub-set of small-cell lung carcinoma (SCLC) cells. Moreover, in a panel of 53 NSCLC cell lines NAMPT mRNA and protein levels inversely correlated with sensitivity to the NAMPT inhibitor GNE-618 [154]. Thus, NAMPT itself may serve as predictive biomarker for NAMPT inhibitor sensitivity.

The Preiss-Handler pathway leading to NAD<sup>+</sup> synthesis starting from nicotinic acid (NA) is frequently found to be inactive in cancer cells due to lack of expression of the rate-limiting enzyme nicotinic acid phosphoribosyltransferase (NAPRT1), thus making them more dependent on NAMPT for NAD<sup>+</sup> generation and cell survival and more susceptible to the cytotoxic effects of NAMPT inhibitors [134]. In NAPRT1-deficient tumors, addition of nicotinic acid to the media was not sufficient to mitigate the cytotoxic effects of NAMPT inhibition. Loss of NAPRT1 expression was reported to be caused not by the presence of NAPRT1 mutations or loss of heterozygosity but by tumor-specific promoter methylation, which provides a novel predictive biomarker for NAMPT inhibitors. NA rescue status was evaluated in a panel of more than 400 cancer cell lines. A subset of cell lines representing a range of tumor types was found to be NAPRT1-deficient (approximately 10-20% of colorectal, ovarian, non-small cell carcinoma and glioblastoma cell lines analyzed) or expressed undetectable NAPRT1 levels. Tumor-specific promoter hypermethylation of a CpG island that

overlaps with the NAPRT1 gene transcription start site inactivated this NAD<sup>+</sup> salvage pathways, resulting in synthetic lethality with the co-administration of a NAMPT inhibitor [155].

Finally, as for several other targeted therapies, also for NAMPT inhibition the development of target-specific drug resistance has been described.

We developed a model of FK866 resistance derived from Jurkat T-ALL cells, which was independent from NAMPT mutations but able to survive drug treatment maintaining a sufficient NAD<sup>+</sup> pool, restoring ATP intracellular content and resuming translation. In the resistant cells, NAMPT mRNA levels were reduced up to 50% with respect to parental cells whereas NAD<sup>+</sup> levels after treatment with the drug were restored up to 50% (in parental cells they were almost completely abolished).

The molecular mechanism of drug resistance has not been fully understood yet. However, NAMPT reduced levels have to be counterbalanced to support NAD<sup>+</sup> synthesis and cell survival, possibly by activation of NAMPT-independent pathways of NAD<sup>+</sup> synthesis. A major candidate for restoring NAD<sup>+</sup> is the *de novo* pathway, which is based on the transport of tryptophan within the cells by the L-type amino acid transporter 1 (LAT1) [156]. Tryptophan is then catabolized by the rate-limiting enzyme IDO1, which catalyzes the conversion of tryptophan to kynurenine and NAD<sup>+</sup> [157]. In FK866-resistant models, IDO1 gene expression was found to be up-regulated and might support the alternative pathway of NAD<sup>+</sup> synthesis. Therefore, we will investigate the involvement of tryptophan in the mechanism of resistance. Moreover, the requirement of LAT1-mediated tryptophan transportation in FK866-resistant models to support *de novo* NAD<sup>+</sup> biosynthesis will be tested by checking the response to JPH203, a LAT1 selective inhibitor [158], and by tryptophan deprivation through removal from culture media. LAT1 over-expression in T-ALL cancer cells was reported to reflect an addiction towards increased nutrients uptake for mTOR and AKT activation and reprogrammed metabolism [158].

NAD<sup>+</sup> synthesis based on the *de novo* pathway relying on tryptophan transport seems to be therefore the most promising pathway to be worth of investigation. In addition, we will evaluate the activity of ectoenzymes such as CD73, which

enables the utilization of extracellular NMN as precursor for intracellular NAD<sup>+</sup> biosynthesis bypassing NAMPT inhibition, and CD38, which degrades NMN and generates nicotinamide.

In addition, the level of the rate-limiting enzyme in NAD<sup>+</sup> synthesis from nicotinic acid, nicotinic acid phosphoribosyltransferase (NAPRT1), will be evaluated. NAPRT1 activity constitutes a possible rescue mechanism able to mitigate the cytotoxic effects of NAMPT inhibition.

In conclusion, understanding the molecular mechanism of FK866 resistance will provide insights in the regulation of NAD<sup>+</sup> content in cancer cells, contributing to the development of new specific and effective combinatorial drug therapies.

## REFERENCES

- [1] D. Hanahan and R. A. Weinberg, "Hallmarks of cancer: the next generation.," *Cell*, vol. 144, no. 5, pp. 646–74, Mar. 2011.
- [2] O. Warburg, "On respiratory impairment in cancer cells.," *Science*, vol. 124, no. 3215, pp. 269–70, Aug. 1956.
- [3] E. Bustamante, H. P. Morris, and P. L. Pedersen, "Energy metabolism of tumor cells. Requirement for a form of hexokinase with a propensity for mitochondrial binding.," *J. Biol. Chem.*, vol. 256, no. 16, pp. 8699–704, Aug. 1981.
- [4] P. S. Ward and C. B. Thompson, "Metabolic reprogramming: a cancer hallmark even warburg did not anticipate.," *Cancer Cell*, vol. 21, no. 3, pp. 297–308, Mar. 2012.
- [5] T. Soga, "Cancer metabolism: key players in metabolic reprogramming.," *Cancer Sci.*, vol. 104, no. 3, pp. 275–81, Mar. 2013.
- [6] R. G. Jones and C. B. Thompson, "Tumor suppressors and cell metabolism: a recipe for cancer growth," *Genes Dev.*, vol. 23, no. 5, pp. 537–548, Mar. 2009.
- [7] A. Chiarugi, C. Dölle, R. Felici, and M. Ziegler, "The NAD metabolome — a key determinant of cancer cell biology," *Nat. Rev. Cancer*, vol. 12, no. 11, pp. 741–752, Sep. 2012.
- [8] F. Berger, M. H. Ramírez-Hernández, and M. Ziegler, "The new life of a centenarian: signalling functions of NAD(P).," *Trends Biochem. Sci.*, vol. 29, no. 3, pp. 111–8, Mar. 2004.
- [9] D. Corda and M. Di Girolamo, "Functional aspects of protein mono-ADP-ribosylation.," *EMBO J.*, vol. 22, no. 9, pp. 1953–8, May 2003.
- [10] R. H. Houtkooper, C. Cantó, R. J. Wanders, and J. Auwerx, "The Secret Life of NAD +: An Old Metabolite Controlling New Metabolic Signaling Pathways," *Endocr. Rev.*, vol. 31, no. 2, pp. 194–223, Apr. 2010.
- [11] Q. Zhang, D. W. Piston, and R. H. Goodman, "Regulation of corepressor function by nuclear NADH.," *Science*, vol. 295, no. 5561, pp. 1895–7, Mar. 2002.
- [12] N. Pollak, C. Dölle, and M. Ziegler, "The power to reduce: pyridine nucleotides--small molecules with a multitude of functions.," *Biochem. J.*, vol. 402, no. 2, pp. 205–18, Mar. 2007.
- [13] P. Bieganski and C. Brenner, "Discoveries of nicotinamide riboside as a nutrient and conserved NRK genes establish a Preiss-Handler independent route to NAD+ in fungi and humans.," *Cell*, vol. 117, no. 4, pp. 495–502, May 2004.

- [14] W. A. Krehl, L. J. Teply, P. S. Sarma, and C. A. Elvehjem, "Growth-retarding effect of corn in Nicotinic Acid-low rations and its counteraction by Tryptophane.," *Science*, vol. 101, no. 2628, pp. 489–90, May 1945.
- [15] D. A. Bender and R. Olufunwa, "Utilization of tryptophan, nicotinamide and nicotinic acid as precursors for nicotinamide nucleotide synthesis in isolated rat liver cells.," *Br. J. Nutr.*, vol. 59, no. 2, pp. 279–87, Mar. 1988.
- [16] G. Schutz and P. Feigelson, "Purification and properties of rat liver tryptophan oxygenase.," *J. Biol. Chem.*, vol. 247, no. 17, pp. 5327–32, Sep. 1972.
- [17] F. Yamazaki, T. Kuroiwa, O. Takikawa, and R. Kido, "Human indolylamine 2,3-dioxygenase. Its tissue distribution, and characterization of the placental enzyme.," *Biochem. J.*, vol. 230, no. 3, pp. 635–8, Sep. 1985.
- [18] O. Takikawa, R. Yoshida, R. Kido, and O. Hayaishi, "Tryptophan degradation in mice initiated by indoleamine 2,3-dioxygenase.," *J. Biol. Chem.*, vol. 261, no. 8, pp. 3648–53, Mar. 1986.
- [19] D. A. Bender, "Biochemistry of tryptophan in health and disease.," *Mol. Aspects Med.*, vol. 6, no. 2, pp. 101–97, Jan. 1983.
- [20] V. Mori, A. Amici, F. Mazzola, M. Di Stefano, L. Conforti, G. Magni, S. Ruggieri, N. Raffaelli, and G. Orsomando, "Metabolic Profiling of Alternative NAD Biosynthetic Routes in Mouse Tissues," *PLoS One*, vol. 9, no. 11, p. e113939, Nov. 2014.
- [21] E. L. Jacobson, A. J. Dame, J. S. Pyrek, and M. K. Jacobson, "Evaluating the role of niacin in human carcinogenesis.," *Biochimie*, vol. 77, no. 5, pp. 394–8, Jan. 1995.
- [22] J. PREISS and P. HANDLER, "Biosynthesis of diphosphopyridine nucleotide. I. Identification of intermediates.," *J. Biol. Chem.*, vol. 233, no. 2, pp. 488–92, Aug. 1958.
- [23] A. Rongvaux, F. Andris, F. Van Gool, and O. Leo, "Reconstructing eukaryotic NAD metabolism," *BioEssays*, vol. 25, no. 7, pp. 683–690, Jul. 2003.
- [24] M. Schweiger, K. Hennig, F. Lerner, M. Niere, M. Hirsch-Kauffmann, T. Specht, C. Weise, S. L. Oei, and M. Ziegler, "Characterization of recombinant human nicotinamide mononucleotide adenylyl transferase (NMNAT), a nuclear enzyme essential for NAD synthesis.," *FEBS Lett.*, vol. 492, no. 1–2, pp. 95–100, Mar. 2001.
- [25] X. Zhang, O. V Kurnasov, S. Karthikeyan, N. V Grishin, A. L. Osterman, and H. Zhang, "Structural characterization of a human cytosolic NMN/NaMN adenylyltransferase and implication in human NAD biosynthesis.," *J. Biol. Chem.*, vol. 278, no. 15, pp. 13503–11, Apr. 2003.
- [26] B. Samal, Y. Sun, G. Stearns, C. Xie, S. Suggs, and I. McNiece, "Cloning and characterization of the cDNA encoding a novel human pre-B-cell colony-enhancing factor.," *Mol. Cell. Biol.*, vol. 14, no. 2, pp. 1431–7, Feb. 1994.

- [27] A. Rongvaux, R. J. Shea, M. H. Mulks, D. Gigot, J. Urbain, O. Leo, and F. Andris, "Pre-B-cell colony-enhancing factor, whose expression is up-regulated in activated lymphocytes, is a nicotinamide phosphoribosyltransferase, a cytosolic enzyme involved in NAD biosynthesis.," *Eur. J. Immunol.*, vol. 32, no. 11, pp. 3225–34, Nov. 2002.
- [28] J. A. Khan, X. Tao, and L. Tong, "Molecular basis for the inhibition of human NMPRTase, a novel target for anticancer agents.," *Nat. Struct. Mol. Biol.*, vol. 13, no. 7, pp. 582–8, Jul. 2006.
- [29] E. S. Burgos and V. L. Schramm, "Weak Coupling of ATP Hydrolysis to the Chemical Equilibrium of Human Nicotinamide Phosphoribosyltransferase †," *Biochemistry*, vol. 47, no. 42, pp. 11086–11096, Oct. 2008.
- [30] A. Fukuhara, M. Matsuda, M. Nishizawa, K. Segawa, M. Tanaka, K. Kishimoto, Y. Matsuki, M. Murakami, T. Ichisaka, H. Murakami, E. Watanabe, T. Takagi, M. Akiyoshi, T. Ohtsubo, S. Kihara, S. Yamashita, M. Makishima, T. Funahashi, S. Yamanaka, R. Hiramatsu, Y. Matsuzawa, and I. Shimomura, "Visfatin: a protein secreted by visceral fat that mimics the effects of insulin.," *Science*, vol. 307, no. 5708, pp. 426–30, Jan. 2005.
- [31] A. Fukuhara, M. Matsuda, M. Nishizawa, K. Segawa, M. Tanaka, K. Kishimoto, Y. Matsuki, M. Murakami, T. Ichisaka, H. Murakami, E. Watanabe, T. Takagi, M. Akiyoshi, T. Ohtsubo, S. Kihara, S. Yamashita, M. Makishima, T. Funahashi, S. Yamanaka, R. Hiramatsu, Y. Matsuzawa, and I. Shimomura, "Retraction.," *Science*, vol. 318, no. 5850, p. 565, Oct. 2007.
- [32] J. R. Revollo, A. Körner, K. F. Mills, A. Satoh, T. Wang, A. Garten, B. Dasgupta, Y. Sasaki, C. Wolberger, R. R. Townsend, J. Milbrandt, W. Kiess, and S.-I. Imai, "Nampt/PBEF/Visfatin regulates insulin secretion in beta cells as a systemic NAD biosynthetic enzyme.," *Cell Metab.*, vol. 6, no. 5, pp. 363–75, Nov. 2007.
- [33] P. R. Martin, R. J. Shea, and M. H. Mulks, "Identification of a plasmid-encoded gene from *Haemophilus ducreyi* which confers NAD independence.," *J. Bacteriol.*, vol. 183, no. 4, pp. 1168–74, Feb. 2001.
- [34] T. Kitani, S. Okuno, and H. Fujisawa, "Growth phase-dependent changes in the subcellular localization of pre-B-cell colony-enhancing factor.," *FEBS Lett.*, vol. 544, no. 1–3, pp. 74–8, Jun. 2003.
- [35] H. Yang, T. Yang, J. A. Baur, E. Perez, T. Matsui, J. J. Carmona, D. W. Lamming, N. C. Souza-Pinto, V. A. Bohr, A. Rosenzweig, R. de Cabo, A. A. Sauve, and D. A. Sinclair, "Nutrient-sensitive mitochondrial NAD<sup>+</sup> levels dictate cell survival.," *Cell*, vol. 130, no. 6, pp. 1095–107, Sep. 2007.
- [36] K. M. Ramsey, J. Yoshino, C. S. Brace, D. Abrassart, Y. Kobayashi, B. Marcheva, H.-K. Hong, J. L. Chong, E. D. Buhr, C. Lee, J. S. Takahashi, S.-I. Imai, and J. Bass, "Circadian clock feedback cycle through NAMPT-mediated NAD<sup>+</sup> biosynthesis.," *Science*, vol. 324, no. 5927, pp. 651–4, May 2009.

- [37] Y. Nakahata, S. Sahar, G. Astarita, M. Kaluzova, and P. Sassone-Corsi, "Circadian Control of the NAD<sup>+</sup> Salvage Pathway by CLOCK-SIRT1," *Science* (80-. ), vol. 324, no. 5927, pp. 654–657, Mar. 2009.
- [38] J. Hector, B. Schwarzloh, J. Goehring, T. G. Strate, U. F. Hess, G. Deuretzbacher, N. Hansen-Algenstaedt, F.-U. Beil, and P. Algenstaedt, "TNF-alpha alters visfatin and adiponectin levels in human fat.," *Horm. Metab. Res.*, vol. 39, no. 4, pp. 250–5, Apr. 2007.
- [39] M. A. Nowell, P. J. Richards, C. A. Fielding, S. Ognjanovic, N. Topley, A. S. Williams, G. Bryant-Greenwood, and S. A. Jones, "Regulation of pre-B cell colony-enhancing factor by STAT-3-dependent interleukin-6 trans-signaling: implications in the pathogenesis of rheumatoid arthritis.," *Arthritis Rheum.*, vol. 54, no. 7, pp. 2084–95, Jul. 2006.
- [40] S.-K. Bae, S.-R. Kim, J. G. Kim, J. Y. Kim, T. H. Koo, H.-O. Jang, I. Yun, M.-A. Yoo, and M.-K. Bae, "Hypoxic induction of human visfatin gene is directly mediated by hypoxia-inducible factor-1.," *FEBS Lett.*, vol. 580, no. 17, pp. 4105–13, Jul. 2006.
- [41] S. H. Jia, Y. Li, J. Parodo, A. Kapus, L. Fan, O. D. Rotstein, and J. C. Marshall, "Pre-B cell colony-enhancing factor inhibits neutrophil apoptosis in experimental inflammation and clinical sepsis.," *J. Clin. Invest.*, vol. 113, no. 9, pp. 1318–27, May 2004.
- [42] S. Q. Ye, B. A. Simon, J. P. Maloney, A. Zambelli-Weiner, L. Gao, A. Grant, R. B. Easley, B. J. McVerry, R. M. Tuder, T. Standiford, R. G. Brower, K. C. Barnes, and J. G. N. Garcia, "Pre-B-Cell Colony-enhancing Factor as a Potential Novel Biomarker in Acute Lung Injury," *Am. J. Respir. Crit. Care Med.*, vol. 171, no. 4, pp. 361–370, Feb. 2005.
- [43] F. Brentano, O. Schorr, C. Ospelt, J. Stanczyk, R. E. Gay, S. Gay, and D. Kyburz, "Pre-B cell colony-enhancing factor/visfatin, a new marker of inflammation in rheumatoid arthritis with proinflammatory and matrix-degrading activities," *Arthritis Rheum.*, vol. 56, no. 9, pp. 2829–2839, Sep. 2007.
- [44] T. B. Dahl, A. Yndestad, M. Skjelland, E. Øie, A. Dahl, A. Michelsen, J. K. Damås, S. H. Tunheim, T. Ueland, C. Smith, B. Bendz, S. Tonstad, L. Gullestad, S. S. Frøland, K. Krohg-Sørensen, D. Russell, P. Aukrust, and B. Halvorsen, "Increased expression of visfatin in macrophages of human unstable carotid and coronary atherosclerosis: possible role in inflammation and plaque destabilization.," *Circulation*, vol. 115, no. 8, pp. 972–80, Feb. 2007.
- [45] S. E. Hufton, P. T. Moerkerk, R. Brandwijk, A. P. de Bruïne, J. W. Arends, and H. R. Hoogenboom, "A profile of differentially expressed genes in primary colorectal cancer using suppression subtractive hybridization.," *FEBS Lett.*, vol. 463, no. 1–2, pp. 77–82, Dec. 1999.
- [46] W. Xia, Z. Wang, Q. Wang, J. Han, C. Zhao, Y. Hong, L. Zeng, L. Tang, and W. Ying, "Roles of NAD(+) / NADH and NADP(+) / NADPH in cell death.," *Curr. Pharm. Des.*, vol. 15, no. 1, pp. 12–9, Jan. 2009.

- [47] R. Adya, B. K. Tan, A. Punn, J. Chen, and H. S. Randeve, "Visfatin induces human endothelial VEGF and MMP-2/9 production via MAPK and PI3K/Akt signalling pathways: novel insights into visfatin-induced angiogenesis," *Cardiovasc. Res.*, vol. 78, no. 2, pp. 356–365, Feb. 2008.
- [48] Y.-H. Bae, M.-K. Bae, S.-R. Kim, J. H. Lee, H.-J. Wee, and S.-K. Bae, "Upregulation of fibroblast growth factor-2 by visfatin that promotes endothelial angiogenesis," *Biochem. Biophys. Res. Commun.*, vol. 379, no. 2, pp. 206–11, Feb. 2009.
- [49] T. Zhou, T. Wang, and J. G. N. Garcia, "Expression of Nicotinamide Phosphoribosyltransferase-Influenced Genes Predicts Recurrence-Free Survival in Lung and Breast Cancers," *Sci. Rep.*, vol. 4, p. 6107, Aug. 2014.
- [50] R. E. Shackelford, M. M. Bui, D. Coppola, and A. Hakam, "Over-expression of nicotinamide phosphoribosyltransferase in ovarian cancers.," *Int. J. Clin. Exp. Pathol.*, vol. 3, no. 5, pp. 522–7, Jan. 2010.
- [51] M. A. A. K. Folgueira, D. M. Carraro, H. Brentani, D. F. da C. Patrão, E. M. Barbosa, M. M. Netto, J. R. F. Caldeira, M. L. H. Katayama, F. A. Soares, C. T. Oliveira, L. F. L. Reis, J. H. L. Kaiano, L. P. Camargo, R. Z. N. Vêncio, I. M. L. Snitcovsky, F. B. A. Makdissi, P. J. da S. e Silva, J. C. G. S. Góes, and M. M. Brentani, "Gene expression profile associated with response to doxorubicin-based therapy in breast cancer.," *Clin. Cancer Res.*, vol. 11, no. 20, pp. 7434–43, Oct. 2005.
- [52] T.-Q. Bi, X.-M. Che, X.-H. Liao, D.-J. Zhang, H.-L. Long, H.-J. Li, and W. Zhao, "Overexpression of Nampt in gastric cancer and chemopotentiating effects of the Nampt inhibitor FK866 in combination with fluorouracil.," *Oncol. Rep.*, vol. 26, no. 5, pp. 1251–7, Nov. 2011.
- [53] B. Wang, M. K. Hasan, E. Alvarado, H. Yuan, H. Wu, and W. Y. Chen, "NAMPT overexpression in prostate cancer and its contribution to tumor cell survival and stress response.," *Oncogene*, vol. 30, no. 8, pp. 907–21, Feb. 2011.
- [54] R. Shackelford, S. Hirsh, K. Henry, A. Abdel-Mageed, E. Kandil, and D. Coppola, "Nicotinamide phosphoribosyltransferase and SIRT3 expression are increased in well-differentiated thyroid carcinomas.," *Anticancer Res.*, vol. 33, no. 8, pp. 3047–52, Aug. 2013.
- [55] W. Tian, Y. Zhu, Y. Wang, F. Teng, H. Zhang, G. Liu, X. Ma, D. Sun, T. Rohan, and F. Xue, "Visfatin, a potential biomarker and prognostic factor for endometrial cancer.," *Gynecol. Oncol.*, vol. 129, no. 3, pp. 505–12, Jun. 2013.
- [56] S. U. Venkateshaiah, S. Khan, W. Ling, R. Bam, X. Li, F. van Rhee, S. Usmani, B. Barlogie, J. Epstein, and S. Yaccoby, "NAMPT/PBEF1 enzymatic activity is indispensable for myeloma cell growth and osteoclast activity.," *Exp. Hematol.*, vol. 41, no. 6, pp. 547–557.e2, Jun. 2013.
- [57] R. Bułdak, "Visfatin affects redox adaptative responses and proliferation in Me45 human malignant melanoma cells: An in vitro study," *Oncol. Rep.*, vol. 29, no. 2, pp. 771–8, Dec. 2012.

- [58] P. S. Reddy, S. Umesh, B. Thota, A. Tandon, P. Pandey, A. S. Hegde, A. Balasubramaniam, B. A. Chandramouli, V. Santosh, M. R. S. Rao, P. Kondaiah, and K. Somasundaram, "PBEF1/NAMPRase/Visfatin: a potential malignant astrocytoma/glioblastoma serum marker with prognostic value.," *Cancer Biol. Ther.*, vol. 7, no. 5, pp. 663–8, May 2008.
- [59] U. H. Olesen, N. Hastrup, and M. Sehested, "Expression patterns of nicotinamide phosphoribosyltransferase and nicotinic acid phosphoribosyltransferase in human malignant lymphomas.," *APMIS*, vol. 119, no. 4–5, pp. 296–303, Apr. 2011.
- [60] H.-J. Park, S.-R. Kim, S. S. Kim, H.-J. Wee, M.-K. Bae, M. H. Ryu, and S.-K. Bae, "Visfatin promotes cell and tumor growth by upregulating Notch1 in breast cancer.," *Oncotarget*, vol. 5, no. 13, pp. 5087–99, Jul. 2014.
- [61] C. C. S. Chini, A. M. G. Guerrico, V. Nin, J. Camacho-Pereira, C. Escande, M. T. Barbosa, and E. N. Chini, "Targeting of NAD metabolism in pancreatic cancer cells: potential novel therapy for pancreatic tumors.," *Clin. Cancer Res.*, vol. 20, no. 1, pp. 120–30, Jan. 2014.
- [62] S. Ninomiya, M. Shimizu, K. Imai, K. Takai, M. Shiraki, T. Hara, H. Tsurumi, S. Ishizaki, and H. Moriwaki, "Possible role of visfatin in hepatoma progression and the effects of branched-chain amino acids on visfatin-induced proliferation in human hepatoma cells.," *Cancer Prev. Res. (Phila.)*, vol. 4, no. 12, pp. 2092–100, Dec. 2011.
- [63] D. Soncini, I. Caffa, G. Zoppoli, M. Cea, A. Cagnetta, M. Passalacqua, L. Mastracci, S. Boero, F. Montecucco, G. Sociali, D. Lasigliè, P. Damonte, A. Grozio, E. Mannino, A. Poggi, V. G. D'Agostino, F. Monacelli, A. Provenzani, P. Odetti, A. Ballestrero, S. Bruzzone, and A. Nencioni, "Nicotinamide Phosphoribosyltransferase Promotes Epithelial-to-Mesenchymal Transition as a Soluble Factor Independent of Its Enzymatic Activity," *J. Biol. Chem.*, vol. 289, no. 49, pp. 34189–34204, 2014.
- [64] M. Hasmann and I. Schemainda, "FK866, a highly specific noncompetitive inhibitor of nicotinamide phosphoribosyltransferase, represents a novel mechanism for induction of tumor cell apoptosis.," *Cancer Res.*, vol. 63, no. 21, pp. 7436–42, Nov. 2003.
- [65] M.-K. Kim, J. H. Lee, H. Kim, S. J. Park, S. H. Kim, G. B. Kang, Y. S. Lee, J. B. Kim, K. K. Kim, S. W. Suh, and S. H. Eom, "Crystal structure of visfatin/pre-B cell colony-enhancing factor 1/nicotinamide phosphoribosyltransferase, free and in complex with the anti-cancer agent FK-866.," *J. Mol. Biol.*, vol. 362, no. 1, pp. 66–77, Sep. 2006.
- [66] B. Tan, D. A. Young, Z.-H. Lu, T. Wang, T. I. Meier, R. L. Shepard, K. Roth, Y. Zhai, K. Huss, M.-S. Kuo, J. Gillig, S. Parthasarathy, T. P. Burkholder, M. C. Smith, S. Geeganage, and G. Zhao, "Pharmacological inhibition of nicotinamide phosphoribosyltransferase (NAMPT), an enzyme essential for NAD<sup>+</sup> biosynthesis, in human cancer cells: metabolic basis and potential clinical implications.," *J. Biol. Chem.*, vol. 288, no. 5, pp. 3500–11, Feb. 2013.

- [67] M. Muruganandham, A. A. Alfieri, C. Matei, Y. Chen, G. Sukenick, I. Schemainda, M. Hasmann, L. B. Saltz, and J. A. Koutcher, "Metabolic signatures associated with a NAD synthesis inhibitor-induced tumor apoptosis identified by 1H-decoupled-31P magnetic resonance spectroscopy.," *Clin. Cancer Res.*, vol. 11, no. 9, pp. 3503–13, May 2005.
- [68] K. Wosikowski, K. Mattern, I. Schemainda, M. Hasmann, B. Rattel, and R. Löser, "WK175, a novel antitumor agent, decreases the intracellular nicotinamide adenine dinucleotide concentration and induces the apoptotic cascade in human leukemia cells.," *Cancer Res.*, vol. 62, no. 4, pp. 1057–62, Feb. 2002.
- [69] R. A. Billington, A. A. Genazzani, C. Travelli, and F. Condorelli, "NAD depletion by FK866 induces autophagy.," *Autophagy*, vol. 4, no. 3, pp. 385–7, Apr. 2008.
- [70] C. Travelli, V. Drago, E. Maldi, N. Kaludercic, U. Galli, R. Boldorini, F. Di Lisa, G. C. Tron, P. L. Canonico, and A. A. Genazzani, "Reciprocal potentiation of the antitumoral activities of FK866, an inhibitor of nicotinamide phosphoribosyltransferase, and etoposide or cisplatin in neuroblastoma cells.," *J. Pharmacol. Exp. Ther.*, vol. 338, no. 3, pp. 829–40, Sep. 2011.
- [71] J. Dreves, R. Löser, B. Rattel, and N. Esser, "Antiangiogenic potency of FK866/K22.175, a new inhibitor of intracellular NAD biosynthesis, in murine renal cell carcinoma.," *Anticancer Res.*, vol. 23, no. 6C, pp. 4853–8, Jan. .
- [72] A. Nahimana, A. Attinger, D. Aubry, P. Greaney, C. Ireson, A. V Thougard, J. Tjørnelund, K. M. Dawson, M. Dupuis, and M. A. Duchosal, "The NAD biosynthesis inhibitor APO866 has potent antitumor activity against hematologic malignancies.," *Blood*, vol. 113, no. 14, pp. 3276–86, Apr. 2009.
- [73] M. Cea, G. Zoppoli, S. Bruzzone, F. Fruscione, E. Moran, A. Garuti, I. Rocco, G. Cirmena, S. Casciaro, F. Olcese, I. Pierri, A. Cagnetta, F. Ferrando, R. Ghio, M. Gobbi, A. Ballestrero, F. Patrone, and A. Nencioni, "APO866 activity in hematologic malignancies: a preclinical in vitro study.," *Blood*, vol. 113, no. 23, pp. 6035–7; author reply 6037–8, Jun. 2009.
- [74] G. Zoppoli, M. Cea, D. Soncini, F. Fruscione, J. Rudner, E. Moran, I. Caffa, D. Bedognetti, G. Motta, R. Ghio, F. Ferrando, A. Ballestrero, S. Parodi, C. Belka, F. Patrone, S. Bruzzone, and A. Nencioni, "Potent synergistic interaction between the Nampt inhibitor APO866 and the apoptosis activator TRAIL in human leukemia cells.," *Exp. Hematol.*, vol. 38, no. 11, pp. 979–88, Nov. 2010.
- [75] I. Gehrke, E. D. J. Bouchard, S. Beiggi, A. G. Poepl, J. B. Johnston, S. B. Gibson, and V. Banerji, "On-target effect of FK866, a nicotinamide phosphoribosyl transferase inhibitor, by apoptosis-mediated death in chronic lymphocytic leukemia cells.," *Clin. Cancer Res.*, vol. 20, no. 18, pp. 4861–72, Sep. 2014.
- [76] M. Cea, A. Cagnetta, M. Fulciniti, Y.-T. Tai, T. Hideshima, D. Chauhan, A. Roccaro, A. Sacco, T. Calimeri, F. Cottini, J. Jakubikova, S.-Y. Kong, F. Patrone, A. Nencioni, M. Gobbi, P. Richardson, N. Munshi, and K. C. Anderson, "Targeting NAD<sup>+</sup> salvage pathway induces autophagy in multiple myeloma cells

- via mTORC1 and extracellular signal-regulated kinase (ERK1/2) inhibition.," *Blood*, vol. 120, no. 17, pp. 3519–29, Oct. 2012.
- [77] A. Cagnetta, M. Cea, T. Calimeri, C. Acharya, M. Fulciniti, Y.-T. Tai, T. Hideshima, D. Chauhan, M. Y. Zhong, F. Patrone, A. Nencioni, M. Gobbi, P. Richardson, N. Munshi, and K. C. Anderson, "Intracellular NAD<sup>+</sup> depletion enhances bortezomib-induced anti-myeloma activity.," *Blood*, vol. 122, no. 7, pp. 1243–55, Aug. 2013.
- [78] A. Nahimana, D. Aubry, C. S. Breton, S. R. Majjigapu, B. Sordat, P. Vogel, and M. A. Duchosal, "The anti-lymphoma activity of APO866, an inhibitor of nicotinamide adenine dinucleotide biosynthesis, is potentialized when used in combination with anti-CD20 antibody.," *Leuk. Lymphoma*, vol. 55, no. 9, pp. 2141–50, Sep. 2014.
- [79] K. Holen, L. B. Saltz, E. Hollywood, K. Burk, and A.-R. Hanauske, "The pharmacokinetics, toxicities, and biologic effects of FK866, a nicotinamide adenine dinucleotide biosynthesis inhibitor.," *Invest. New Drugs*, vol. 26, no. 1, pp. 45–51, Feb. 2008.
- [80] M. Cea, A. Cagnetta, F. Patrone, A. Nencioni, M. Gobbi, and K. C. Anderson, "Intracellular NAD(+) depletion induces autophagic death in multiple myeloma cells.," *Autophagy*, vol. 9, no. 3, pp. 410–2, Mar. 2013.
- [81] A. Grozio, G. Sociali, L. Sturla, I. Caffa, D. Soncini, A. Salis, N. Raffaelli, A. De Flora, A. Nencioni, and S. Bruzzone, "CD73 Protein as a Source of Extracellular Precursors for Sustained NAD<sup>+</sup> Biosynthesis in FK866-treated Tumor Cells," *J. Biol. Chem.*, vol. 288, no. 36, pp. 25938–25949, Jul. 2013.
- [82] W. van Veelen, S. E. Korsse, L. van de Laar, and M. P. Peppelenbosch, "The long and winding road to rational treatment of cancer associated with LKB1/AMPK/TSC/mTORC1 signaling.," *Oncogene*, vol. 30, no. 20, pp. 2289–303, May 2011.
- [83] S. Schuster, M. Penke, T. Gorski, R. Gebhardt, T. S. Weiss, W. Kiess, and A. Garten, "FK866-induced NAMPT inhibition activates AMPK and downregulates mTOR signaling in hepatocarcinoma cells.," *Biochem. Biophys. Res. Commun.*, vol. 458, no. 2, pp. 334–40, Mar. 2015.
- [84] A. Hemminki, D. Markie, I. Tomlinson, E. Avizienyte, S. Roth, A. Loukola, G. Bignell, W. Warren, M. Aminoff, P. Höglund, H. Järvinen, P. Kristo, K. Pelin, M. Ridanpää, R. Salovaara, T. Toro, W. Bodmer, S. Olschwang, A. S. Olsen, M. R. Stratton, A. de la Chapelle, and L. A. Aaltonen, "A serine/threonine kinase gene defective in Peutz-Jeghers syndrome.," *Nature*, vol. 391, no. 6663, pp. 184–7, Jan. 1998.
- [85] J. Boudeau, A. F. Baas, M. Deak, N. A. Morrice, A. Kieloch, M. Schutkowski, A. R. Prescott, H. C. Clevers, and D. R. Alessi, "MO25alpha/beta interact with STRADalpha/beta enhancing their ability to bind, activate and localize LKB1 in the cytoplasm.," *EMBO J.*, vol. 22, no. 19, pp. 5102–14, Oct. 2003.

- [86] S. A. Hawley, J. Boudeau, J. L. Reid, K. J. Mustard, L. Udd, T. P. Mäkelä, D. R. Alessi, and D. G. Hardie, "Complexes between the LKB1 tumor suppressor, STRAD alpha/beta and MO25 alpha/beta are upstream kinases in the AMP-activated protein kinase cascade.," *J. Biol.*, vol. 2, no. 4, p. 28, Jan. 2003.
- [87] R. J. Shaw, M. Kosmatka, N. Bardeesy, R. L. Hurley, L. A. Witters, R. A. DePinho, and L. C. Cantley, "The tumor suppressor LKB1 kinase directly activates AMP-activated kinase and regulates apoptosis in response to energy stress.," *Proc. Natl. Acad. Sci. U. S. A.*, vol. 101, no. 10, pp. 3329–35, Mar. 2004.
- [88] M. Tiainen, K. Vaahtomeri, A. Ylikorkala, and T. P. Mäkelä, "Growth arrest by the LKB1 tumor suppressor: induction of p21(WAF1/CIP1).," *Hum. Mol. Genet.*, vol. 11, no. 13, pp. 1497–504, Jun. 2002.
- [89] B. Xiao, M. J. Sanders, E. Underwood, R. Heath, F. V Mayer, D. Carmena, C. Jing, P. A. Walker, J. F. Eccleston, L. F. Haire, P. Saiu, S. A. Howell, R. Aasland, S. R. Martin, D. Carling, and S. J. Gambin, "Structure of mammalian AMPK and its regulation by ADP.," *Nature*, vol. 472, no. 7342, pp. 230–3, Apr. 2011.
- [90] S. A. Hawley, M. A. Selbert, E. G. Goldstein, A. M. Edelman, D. Carling, and D. G. Hardie, "5'-AMP activates the AMP-activated protein kinase cascade, and Ca<sup>2+</sup>/calmodulin activates the calmodulin-dependent protein kinase I cascade, via three independent mechanisms.," *J. Biol. Chem.*, vol. 270, no. 45, pp. 27186–91, Nov. 1995.
- [91] L. Tong, "Acetyl-coenzyme A carboxylase: crucial metabolic enzyme and attractive target for drug discovery.," *Cell. Mol. Life Sci.*, vol. 62, no. 16, pp. 1784–803, Aug. 2005.
- [92] G. Zhou, R. Myers, Y. Li, Y. Chen, X. Shen, J. Fenyk-Melody, M. Wu, J. Ventre, T. Doebber, N. Fujii, N. Musi, M. F. Hirshman, L. J. Goodyear, and D. E. Moller, "Role of AMP-activated protein kinase in mechanism of metformin action.," *J. Clin. Invest.*, vol. 108, no. 8, pp. 1167–74, Oct. 2001.
- [93] B. Faubert, G. Boily, S. Izreig, T. Griss, B. Samborska, Z. Dong, F. Dupuy, C. Chambers, B. J. Fuerth, B. Viollet, O. A. Mamer, D. Avizonis, R. J. DeBerardinis, P. M. Siegel, and R. G. Jones, "AMPK is a negative regulator of the Warburg effect and suppresses tumor growth in vivo.," *Cell Metab.*, vol. 17, no. 1, pp. 113–24, Jan. 2013.
- [94] C.-W. Lee, L. L.-Y. Wong, E. Y.-T. Tse, H.-F. Liu, V. Y.-L. Leong, J. M.-F. Lee, D. G. Hardie, I. O.-L. Ng, and Y.-P. Ching, "AMPK promotes p53 acetylation via phosphorylation and inactivation of SIRT1 in liver cancer cells.," *Cancer Res.*, vol. 72, no. 17, pp. 4394–404, Sep. 2012.
- [95] R. J. Shaw, N. Bardeesy, B. D. Manning, L. Lopez, M. Kosmatka, R. A. DePinho, and L. C. Cantley, "The LKB1 tumor suppressor negatively regulates mTOR signaling.," *Cancer Cell*, vol. 6, no. 1, pp. 91–9, Jul. 2004.

- [96] A. F. Castro, J. F. Rebhun, G. J. Clark, and L. A. Quilliam, "Rheb binds tuberous sclerosis complex 2 (TSC2) and promotes S6 kinase activation in a rapamycin- and farnesylation-dependent manner.," *J. Biol. Chem.*, vol. 278, no. 35, pp. 32493–6, Aug. 2003.
- [97] G. Benvenuto, S. Li, S. J. Brown, R. Braverman, W. C. Vass, J. P. Cheadle, D. J. Halley, J. R. Sampson, R. Wienecke, and J. E. DeClue, "The tuberous sclerosis-1 (TSC1) gene product hamartin suppresses cell growth and augments the expression of the TSC2 product tuberin by inhibiting its ubiquitination.," *Oncogene*, vol. 19, no. 54, pp. 6306–16, Dec. 2000.
- [98] A. Hahn-Windgassen, V. Nogueira, C.-C. Chen, J. E. Skeen, N. Sonenberg, and N. Hay, "Akt Activates the Mammalian Target of Rapamycin by Regulating Cellular ATP Level and AMPK Activity," *J. Biol. Chem.*, vol. 280, no. 37, pp. 32081–32089, Jul. 2005.
- [99] D. M. Gwinn, D. B. Shackelford, D. F. Egan, M. M. Mihaylova, A. Mery, D. S. Vasquez, B. E. Turk, and R. J. Shaw, "AMPK phosphorylation of raptor mediates a metabolic checkpoint.," *Mol. Cell*, vol. 30, no. 2, pp. 214–26, Apr. 2008.
- [100] S. Wullschleger, R. Loewith, and M. N. Hall, "TOR signaling in growth and metabolism.," *Cell*, vol. 124, no. 3, pp. 471–84, Feb. 2006.
- [101] W. J. Oh and E. Jacinto, "mTOR complex 2 signaling and functions.," *Cell Cycle*, vol. 10, no. 14, pp. 2305–16, Jul. 2011.
- [102] Y. Zhang, X. Gao, L. J. Saucedo, B. Ru, B. A. Edgar, and D. Pan, "Rheb is a direct target of the tuberous sclerosis tumour suppressor proteins," *Nat. Cell Biol.*, vol. 5, no. 6, pp. 578–581, May 2003.
- [103] D. M. Sabatini, "mTOR and cancer: insights into a complex relationship.," *Nat. Rev. Cancer*, vol. 6, no. 9, pp. 729–34, Sep. 2006.
- [104] K. Hara, Y. Maruki, X. Long, K. Yoshino, N. Oshiro, S. Hidayat, C. Tokunaga, J. Avruch, and K. Yonezawa, "Raptor, a binding partner of target of rapamycin (TOR), mediates TOR action.," *Cell*, vol. 110, no. 2, pp. 177–89, Jul. 2002.
- [105] A. A. Michels, A. M. Robitaille, D. Buczynski-Ruchonnet, W. Hodroj, J. H. Reina, M. N. Hall, and N. Hernandez, "mTORC1 directly phosphorylates and regulates human MAF1.," *Mol. Cell. Biol.*, vol. 30, no. 15, pp. 3749–57, Aug. 2010.
- [106] C. C. Hudson, M. Liu, G. G. Chiang, D. M. Otterness, D. C. Loomis, F. Kaper, A. J. Giaccia, and R. T. Abraham, "Regulation of hypoxia-inducible factor 1alpha expression and function by the mammalian target of rapamycin.," *Mol. Cell. Biol.*, vol. 22, no. 20, pp. 7004–14, Oct. 2002.
- [107] C. H. Jung, C. B. Jun, S.-H. Ro, Y.-M. Kim, N. M. Otto, J. Cao, M. Kundu, and D.-H. Kim, "ULK-Atg13-FIP200 complexes mediate mTOR signaling to the autophagy machinery.," *Mol. Biol. Cell*, vol. 20, no. 7, pp. 1992–2003, Apr. 2009.
- [108] P. Wang, Y.-F. Guan, H. Du, Q.-W. Zhai, D.-F. Su, and C.-Y. Miao, "Induction of autophagy contributes to the neuroprotection of nicotinamide

- phosphoribosyltransferase in cerebral ischemia.," *Autophagy*, vol. 8, no. 1, pp. 77–87, Jan. 2012.
- [109] M. S. Song, L. Salmena, and P. P. Pandolfi, "The functions and regulation of the PTEN tumour suppressor.," *Nat. Rev. Mol. Cell Biol.*, vol. 13, no. 5, pp. 283–96, May 2012.
- [110] B. F. Teske, S. A. Wek, P. Bunpo, J. K. Cundiff, J. N. McClintick, T. G. Anthony, and R. C. Wek, "The eIF2 kinase PERK and the integrated stress response facilitate activation of ATF6 during endoplasmic reticulum stress.," *Mol. Biol. Cell*, vol. 22, no. 22, pp. 4390–405, Nov. 2011.
- [111] D. T. Rutkowski, S. M. Arnold, C. N. Miller, J. Wu, J. Li, K. M. Gunnison, K. Mori, A. A. Sadighi Akha, D. Raden, and R. J. Kaufman, "Adaptation to ER stress is mediated by differential stabilities of pro-survival and pro-apoptotic mRNAs and proteins.," *PLoS Biol.*, vol. 4, no. 11, p. e374, Nov. 2006.
- [112] S. J. Marciniak and D. Ron, "Endoplasmic reticulum stress signaling in disease.," *Physiol. Rev.*, vol. 86, no. 4, pp. 1133–49, Oct. 2006.
- [113] D. Ron and P. Walter, "Signal integration in the endoplasmic reticulum unfolded protein response.," *Nat. Rev. Mol. Cell Biol.*, vol. 8, no. 7, pp. 519–29, Jul. 2007.
- [114] D. Senft and Z. A. Ronai, "UPR, autophagy, and mitochondria crosstalk underlies the ER stress response," *Trends Biochem. Sci.*, vol. 40, no. 3, pp. 141–8, Feb. 2015.
- [115] M. Wang, S. Wey, Y. Zhang, R. Ye, and A. S. Lee, "Role of the unfolded protein response regulator GRP78/BiP in development, cancer, and neurological disorders.," *Antioxid. Redox Signal.*, vol. 11, no. 9, pp. 2307–16, Sep. 2009.
- [116] A. Bertolotti, Y. Zhang, L. M. Hendershot, H. P. Harding, and D. Ron, "Dynamic interaction of BiP and ER stress transducers in the unfolded-protein response.," *Nat. Cell Biol.*, vol. 2, no. 6, pp. 326–32, Jun. 2000.
- [117] H. P. Harding, Y. Zhang, and D. Ron, "Protein translation and folding are coupled by an endoplasmic-reticulum-resident kinase.," *Nature*, vol. 397, no. 6716, pp. 271–4, Jan. 1999.
- [118] K. M. Vattem and R. C. Wek, "Reinitiation involving upstream ORFs regulates ATF4 mRNA translation in mammalian cells.," *Proc. Natl. Acad. Sci. U. S. A.*, vol. 101, no. 31, pp. 11269–74, Aug. 2004.
- [119] Y. Shi, K. M. Vattem, R. Sood, J. An, J. Liang, L. Stramm, and R. C. Wek, "Identification and characterization of pancreatic eukaryotic initiation factor 2 alpha-subunit kinase, PEK, involved in translational control.," *Mol. Cell. Biol.*, vol. 18, no. 12, pp. 7499–509, Dec. 1998.
- [120] J. J. Chen and I. M. London, "Regulation of protein synthesis by heme-regulated eIF-2 alpha kinase.," *Trends Biochem. Sci.*, vol. 20, no. 3, pp. 105–8, Mar. 1995.

- [121] B. A. Castilho, R. Shanmugam, R. C. Silva, R. Ramesh, B. M. Himme, and E. Sattlegger, "Keeping the eIF2 alpha kinase Gcn2 in check.," *Biochim. Biophys. Acta*, vol. 1843, no. 9, pp. 1948–68, Sep. 2014.
- [122] R. Iurlaro and C. Muñoz Pinedo, "Cell death induced by endoplasmic reticulum stress.," *FEBS J.*, Nov. 2015.
- [123] M. Pizzato, O. Erlwein, D. Bonsall, S. Kaye, D. Muir, and M. O. McClure, "A one-step SYBR Green I-based product-enhanced reverse transcriptase assay for the quantitation of retroviruses in cell culture supernatants.," *J. Virol. Methods*, vol. 156, no. 1–2, pp. 1–7, Mar. 2009.
- [124] T. Pemovska, M. Kontro, B. Yadav, H. Edgren, S. Eldfors, A. Szwajda, H. Almusa, M. M. Beshpalov, P. Ellonen, E. Elonen, B. T. Gjertsen, R. Karjalainen, E. Kuleskiy, S. Lagström, A. Lehto, M. Lepistö, T. Lundán, M. M. Majumder, J. M. L. Marti, P. Mattila, A. Murumägi, S. Mustjoki, A. Palva, A. Parsons, T. Pirttinen, M. E. Rämetsä, M. Suvela, L. Turunen, I. Väström, M. Wolf, J. Knowles, T. Aittokallio, C. A. Heckman, K. Porkka, O. Kallioniemi, and K. Wennerberg, "Individualized systems medicine strategy to tailor treatments for patients with chemorefractory acute myeloid leukemia.," *Cancer Discov.*, vol. 3, no. 12, pp. 1416–29, Dec. 2013.
- [125] B. Yadav, T. Pemovska, A. Szwajda, E. Kuleskiy, M. Kontro, R. Karjalainen, M. M. Majumder, D. Malani, A. Murumägi, J. Knowles, K. Porkka, C. Heckman, O. Kallioniemi, K. Wennerberg, and T. Aittokallio, "Quantitative scoring of differential drug sensitivity for individually optimized anticancer therapies.," *Sci. Rep.*, vol. 4, p. 5193, Jan. 2014.
- [126] T.-C. Chou, "Drug combination studies and their synergy quantification using the Chou-Talalay method.," *Cancer Res.*, vol. 70, no. 2, pp. 440–6, Jan. 2010.
- [127] I. R. Powley, A. Kondrashov, L. A. Young, H. C. Dobbyn, K. Hill, I. G. Cannell, M. Stoneley, Y.-W. Kong, J. A. Cotes, G. C. M. Smith, R. Wek, C. Hayes, T. W. Gant, K. A. Spriggs, M. Bushell, and A. E. Willis, "Translational reprogramming following UVB irradiation is mediated by DNA-PKcs and allows selective recruitment to the polysomes of mRNAs encoding DNA repair enzymes.," *Genes Dev.*, vol. 23, no. 10, pp. 1207–20, May 2009.
- [128] T. D. Baird and R. C. Wek, "Eukaryotic initiation factor 2 phosphorylation and translational control in metabolism.," *Adv. Nutr.*, vol. 3, no. 3, pp. 307–21, May 2012.
- [129] J. R. Mills, Y. Hippo, F. Robert, S. M. H. Chen, A. Malina, C.-J. Lin, U. Trojahn, H.-G. Wendel, A. Charest, R. T. Bronson, S. C. Kogan, R. Nadon, D. E. Housman, S. W. Lowe, and J. Pelletier, "mTORC1 promotes survival through translational control of Mcl-1," *Proc. Natl. Acad. Sci.*, vol. 105, no. 31, pp. 10853–10858, Jul. 2008.
- [130] R. M. Fritsch, G. Schneider, D. Saur, M. Scheibel, and R. M. Schmid, "Translational repression of MCL-1 couples stress-induced eIF2 alpha phosphorylation to mitochondrial apoptosis initiation.," *J. Biol. Chem.*, vol. 282, no. 31, pp. 22551–62, Aug. 2007.

- [131] L. A. Pradelli, M. Bénéteau, C. Chauvin, M. A. Jacquin, S. Marchetti, C. Muñoz-Pinedo, P. Auberger, M. Pende, and J.-E. Ricci, "Glycolysis inhibition sensitizes tumor cells to death receptors-induced apoptosis by AMP kinase activation leading to Mcl-1 block in translation.," *Oncogene*, vol. 29, no. 11, pp. 1641–52, Mar. 2010.
- [132] I. Sugawara, "Expression and functions of P-glycoprotein (mdr1 gene product) in normal and malignant tissues.," *Acta Pathol. Jpn.*, vol. 40, no. 8, pp. 545–53, Aug. 1990.
- [133] R. Malayeri, M. Filipits, R. W. Suchomel, S. Zöchbauer, K. Lechner, and R. Pirker, "Multidrug resistance in leukemias and its reversal.," *Leuk. Lymphoma*, vol. 23, no. 5–6, pp. 451–8, Nov. 1996.
- [134] M. Watson, A. Roulston, L. Bélec, X. Billot, R. Marcellus, D. Bédard, C. Bernier, S. Branchaud, H. Chan, K. Dairi, K. Gilbert, D. Goulet, M.-O. Gratton, H. Isakau, A. Jang, A. Khadir, E. Koch, M. Lavoie, M. Lawless, M. Nguyen, D. Paquette, E. Turcotte, A. Berger, M. Mitchell, G. C. Shore, and P. Beauparlant, "The small molecule GMX1778 is a potent inhibitor of NAD<sup>+</sup> biosynthesis: strategy for enhanced therapy in nicotinic acid phosphoribosyltransferase 1-deficient tumors.," *Mol. Cell. Biol.*, vol. 29, no. 21, pp. 5872–88, Nov. 2009.
- [135] U. H. Olesen, J. G. Petersen, A. Garten, W. Kiess, J. Yoshino, S.-I. Imai, M. K. Christensen, P. Fristrup, A. V Thougard, F. Björkling, P. B. Jensen, S. J. Nielsen, and M. Sehested, "Target enzyme mutations are the molecular basis for resistance towards pharmacological inhibition of nicotinamide phosphoribosyltransferase.," *BMC Cancer*, 2010.
- [136] W. Wang, K. Elkins, A. Oh, Y.-C. Ho, J. Wu, H. Li, Y. Xiao, M. Kwong, M. Coons, B. Brillantes, E. Cheng, L. Crocker, P. S. Dragovich, D. Sampath, X. Zheng, K. W. Bair, T. O'Brien, and L. D. Belmont, "Structural basis for resistance to diverse classes of NAMPT inhibitors.," *PLoS One*, vol. 9, no. 10, p. e109366, Jan. 2014.
- [137] M. McDermott, A. J. Eustace, S. Busschots, L. Breen, J. Crown, M. Clynes, N. O'Donovan, and B. Stordal, "In vitro Development of Chemotherapy and Targeted Therapy Drug-Resistant Cancer Cell Lines: A Practical Guide with Case Studies.," *Front. Oncol.*, vol. 4, no. March, p. 40, 2014.
- [138] G. Wei, D. Twomey, J. Lamb, K. Schlis, J. Agarwal, R. W. Stam, J. T. Opferman, S. E. Sallan, M. L. den Boer, R. Pieters, T. R. Golub, and S. A. Armstrong, "Gene expression-based chemical genomics identifies rapamycin as a modulator of MCL1 and glucocorticoid resistance.," *Cancer Cell*, vol. 10, no. 4, pp. 331–42, Oct. 2006.
- [139] N. Z. Lu and J. a Cidlowski, "Translational regulatory mechanisms generate N-terminal glucocorticoid receptor isoforms with unique transcriptional target genes.," *Mol. Cell*, vol. 18, no. 3, pp. 331–42, Apr. 2005.
- [140] G. Zoppoli, M. Cea, D. Soncini, F. Fruscione, J. Rudner, E. Moran, I. Caffa, D. Bedognetti, G. Motta, R. Ghio, F. Ferrando, A. Ballestrero, S. Parodi, C. Belka, F. Patrone, S. Bruzzone, and A. Nencioni, "Potent synergistic interaction

between the Nampt inhibitor APO866 and the apoptosis activator TRAIL in human leukemia cells.," *Exp. Hematol.*, vol. 38, no. 11, pp. 979–88, Nov. 2010.

- [141] A. Cagnetta, M. Cea, T. Calimeri, C. Acharya, M. Fulciniti, Y.-T. Tai, T. Hideshima, D. Chauhan, M. Y. Zhong, F. Patrone, A. Nencioni, M. Gobbi, P. Richardson, N. Munshi, and K. C. Anderson, "Intracellular NAD<sup>+</sup> depletion enhances bortezomib-induced anti-myeloma activity.," *Blood*, vol. 122, no. 7, pp. 1243–55, Aug. 2013.
- [142] J. Barretina, G. Caponigro, N. Stransky, K. Venkatesan, A. A. Margolin, S. Kim, C. J. Wilson, J. Lehár, G. V Kryukov, D. Sonkin, A. Reddy, M. Liu, L. Murray, M. F. Berger, J. E. Monahan, P. Morais, J. Meltzer, A. Korejwa, J. Jané-Valbuena, F. A. Mapa, J. Thibault, E. Bric-Furlong, P. Raman, A. Shipway, I. H. Engels, J. Cheng, G. K. Yu, J. Yu, P. Aspesi, M. de Silva, K. Jagtap, M. D. Jones, L. Wang, C. Hatton, E. Palesscandolo, S. Gupta, S. Mahan, C. Sougnez, R. C. Onofrio, T. Liefeld, L. MacConaill, W. Winckler, M. Reich, N. Li, J. P. Mesirov, S. B. Gabriel, G. Getz, K. Ardlie, V. Chan, V. E. Myer, B. L. Weber, J. Porter, M. Warmuth, P. Finan, J. L. Harris, M. Meyerson, T. R. Golub, M. P. Morrissey, W. R. Sellers, R. Schlegel, and L. A. Garraway, "The Cancer Cell Line Encyclopedia enables predictive modelling of anticancer drug sensitivity.," *Nature*, vol. 483, no. 7391, pp. 603–7, Mar. 2012.
- [143] A. Cagnetta, I. Caffa, C. Acharya, D. Soncini, P. Acharya, S. Adamia, I. Pierri, M. Bergamaschi, A. Garuti, G. Fraternali, L. Mastracci, A. Provenzani, C. Zucal, G. Damonte, A. Salis, F. Montecucco, F. Patrone, A. Ballestrero, S. Bruzzone, M. Gobbi, A. Nencioni, and M. Cea, "APO866 Increases Antitumor Activity of Cyclosporin-A by Inducing Mitochondrial and Endoplasmic Reticulum Stress in Leukemia Cells.," *Clin. Cancer Res.*, vol. 21, no. 17, pp. 3934–45, Sep. 2015.
- [144] P. J. Hjarnaa, E. Jonsson, S. Latini, S. Dhar, R. Larsson, E. Bramm, T. Skov, and L. Binderup, "CHS 828, a novel pyridyl cyanoguanidine with potent antitumor activity in vitro and in vivo.," *Cancer Res.*, vol. 59, no. 22, pp. 5751–7, Nov. 1999.
- [145] M. Cea, D. Soncini, F. Fruscione, L. Raffaghello, A. Garuti, L. Emionite, E. Moran, M. Magnone, G. Zoppoli, D. Reverberi, I. Caffa, A. Salis, A. Cagnetta, M. Bergamaschi, S. Casciaro, I. Pierri, G. Damonte, F. Ansaldi, M. Gobbi, V. Pistoia, A. Ballestrero, F. Patrone, S. Bruzzone, and A. Nencioni, "Synergistic interactions between HDAC and sirtuin inhibitors in human leukemia cells.," *PLoS One*, vol. 6, no. 7, p. e22739, Jan. 2011.
- [146] I. Bajrami, A. Kigozi, A. Van Weverwijk, R. Brough, J. Frankum, C. J. Lord, and A. Ashworth, "Synthetic lethality of PARP and NAMPT inhibition in triple-negative breast cancer cells.," *EMBO Mol. Med.*, vol. 4, no. 10, pp. 1087–96, Oct. 2012.
- [147] A. von Heideman, A. Berglund, R. Larsson, and P. Nygren, "Safety and efficacy of NAD depleting cancer drugs: results of a phase I clinical trial of CHS 828 and overview of published data.," *Cancer Chemother. Pharmacol.*, vol. 65, no. 6, pp. 1165–72, May 2010.
- [148] D. B. Shackelford, E. Abt, L. Gerken, D. S. Vasquez, A. Seki, M. Leblanc, L. Wei, M. C. Fishbein, J. Czernin, P. S. Mischel, and R. J. Shaw, "LKB1

- Inactivation Dictates Therapeutic Response of Non-Small Cell Lung Cancer to the Metabolism Drug Phenformin,” *Cancer Cell*, vol. 23, no. 2, pp. 143–158, Feb. 2013.
- [149] T. Zhou, G. Li, B. Cao, L. Liu, Q. Cheng, H. Kong, C. Shan, X. Huang, J. Chen, and N. Gao, “Downregulation of Mcl-1 through inhibition of translation contributes to benzyl isothiocyanate-induced cell cycle arrest and apoptosis in human leukemia cells.,” *Cell Death Dis.*, vol. 4, p. e515, Jan. 2013.
- [150] A. A. Sauve, C. Munshi, H. C. Lee, and V. L. Schramm, “The reaction mechanism for CD38. A single intermediate is responsible for cyclization, hydrolysis, and base-exchange chemistries.,” *Biochemistry*, vol. 37, no. 38, pp. 13239–49, Sep. 1998.
- [151] S. Garavaglia, S. Bruzzone, C. Cassani, L. Canella, G. Allegrone, L. Sturla, E. Mannino, E. Millo, A. De Flora, and M. Rizzi, “The high-resolution crystal structure of periplasmic Haemophilus influenzae NAD nucleotidase reveals a novel enzymatic function of human CD73 related to NAD metabolism.,” *Biochem. J.*, vol. 441, no. 1, pp. 131–41, Jan. 2012.
- [152] J. Stagg, U. Divisekera, N. McLaughlin, J. Sharkey, S. Pommey, D. Denoyer, K. M. Dwyer, and M. J. Smyth, “Anti-CD73 antibody therapy inhibits breast tumor growth and metastasis.,” *Proc. Natl. Acad. Sci. U. S. A.*, vol. 107, no. 4, pp. 1547–52, Jan. 2010.
- [153] E. Ferrero and F. Malavasi, “The metamorphosis of a molecule: from soluble enzyme to the leukocyte receptor CD38.,” *J. Leukoc. Biol.*, vol. 65, no. 2, pp. 151–61, Feb. 1999.
- [154] Y. Xiao, K. Elkins, J. K. Durieux, L. Lee, J. Oeh, L. X. Yang, X. Liang, C. Delnagro, J. Tremayne, M. Kwong, B. M. Liederer, P. K. Jackson, L. D. Belmont, D. Sampath, and T. O’Brien, “Dependence of Tumor Cell Lines and Patient-Derived Tumors on the NAD Salvage Pathway Renders Them Sensitive to NAMPT Inhibition with GNE-618.,” *Neoplasia*, vol. 15, no. 10, pp. 1151–60, Oct. 2013.
- [155] D. S. Shames, K. Elkins, K. Walter, T. Holcomb, P. Du, D. Mohl, Y. Xiao, T. Pham, P. M. Haverty, B. Liederer, X. Liang, R. L. Yauch, T. O’Brien, R. Bourgon, H. Koeppen, and L. D. Belmont, “Loss of NAPRT1 Expression by Tumor-Specific Promoter Methylation Provides a Novel Predictive Biomarker for NAMPT Inhibitors,” *Clin. Cancer Res.*, vol. 19, no. 24, pp. 6912–6923, Oct. 2013.
- [156] M. Patel, P. Dalvi, M. Gokulgandhi, S. Kesh, T. Kohli, D. Pal, and A. K. Mitra, “Functional characterization and molecular expression of large neutral amino acid transporter (LAT1) in human prostate cancer cells.,” *Int. J. Pharm.*, vol. 443, no. 1–2, pp. 245–53, Feb. 2013.
- [157] M. Platten, W. Wick, and B. J. Van den Eynde, “Tryptophan Catabolism in Cancer: Beyond IDO and Tryptophan Depletion,” *Cancer Res.*, vol. 72, no. 21, pp. 5435–5440, Oct. 2012.

- [158] C. Rosilio, M. Nebout, V. Imbert, E. Griessinger, Z. Neffati, J. Benadiba, T. Hagenbeek, H. Spits, J. Reverso, D. Ambrosetti, J.-F. Michiels, B. Bailly-Maitre, H. Endou, M. F. Wempe, and J.-F. Peyron, "L-type amino-acid transporter 1 (LAT1): a therapeutic target supporting growth and survival of T-cell lymphoblastic lymphoma/T-cell acute lymphoblastic leukemia.," *Leukemia*, Dec. 2014.

## ORIGINAL AUTHORSHIP

I Chiara Zucal confirm that this is my own work and the use of all material from other sources has been properly and fully acknowledged.

A handwritten signature in black ink on a light gray background. The signature reads "Chiara Zucal" in a cursive, slightly slanted script.

## SIDE PROJECTS

During my PhD I have also been involved in side projects mainly focused on the RNA binding protein HuR/ELAVL1, a widely characterized eukaryotic post-transcriptional regulator. HuR mediates cellular response to different kinds of stimuli, namely proliferation, survival and apoptosis, helping to determine cell fate by binding to many target mRNAs and influencing their splicing, shuttling, stability and translation efficiency. An impaired localization and activity of HuR have been associated with many forms of cancer and the protein has generated interest as a potent drug target.

These side projects led to two publications:

**Targeting the Multifaceted HuR Protein, Benefits and Caveats.**

Zucal C *et al.*, *Curr Drug Targets* 2015.

**Dihydropantothine-I interferes with the RNA-binding activity of HuR affecting its posttranscriptional function.**

D'Agostino VG *et al.*, *Sci Rep* 2015.

Since the investigated topics are not closely related to the main project, the side projects have not been discussed in the thesis.

## APPENDIX

**EIF2A-dependent translational arrest protects leukemia cells from the energetic stress induced by NAMPT inhibition.**

Zucal C *et al.*, *BMC Cancer* 2015.....p88

**APO866 Increases Antitumor Activity of Cyclosporin-A by Inducing Mitochondrial and Endoplasmic Reticulum Stress in Leukemia Cells.**

Cagnetta A *et al.*, *Clin Cancer Res* 2015.....p102

Supplementary Tables are provided separately as a compress file (.zip) called "Supplementary Tables".

RESEARCH ARTICLE

Open Access



# EIF2A-dependent translational arrest protects leukemia cells from the energetic stress induced by NAMPT inhibition

Chiara Zucal<sup>1†</sup>, Vito G. D'Agostino<sup>1†</sup>, Antonio Casini<sup>2</sup>, Barbara Mantelli<sup>1</sup>, Natthakan Thongon<sup>1</sup>, Debora Soncini<sup>4</sup>, Irene Caffa<sup>3</sup>, Michele Cea<sup>3</sup>, Alberto Ballestrero<sup>3</sup>, Alessandro Quattrone<sup>4</sup>, Stefano Indraccolo<sup>5</sup>, Alessio Nencioni<sup>3\*</sup> and Alessandro Provenzani<sup>1\*</sup>

## Abstract

**Background:** Nicotinamide phosphoribosyltransferase (NAMPT), the rate-limiting enzyme in NAD<sup>+</sup> biosynthesis from nicotinamide, is one of the major factors regulating cancer cells metabolism and is considered a promising target for treating cancer. The prototypical NAMPT inhibitor FK866 effectively lowers NAD<sup>+</sup> levels in cancer cells, reducing the activity of NAD<sup>+</sup>-dependent enzymes, lowering intracellular ATP, and promoting cell death.

**Results:** We show that FK866 induces a translational arrest in leukemia cells through inhibition of MTOR/4EBP1 signaling and of the initiation factors EIF4E and EIF2A. Specifically, treatment with FK866 is shown to induce 5'AMP-activated protein kinase (AMPK) activation, which, together with EIF2A phosphorylation, is responsible for the inhibition of protein synthesis. Notably, such an effect was also observed in patients' derived primary leukemia cells including T-cell Acute Lymphoblastic Leukemia. Jurkat cells in which AMPK or LKB1 expression was silenced or in which a non-phosphorylatable EIF2A mutant was ectopically expressed showed enhanced sensitivity to the NAMPT inhibitor, confirming a key role for the LKB1-AMPK-EIF2A axis in cell fate determination in response to energetic stress *via* NAD<sup>+</sup> depletion.

**Conclusions:** We identified EIF2A phosphorylation as a novel early molecular event occurring in response to NAMPT inhibition and mediating protein synthesis arrest. In addition, our data suggest that tumors exhibiting an impaired LKB1-AMPK-EIF2A response may be especially susceptible to NAMPT inhibitors and thus become an elective indication for this type of agents.

**Keywords:** NAMPT, EIF2A, AMPK, Energetic stress, Translation arrest, UPR

## Background

Aberrant activation of metabolic pathways has emerged as an hallmark of proliferating cancer cells and pharmaceutical approaches targeting cell metabolism hold potential for treating cancer [1]. Nicotinamide adenine dinucleotide (NAD<sup>+</sup>) plays a key role in different biochemical processes, acting as a coenzyme in redox reactions or as a substrate for NAD<sup>+</sup> degrading enzymes, such as poly(ADP-ribose) polymerases (PARPs), cluster of differentiation 38 (CD38), and sirtuins. Intracellular NAD<sup>+</sup> is continuously

replenished utilizing either tryptophan, nicotinamide, nicotinic acid or nicotinamide riboside as a substrate [2], and nicotinamide phosphoribosyltransferase, NAMPT, is the rate-limiting enzyme for NAD<sup>+</sup> biosynthesis from nicotinamide in mammalian cells [3]. High NAMPT levels, whose activity appears to be also important in the differentiation of myeloid cells [4], were shown to be required to support cancer cell growth, survival and epithelial-mesenchymal transition (EMT) transition [5, 6], and have been reported in different types of tumors [7, 8]. In line with these notions, several studies have highlighted a strong activity of NAMPT inhibitors in preclinical models of inflammatory and malignant disorders, including leukemia [2, 9–11]. FK866, a prototypical NAMPT inhibitor, was found to

\* Correspondence: alessio.nencioni@unige.it; alessandro.provenzani@unitn.it

<sup>†</sup>Equal contributors

<sup>3</sup>Department of Internal Medicine, University of Genoa, Genoa, Italy

<sup>1</sup>Laboratory of Genomic Screening, CIBIO, University of Trento, Trento, Italy

Full list of author information is available at the end of the article

promote cell death in both lymphoid- and myeloid-derived hematological malignancies and its activity clearly resulted from intracellular NAD<sup>+</sup> depletion [12–14]. Notably, opposite to cancer cells, activated immune cells [10], along with many other types of healthy cells, such as hematopoietic stem cells [12], appear unaffected by NAMPT inhibitors, and consistently, agents such as FK866 or CHS-828 are well tolerated in patients [15, 16].

The molecular consequences upon NAMPT inhibition are only partially understood. The induced NAD<sup>+</sup> depletion clearly affects intracellular ATP levels resulting in mitochondrial dysfunction and activation of cell death pathways: reactive oxygen species generation and activation of the apoptotic cascade have both been involved in cell demise in response to NAMPT inhibitors [17]. ATP depletion has been related to the loss of plasma membrane homeostasis invariably leading to oncotic cell death [18]. Different groups have suggested a role for autophagic cell death in the cytotoxic activity of these drugs [10, 12, 13, 19]. In particular, Cea and colleagues proposed that FK866 would induce autophagy *via* activation of transcription factor EB (TFEB), a master regulator of the lysosomal-autophagic pathway [20], and through MTORC1/AKT and ERK1/2 pathway inhibition [21]. There is also evidence that AMP-activated protein kinase (AMPK), an important coordinator of metabolic pathways in response to energetic fluctuations [22], is activated by FK866 in prostate cancer cells affecting lipogenesis [23] and in hepatocarcinoma cells with impact on MTOR/4EBP1 signaling [24]. Moreover, NAMPT-dependent AMPK activation associated with deacetylation of liver kinase B1 (LKB1), an upstream kinase of AMPK, has been linked with modulation of NAD levels and with significant impact on neuron cell survival [25]. Translation inhibition is often observed during cell stress [26] and this event often involves a re-programming of translation leading to differential regulation of mRNAs, occurring also *via* alternative mechanisms, aimed at reorganizing cell physiology to respond to the insult.

In this study, we focused on the pre-toxic molecular events induced by FK866 in acute lymphoblastic leukemia cells, known to be sensitive to the drug [10], in order to define the molecular mechanism favoring cell death or cell survival. A marked global protein synthesis inhibition represented an early cellular response associated with the FK866-induced energetic stress and here we show that AMPK-EIF2A is a central hub in mediating this effect and is responsible for cell fate decisions.

## Methods

### Cell lines, primary B-CLL cell and T-ALL PDX isolation

Human Jurkat T-cell acute lymphoblastic leukemia (T-ALL) cells were purchased from the InterLab Cell Line Collection bank (ICLC HTL01002). SUP-T1 cells were

purchased from ATCC (CRL-1942) and Molt-4 Clone 8 from NIH AIDS Reagent Program (Catalog #: 175). Human lung carcinoma A594 (CCL-185) and H460 (HTB-177) cells were purchased from ATCC. These cells were transduced with retroviral vectors encoding either LKB1 cDNA (pBABE-LKB1) or the pBABE control vector. Cell lines were grown in complete RPMI 1640 (Gibco Life Technologies) supplemented with 10 % fetal bovine serum (FBS, Lonza), 2 mM L-glutamine, 100 U/ml penicillin-streptomycin (Lonza). All cell lines were grown at 37 °C under 5 % CO<sub>2</sub> and regularly tested for mycoplasma contamination. For primary B-CLL cell isolation, a 5 ml blood sample was obtained from patients presenting with marked lymphocytosis (>20000/ $\mu$ l) according to a protocol that was approved by the Ethics Committee of the Hospital IRCCS AOU San Martino IST in Genoa (#840, February 18th 2011). Patients' written informed consent was collected. B-CLL cells were isolated by density gradient centrifugation on Ficoll-Hypaque (Biotest). The phenotype of the obtained cell preparations was confirmed by immunostaining with anti-CD19, anti-CD5, and anti-CD23 (Immunotech), and subsequent flow cytometric analysis. T-ALL xenografts (PD T-ALL) were established from BM (bone marrow) of newly diagnosed ALL pediatric patients, according to a protocol approved by the ethics committee of the University of Padova (Project number 16B/2013). The PD T-ALL cells used in this study have been published elsewhere [27]. At time of PD T-ALL establishment, written informed consent was obtained from the parents of the children. *In vitro* studies were performed with T-ALL cultures established from the spleen of the xenografts. Purity of the cultures (in terms of percentage of human CD5<sup>+</sup> cells) was checked by flow cytometry and was always >85 %. Research carried out on human material was in compliance with the Helsinki Declaration.

### Chemicals

FK866 (sc-205325) was bought from Santa Cruz, Compound C (P5499), Nicotinic acid (N0761), Actinomycin D (A9415), (S)-(+)-Camptothecin (C9911), Cycloheximide (C1988), MG-132 (M7449), Doxorubicin hydrochloride (D1515) and Dexamethasone (D4902) were bought from Sigma-Aldrich, CHS-828 (200484-11-3) from Cayman chemical, Torin 1 (S2827) and Rapamycin (S1039) from Selleck Chemicals, Cisplatin (ALX-400-040) from Enzo Life Sciences and Propidium Iodide Staining Solution from BD Pharmingen. Jurkat cells were treated with drugs dissolved in DMSO at the same cell density (5X10<sup>5</sup> cells/ml).

### Viability assays

Cell viability was assessed with the Annexin V-FITC Apoptosis Detection Kit I and 7-Aminoactinomycin D

(7-AAD) Staining Solution (BD Pharmingen) according to manufacturer's instruction.  $EC_{50}$  values of FK866 were determined by nonlinear regression analysis (GraphPad Prism software v5.01,) vs viable cells in mock conditions (DMSO).

Jurkat, A549 and H460 cell lines were grown and treated in 96 well-plate for 48 h. Cells were then assayed for viability using Thiazolyl blue tetrazolium bromide (MTT) M5655 (Sigma). In brief, MTT (5 mg/ml) at 10 % volume of culture media was added to each well and cells were further incubated for 2 h at 37 °C. Then 100  $\mu$ l of DMSO was used to dissolve formazan. Absorbance was then determined at 565 nm by microplate reader. Cell survival was calculated and  $EC_{50}$  values were determined.

#### Determination of $NAD^+$ -NADH and ATP levels and caspase/protease activity

Intracellular  $NAD^+$ -NADH content was assessed with a  $NAD^+$ -NADH Quantification Kit (BioVision) according to the manufacturer's protocol. Intracellular ATP content was determined using Cell titer Glo Luminescent Cell Viability Assay (Promega).  $NAD^+$ -NADH and ATP values were normalized to the number of viable cells as determined using Trypan Blue (Lonza). EnzChek Protease Assay Kit, containing a casein derivative labeled with green-fluorescent BODIPY FL (Life Technologies), was used to determine protease activity after treatment of  $2 \times 10^6$  cells. Cells were washed once with PBS and lysed in 500  $\mu$ l of 1X digestion buffer, sonicated and centrifuged for 5 min at maximum speed. One  $\mu$ l of the BODIPY casein 100X was added to 100  $\mu$ l of the supernatant and incubated for 1 h protected from light. Fluorescence was measured and normalized to protein concentration in the cell lysates (Bradford Reagent, Sigma). Caspase-Glo 3/7 Assay (Promega) was used to quantify caspase activity.

#### RNA and protein click-iT labeling kits

Click-iT RNA Alexa Fluor 488 Imaging Kit (Life Technologies) was used to quantify the level of global RNA synthesis by flow-cytometry. Jurkat cells ( $3 \times 10^6$ /sample) were treated for 45 h with FK866 (or DMSO) and then incubated for 3 h with 1X EU working solution without removing the drug-containing media. EU detection was performed following the manufacturer's protocol after cell fixation and permeabilization. Click-iT AHA Alexa Fluor 488 Protein Synthesis Assay (Life Technologies) was used to measure the rate of translation. Cells ( $3 \times 10^6$ /sample) were treated for 45 h with FK866, centrifuged and incubated for 3 h with 50  $\mu$ M AHA in L-methionine-free medium (RPMI Medium 1640, Sigma-Aldrich) containing the drug (or DMSO). After fixation and permeabilization, AHA incorporation was

assessed by flow cytometry. 7-AAD Staining Solution (0.25  $\mu$ g/sample) allowed the exclusion of non-viable cells.

#### Western blotting, antibody list and plasmids

Cells were lysed for 5 min on ice in RIPA lysis buffer supplemented with Protease Inhibitor Cocktail (Sigma-Aldrich). After sonication and clarification, equal amounts of proteins were separated by SDS-PAGE and blotted onto PVDF membranes (Immobilon-P, Millipore), as in [28]. The antibodies used were: 4EBP1 (sc-6936), p-4EBP1 (Ser 65/Thr 70; sc-12884), EIF4E (sc-9976), p-EIF4E (Ser 209; sc-12885), AKT1/2/3 (sc-8312), p-AKT1/2/3 (Ser 473; sc-7985), MTOR (sc-8319), BCL-2 (sc-509), NAMPT (sc-130058) from Santa Cruz; EIF2S1 (ab26197), p-EIF2S1 (Ser 51; ab32157), and p-MTOR (Ser 2448; ab1093) from Abcam; AMPK $\alpha$  (2603), p-AMPK $\alpha$  (Thr 172; 2531), ACC (3676) and p-ACC (Ser 79; 3661) and MCL1 (4572) from Cell Signaling. A mouse anti- $\beta$ -actin antibody (3700, Cell Signaling) was used as a protein loading control. eIF2a 1 (Addgene plasmid # 21807), eIF2a 2 (Addgene plasmid # 21808) and eIF2a 3 (Addgene plasmid # 21809) were a gift from David Ron. A549 cells were transfected using Lipofectamine 3000 Reagent from Life Technologies. Cells were plated in 6 well and transfected at 70 % confluence for 24 h with 1  $\mu$ g of DNA. Jurkat cells were transfected for 48 h with 1  $\mu$ g of DNA in 24- well plate.

#### Real-time PCR

Total RNA was extracted with Quick-RNA MiniPrep kit (Zymo Research) and treated with DNase. cDNA was synthesized using RevertAid First Strand cDNA Synthesis Kit (Fermentas) following the manufacturer's recommendation. Real-time PCR reactions were performed using the KAPA SYBR FAST Universal qPCR Kit on a CFX96 Real-Time PCR Detection System (BioRad). Relative mRNA quantification was obtained with the  $\Delta C_q$  method using  $\beta$ -actin (*ACTB*) as housekeeping gene. Primers' sequences are reported as follows: *BiP/Grp78* (Fw: TGTTCAACCAATTATCAGCAAACCTC Rev: TTC TGCTGTATCCTCTTCACCAGT) *ACTB* (Fw: CTGGA ACGGTGAAGGTGACA Rev: AGGGACTTCCTGTAA CAATGCA) *STK11/LKB1* (Fw: GAGCTGATGTCGGT GGGTATG Rev: CACCTTGCCGTAAGAGCCT).

#### Lentiviral particles production and luciferase assay

Lentiviral particles were produced using the pHR-SIN-R-Myc-E, pHR-SIN-F-HCV-R and pHR-SIN-F-CrPV-R transfer vectors [29], coding for reporter genes controlled by a cMyc-5'UTR, HCV or CrPV IRESes regulated translation, by co-transfection of 293 T cells with the packaging plasmid pCMV-deltaR8.91 and the VSV envelope-coding plasmid pMD2.G. Five thousand Jurkat cells/sample were transduced. After treatment with FK866, luciferase activity

was measured using the Dual-Glo Luciferase Assay System (Promega) and normalized for protein concentration.

### Silencing with shRNAs

The pLKO.1-based lentiviral plasmids containing AMPK $\alpha$ 1 shRNA (TRCN0000000859), AMPK $\alpha$ 2 shRNA (TRCN0000002169) or NAMPT shRNA expression cassette (TRCN0000116180) and (TRCN0000116181) were purchased from Sigma-Aldrich. Scramble shRNA (Addgene plasmid #1864 [30]) was used as a control. Vectors were produced in 293 T cells by cotransfection of the different transfer vectors with the packaging plasmid pCMV-deltaR8.91 and the VSV envelope-coding plasmid pMD2.G. 1 million of Jurkat cells were transduced with lentiviral particles expressing the control (shSCR) or NAMPT-silencing short hairpin RNA (shNAMPT) by spinning them down with vector-containing supernatants for 2 h at 1600xg at room temperature and leaving them incubate overnight at 37 °C without replacing the transduction supernatant. After changing the medium, the cells were further incubated for 72 h before collection for WB.

For AMPK silencing experiments, Jurkat cells were first transduced with the shRNA vector targeting the  $\alpha$ 1 subunit (shAMPK $\alpha$ 1) as reported before. After 24 h from the first transduction the cells were then transduced again, following the same protocol, with the lentiviral vector coding for the shRNA targeting the AMPK  $\alpha$ 2 subunit (shAMPK $\alpha$ 2). After changing the medium the next morning, the cells were further incubated for 48 h and then treated for additional 48 h with or without (DMSO) 5 nM of FK866.

To obtain LKB1 silencing, pLKO.1 transfer vectors were prepared by cloning annealed oligos coding for shRNAs (clone TRCN0000000408 for LKB1-A and clone TRCN0000000409 for LKB1-B) into the TRC cloning vector (Addgene plasmid #10878 [31]) according to the TRC standard protocol. Cells were transduced by spinning them down with vector-containing supernatants and leaving them incubate overnight. After changing the medium, the cells were incubated for 72 h and then treated for additional 48 h with or without FK866.

### Statistical analysis

Experiments were performed in biological triplicates. *T*-test was used to calculate final *p*-values, without assuming variances to be equal (Welch's *t*-test). *P*-value <0.05 was considered statistically significant.

## Results

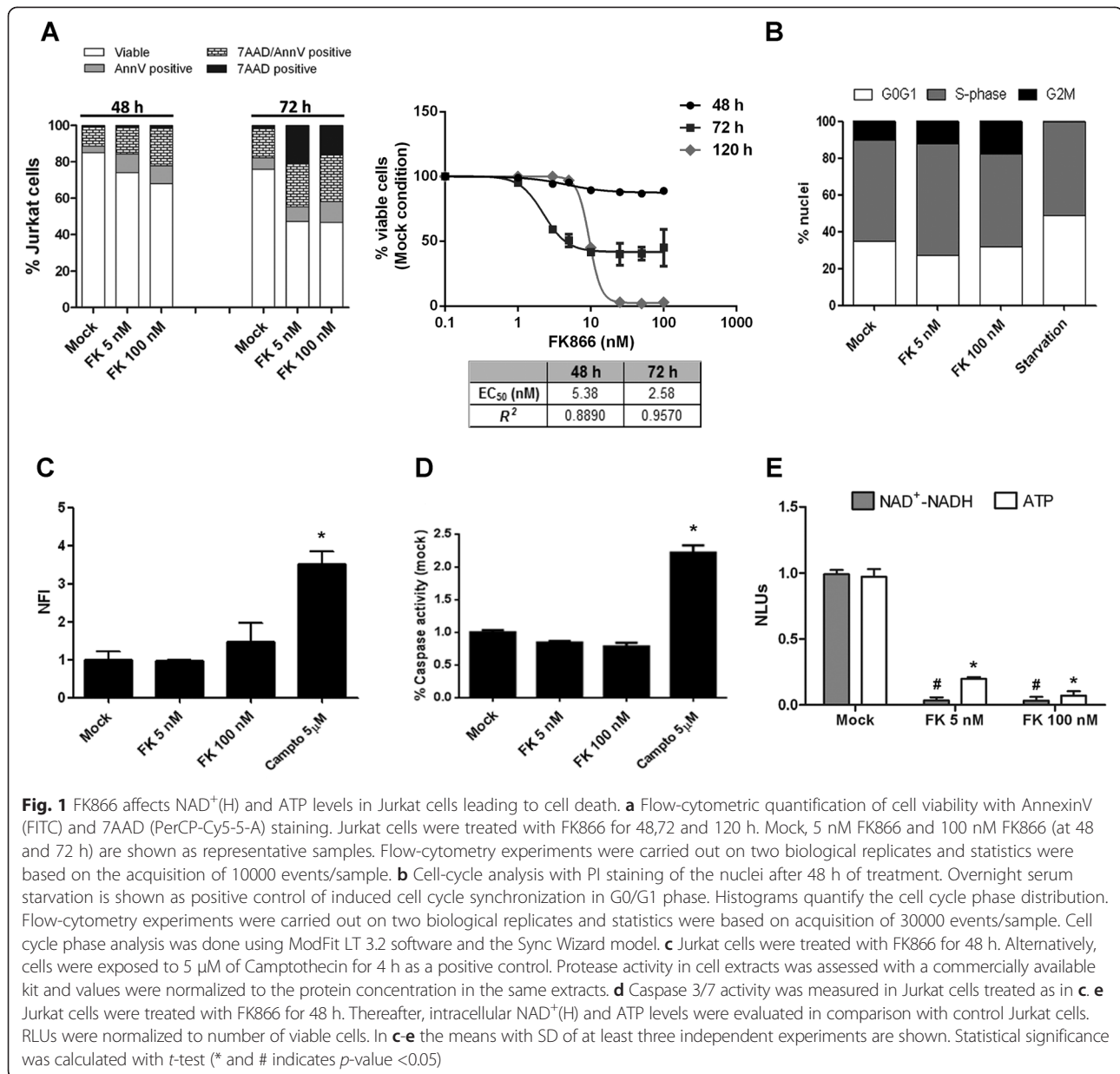
### Sensitivity of leukemia cells to the NAMPT inhibitor FK866

FK866 was previously shown to have cytotoxic activity at nanomolar concentrations against different types of

hematological malignancies, including myeloid and lymphoid leukemias and multiple myeloma [12, 21]. We monitored FK866-induced cell death in Jurkat cells by quantifying early and late apoptosis with 7AAD and Annexin V staining. In line with previous reports, FK866 cytotoxic activity started to become evident between 48 and 72 h of exposure with approximately 74 and 47 % of viable cells left at these time points when cells are treated with FK866 100 nM (Fig. 1a), respectively. This suggests the existence of a lag phase through which cells can cope with the energetic shortage. Starting from a concentration of 10 nM, FK866 cytotoxic activity reached a plateau and an EC<sub>50</sub> of 5.3 nM could be estimated after 48 h of exposure (Fig. 1a). Indeed, at 120 h we measured an effective IC<sub>50</sub> of 10 nM, highlighting the inability of these cells to compensate for the energetic stress induced by FK866 in long term treatment (Fig. 1a). Cell cycle analysis of FK866-treated cells, at 48 h, showed a non-significant accumulation of cells in G2/M phase, while, as predicted, serum starvation resulted in accumulation of cells in G0/G1 phase (Fig. 1b and Additional file 1A). Forty-eight hours treatment with FK866 led to approximately 25 % of cell death, but did not lead to massive protease or caspase activation (Fig. 1c and d). However, 5 nM FK866 was sufficient to effectively reduce NAD<sup>+</sup>(H) and ATP levels in Jurkat cells, representing a pre-toxic experimental condition to apply for further experiments (Fig. 1e).

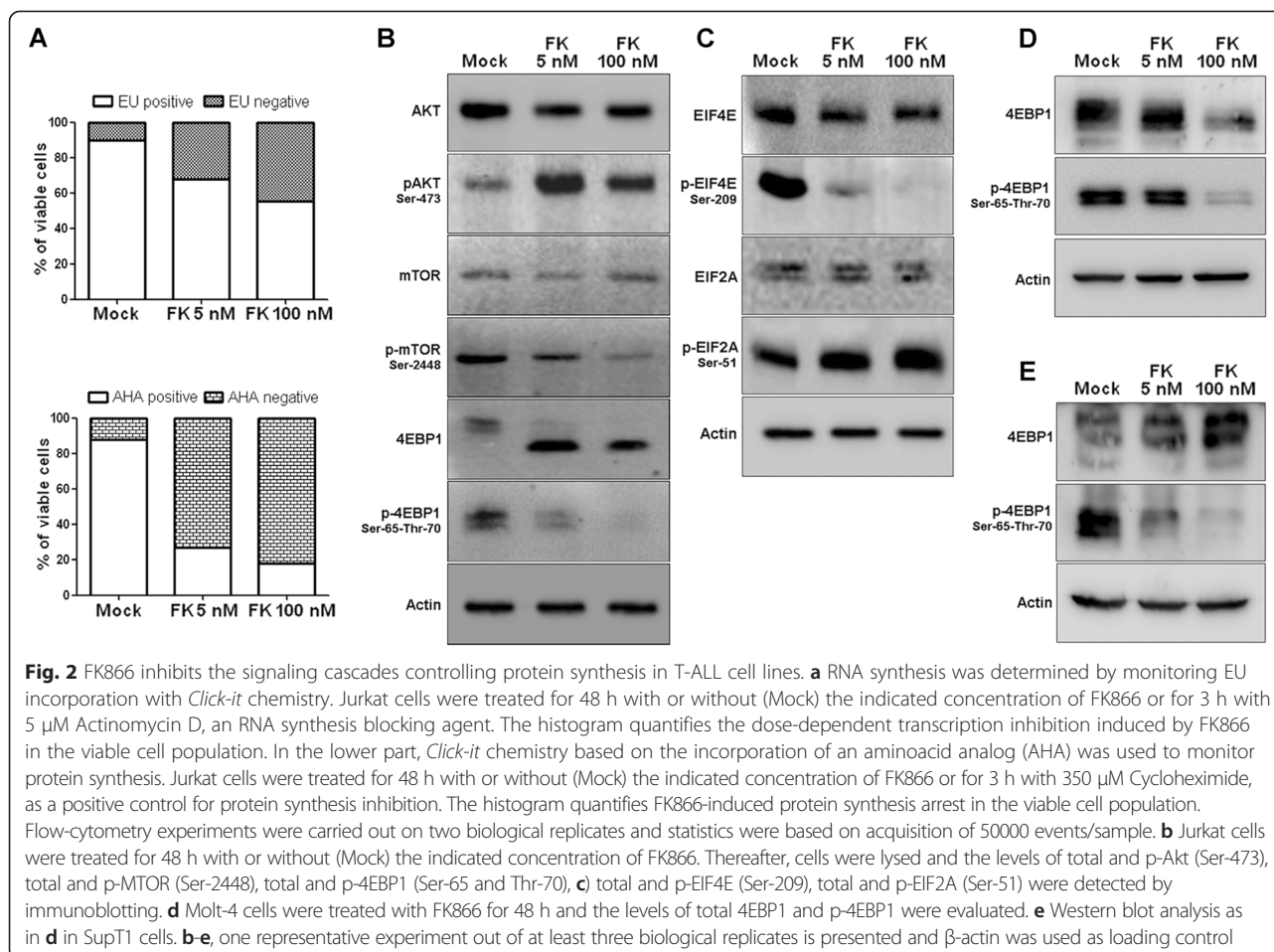
### FK866 and NAMPT ablation blocks cap-dependent translation, but not gene transcription, through MTOR/4EBP1, EIF4E, and EIF2A inhibition in cancer cells

We assessed the impact of FK866 on global transcriptional and translational efficiencies in Jurkat cells. Global RNA transcription and translation were monitored using the *Click-it* chemistry and flow-cytometry by the incorporation of the nucleoside analog 5-ethynyl uridine (EU) and of an aminoacid analog (AHA), respectively. In the viable Jurkat cell population, FK866 caused a reduction in the incorporation of EU in a dose-dependent manner, with 70 and 55 % of transcriptionally active cells in the presence of 5 and 100 nM FK866, respectively. Thus, despite NAD<sup>+</sup> and ATP depletion, cells treated with FK866 for 48 h essentially retained their ability to perform RNA transcription. By contrast, even 5 nM FK866 determined a striking reduction (up to 30 %) of the fraction of viable cells showing active protein synthesis (Fig. 2a and Additional file 1B). The utilization of bicistronic reporter assays to test the efficacy of cap or IRES (Internal Ribosome Entry Site) dependent translation confirmed that FK866 induced a strong translation arrest with a major impact on cap-dependent translation in Jurkat cells (Additional file 2).



Since the initiation phase is considered the limiting step of translation [32], we evaluated the activation of three signaling pathways regulating the canonical cap-dependent translation process. The Mammalian Target of Rapamycin (MTOR) kinase regulates the p70 ribosomal S6 kinase (p70-S6K) and the eukaryotic translation initiation factor 4E-binding protein 4EBP1, whose phosphorylation determines EIF4E availability for its interacting partner EIF4G, which is involved in mRNA recruitment to the ribosomes for protein translation [32]. It has been recently shown that FK866 induces MTOR de-phosphorylation [24], thereby inducing autophagic cell death in multiple myeloma cells [21, 33]. As shown in Fig. 2b, Jurkat cells treated with FK866

indeed showed a marked de-phosphorylation of MTOR and 4EBP1. Enhanced AKT phosphorylation at Ser-473 was also observed (Fig. 2b), which is in line with the paradoxical activation of AKT by MTORC2 complex following inhibition of MTOR as reported with different MTOR inhibitors in multiple myeloma cells [34]. Notably, treatment with FK866 led to a previously unappreciated de-phosphorylation of EIF4E on serine 209, suggesting that the MAP Kinase Interacting Serine/Threonine Kinase (MNK)-dependent pathway is also affected [35] (Fig. 2c), and to an increased phosphorylation on Ser-51 of EIF2A, an initiation factor that transfers methionyl-initiator tRNA (Met) to the small ribosomal subunit. When phosphorylated (Fig. 2c), EIF2A loses its

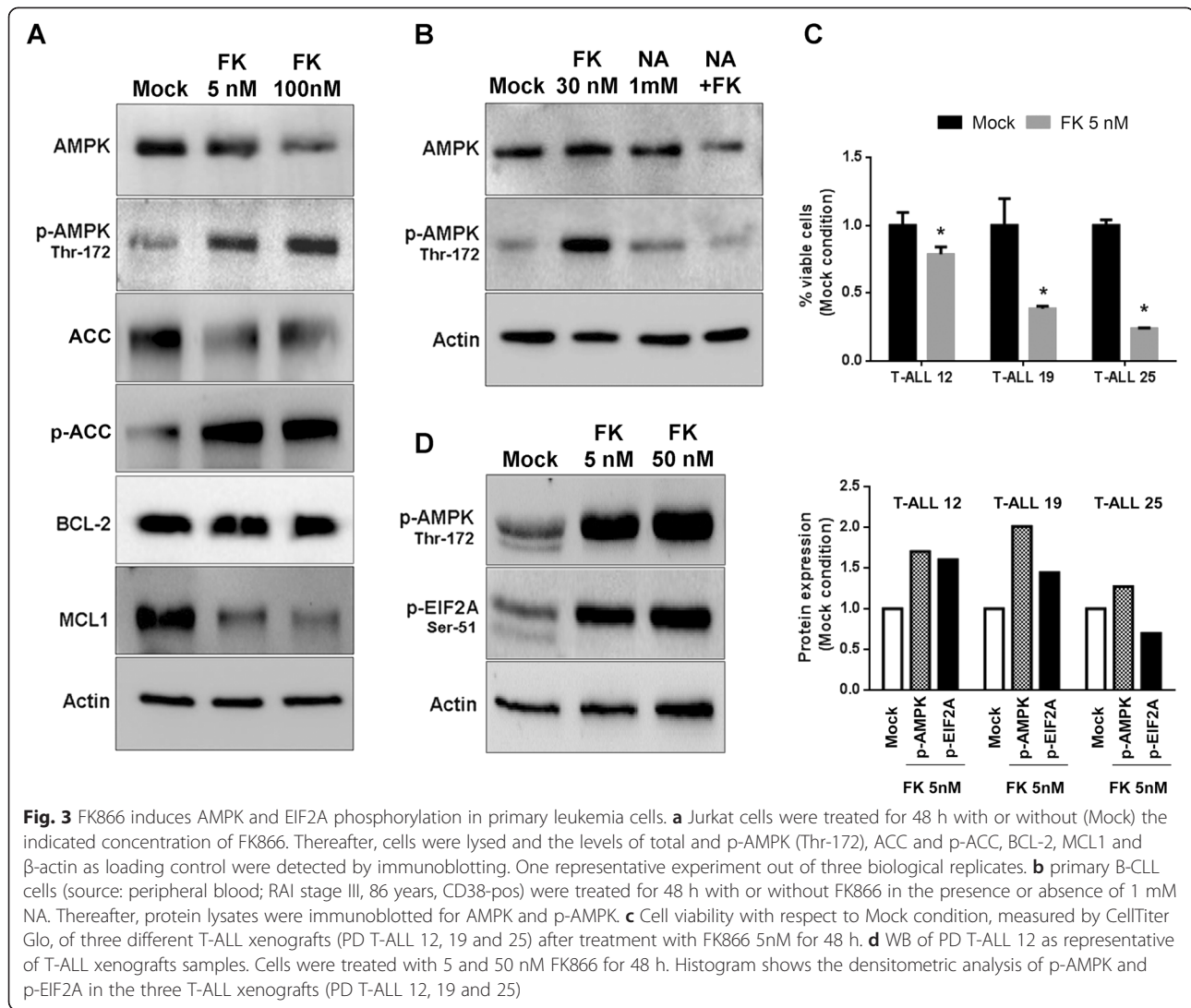


ability to exchange GDP and GTP, impairing the formation of a complex with the EIF2B subunit and thus preventing translation initiation [36]. Analogously, SUP-T1 and Molt-4 Clone 8 T-ALL cell lines presented the same FK866-induced inhibition of the activation of 4EBP1, supporting the existence of a general mechanism underlying the FK866-induced translational arrest in leukemia cells (Fig. 2d, e). These effects were also observed using another inhibitor of NAMPT enzymatic activity, CHS-828 (Additional file 3A), but not with other commonly used chemotherapeutics as cisplatin, doxorubicin, dexamethasone and rapamycin, at equivalent pre-toxic doses. Indeed, FK866 induced a stronger protein synthesis arrest than the mTOR inhibitor rapamycin suggesting that this event is a molecular hallmark of FK866. Additionally, FK866 concomitantly induced EIF2A phosphorylation and 4EBP1 de-phosphorylation, uniquely among all the other drugs, thus mechanistically supporting the strong protein synthesis arrest. The other drugs tested were ineffective (Additional file 3B, C, D). In conclusion, these experiments show the modulation of several hubs of the signaling apparatus controlling translation initiation in response to FK866, providing a robust

explanation for the marked protein synthesis inhibition observed after drug treatment.

#### FK866 induces AMPK and EIF2A phosphorylation in Jurkat and primary leukemia cells

In view of the strong translation inhibition and considering its energy-sensing activity in controlling translation [37], we investigated in Jurkat cells the impact of FK866 and CHS-828 on the phosphorylation status of AMPK, whose activation has been previously shown to be induced by FK866 in prostate and hepatic cancer cells [23, 24]. FK866 caused a partial reduction in total AMPK levels at the highest dose used, but, at a same time, a parallel dose-dependent increase of the phosphorylation of its Thr-172 and of its *bona fide* target ACC (Acetyl-CoA Carboxylase) (Fig. 3a), indicating a significant activation of AMPK. We evaluated the effect of FK866 on two important antiapoptotic factors, MCL1 (Myeloid Cell Leukemia 1) and BCL-2 (B-Cell Lymphoma 2). BCL-2 protein levels were essentially not affected by FK866 treatment as compared to the strong down-regulation of MCL1 (Fig. 3a). Notably, nicotinic acid (NA) supplementation, which blocks FK866 cytotoxic activity by allowing NAD<sup>+</sup> biosynthesis through



an alternative pathway (*via* nicotinic acid phosphoribosyl-transferase, NAPRT1), completely prevented AMPK phosphorylation in primary B-CLL (Fig. 3b, Additional file 3E), confirming that  $\text{NAD}^+$  depletion is responsible for AMPK activation. In patient-derived T-ALL xenografts (PD T-ALL) the drug induced cell death and activated AMPK as well as EIF2A phosphorylation (Fig. 3c and d), demonstrating that this molecular event is not limited to cell line models but is also present in primary leukemia cells.

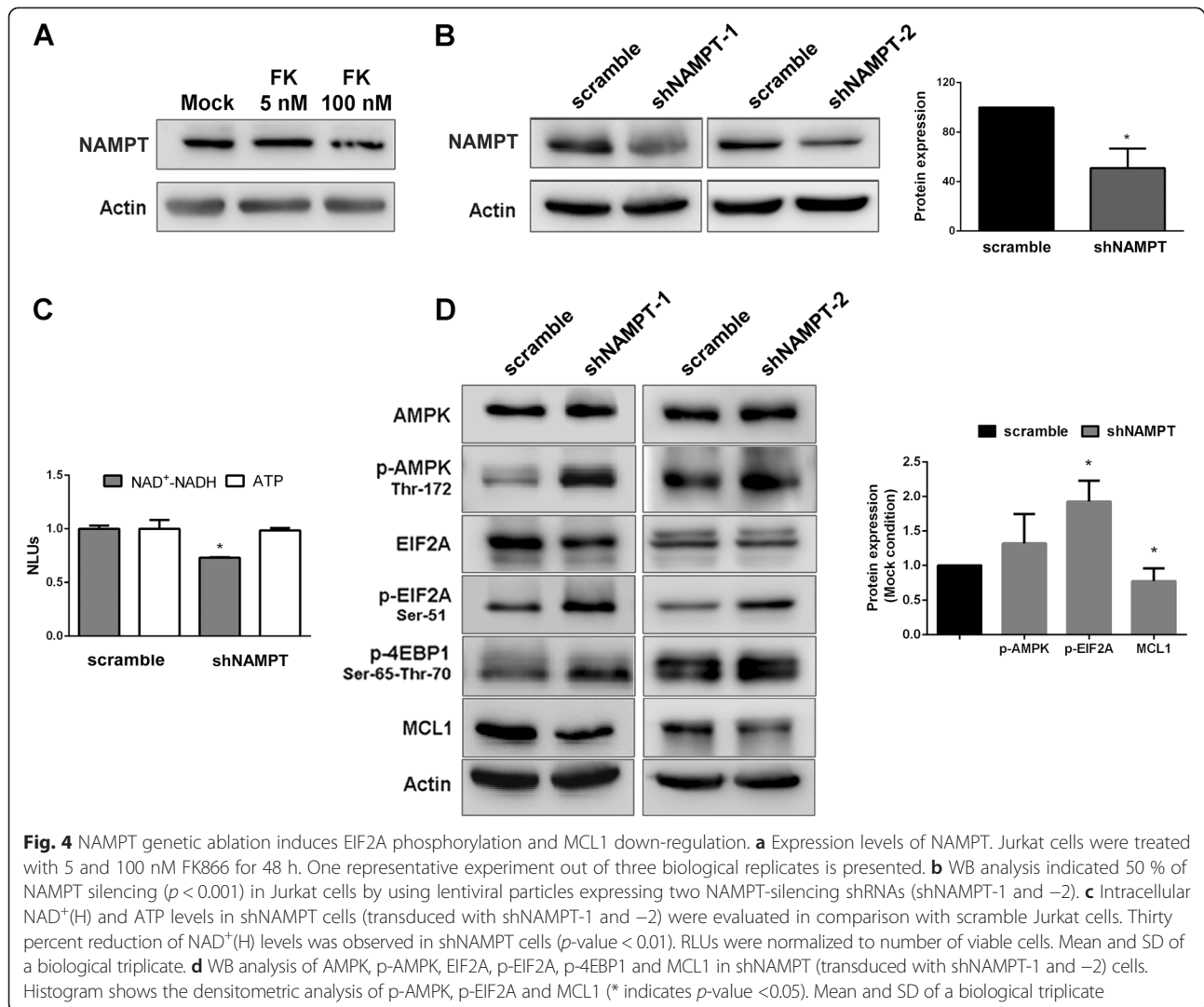
#### EIF2A phosphorylation precedes 4EBP1 de-phosphorylation in Jurkat cells

NAMPT expression level during FK866 treatment remained unchanged as expected (Fig. 4a). Genetic ablation of NAMPT by lentiviral transduction in Jurkat cells (Fig. 4b) lowered  $\text{NAD}^+(\text{H})$  level to 75 % of the control while ATP level was not significantly decreased thus inducing an intermediate condition of energetic stress compared to the one obtained with 5 nM FK866

administration (Fig. 4c). In these conditions of mild stress, AMPK was marginally activated but, nevertheless, we observed a significant phosphorylation of EIF2A but not the de-phosphorylation of 4EBP1, suggesting that the first event precedes the second one (Fig. 4d). Importantly, we observed a clear down-regulation of MCL1, as observed with FK866 treatment (Fig. 3a), suggesting that EIF2A activation is an early response to  $\text{NAD}^+(\text{H})$  shortage.

#### FK866-induced AMPK activation regulates EIF2A phosphorylation

To formally assess the role of AMPK in FK866-induced translational arrest, we pharmacologically blocked AMPK with Compound C, a small molecule inhibitor of this enzyme, although not selective [38]. In addition, we down-regulated AMPK using lentiviral transduction of shRNAs. Compound C administration to Jurkat cells treated with FK866 abrogated AMPK phosphorylation,



reactivated the MTOR/4EBP1 pathway and restored EIF2A in its un-phosphorylated state (Fig. 5a). Rescue experiments with Compound C did not show any down-regulation of MCL1 protein level with no change in BCL2 expression (Fig. 5a). Co-treatment with Compound C partially reverted FK866-induced ATP loss but activated the apoptotic response (Fig. 5b). Down-regulation of AMPK was achieved by targeting both AMPK $\alpha$ 1 and AMPK $\alpha$ 2 isoforms (shAMPK cells). We then exposed silenced and control (scramble) cells to 5 nM of FK866 for 48 h (Fig. 5c). In shAMPK cells we observed a significant decrease of EIF2A phosphorylation but not of 4EBP1 de-phosphorylation. This supports the notion that FK866-induced AMPK activation is primarily involved in the regulation of EIF2A phosphorylation and subsequently in 4EBP1 de-phosphorylation (Fig. 5c). Importantly, shAMPK Jurkat cells showed an increased sensitivity to FK866 with respect to control cells, as revealed by PI staining and flow-cytometry (Fig. 5d),

pointing out the protective effect of AMPK in FK866-induced stress conditions.

#### EIF2A mediates the AMPK pro-survival effect during FK866 treatment

Given the protective role of AMPK in a context of FK866-sensitive cancer cell, we hypothesized that the liver kinase B1 (LKB1), a well-established AMPK regulator, can also exert the same protective effect. Indeed, genetic ablation of LKB1 in Jurkat cells led to an increase toxicity of FK866 treatment (Fig. 6a). Accordingly, we used two lung adenocarcinoma cell lines (H460 and A549), bearing genetic inactivation of LKB1 to prove the dependency of FK866 efficacy on the activation of the LKB1/AMPK pathway. These results provide a rationale for the utilization of NAMPT inhibitors in cancers with this type of genetic background. The cells were stably transduced with retroviral vectors encoding parental LKB1 cDNA (LKB1 WT) or with a control vector

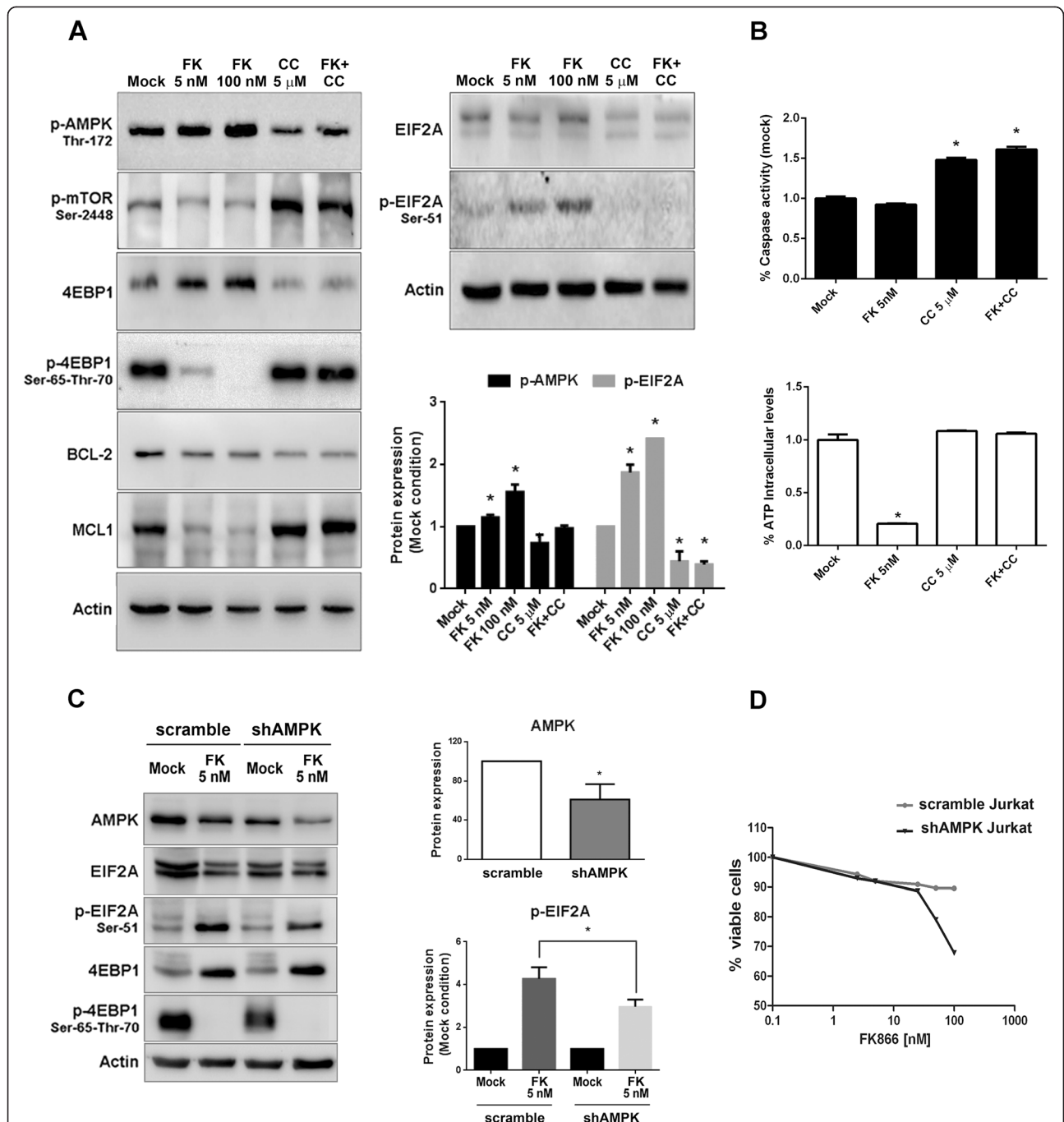
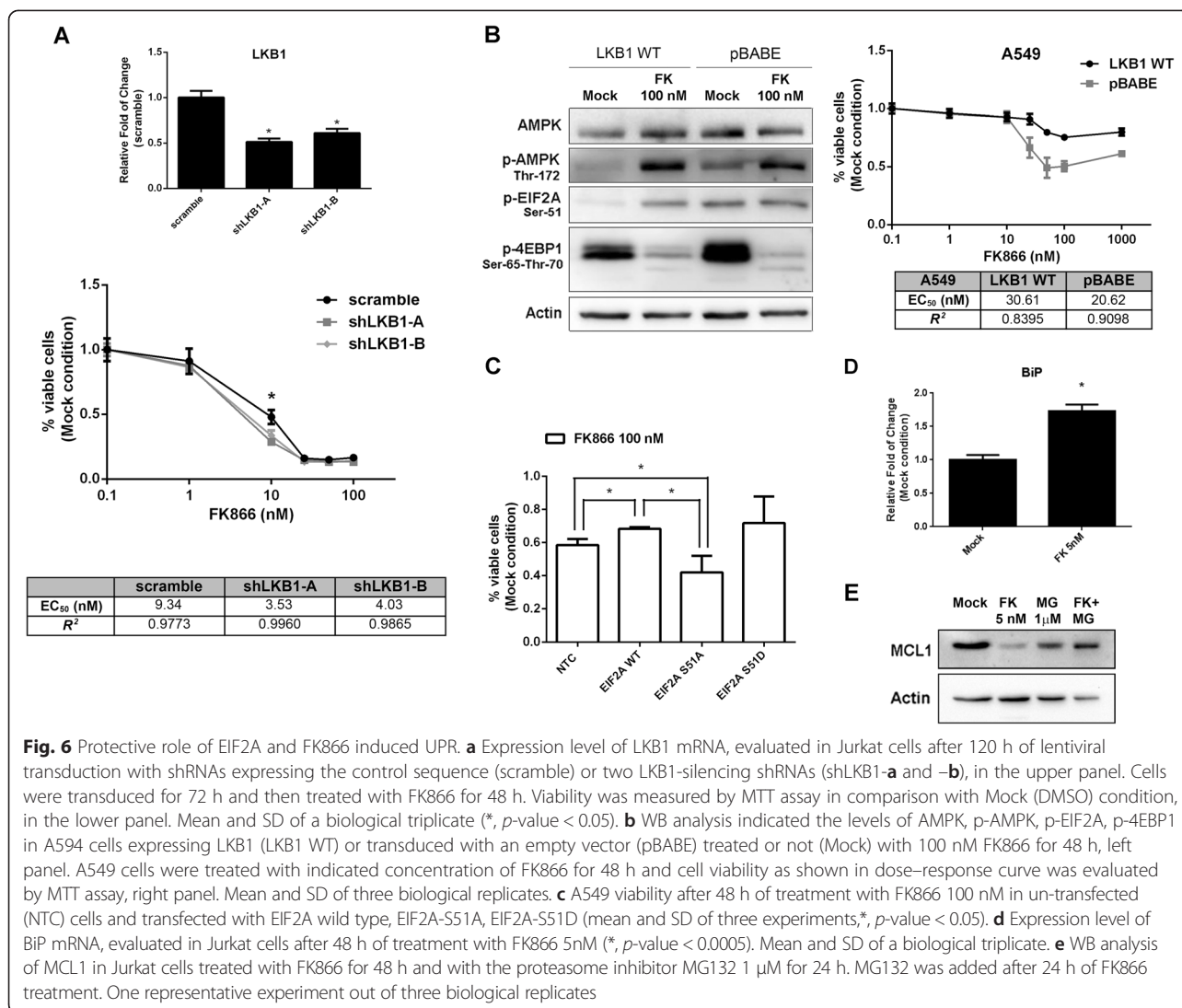


**Fig. 5** AMPK regulates EIF2A phosphorylation and is a pro-survival factor in Jurkat cells. **a** Jurkat cells were treated with or without FK866 at the indicated concentrations in the presence or absence of Compound C 5 μM for 48 h. Thereafter, cells were lysed and the levels of p-AMPK (Thr-172), p-mTOR, 4EBP1, p-4EBP1, BCL-2, MCL1, EIF2A and p-EIF2A were revealed by immunoblotting. Histogram shows the densitometric analysis of p-AMPK and p-EIF2A. **b** In the same samples, caspase 3/7 activity was quantified and relative ATP levels were determined and then normalized to the number of viable cells (\* indicates *p*-value <0.05). **a** and **b** are representative of a biological triplicate (mean and SD). **c** Jurkat cells were transfected with lentiviral particles containing scramble or shAMPK (targeting the α1 and the α2 subunit), then treated for 48 h with or without 5 nM FK866. Cell lysates were used for total AMPK, EIF2A, p-EIF2A, 4EBP1, p-4EBP1 and β-actin immunoblotting. WB analysis indicated 40 % of AMPK silencing (*p*-value < 0.05) and densitometric analysis shows the significant decrease of p-EIF2A in shAMPK Jurkat cells (*p*-value < 0.03). Mean and SD of a biological triplicate. **d** Jurkat scramble and shAMPK cells were treated for 48 h with the indicated doses of FK866. Cell viability was determined by PI staining and flow-cytometry (two biological replicates and statistics based on the acquisition of 10000 events/sample)



(pBABE). FK866 treatment induced AMPK and EIF2A phosphorylation in addition to 4EBP1 de-phosphorylation only when LKB1 was active. On the other hand, albeit to a different extent among the two cell lines, FK866 was not able to activate AMPK or EIF2A but was still effective in de-phosphorylating 4EBP1 when LKB1 was inactive. Viability assays indicated an increased sensitivity of LKB1 negative, EIF2A un-phosphorylated cells to FK866 compared to LKB1 expressing cells (Fig. 6b and Additional file 4A). Finally, in order to assess the relevance of EIF2A in mediating the AMPK induced protection from FK866, we treated with the drug A549 and Jurkat cells transfected with EIF2A, its phosphomimetic mutant S51D or with the non-phosphorylatable mutant S51A. In the context of inactive LKB1, the overexpression of EIF2A and the EIF2A-S51D isoform led to a protective effect, while the alanine mutant induced an increase of cell toxicity (Fig. 6c). The same trend was observed also in Jurkat cells (Additional

file 4B). Therefore, these data indicate that the translation arrest induced by EIF2A mediates the protective effect of AMPK from FK866 induced stress.

#### EIF2A balances pro-survival and pro-death pathways

EIF2A is a key factor regulating the translation machinery in response to a myriad of factors including nutrient depletion, presence of exogenous mRNA and the Unfolded Protein Response (UPR) following the induction of Endoplasmic Reticulum (ER) stress [39]. Indeed, FK866 induced the overexpression of BiP/Grp78 mRNA, coding for a chaperone involved in the folding of ER proteins (Fig. 6d), thus indicating UPR activation in Jurkat cells after 48 h treatment. Moreover, FK866 induced MCL1 down-regulation was dependent on proteasome activation as demonstrated by the rescue of its expression level by MG132 treatment in Jurkat cells (Fig. 6e) [40]. In conclusion, FK866 induces an AMPK-

EIF2A mediated translational arrest, which is responsible for MCL1 down-regulation and the activation of the UPR response, that is a strategic pausing step necessary to protect cells from FK866-induced energetic stress.

## Discussion

We investigated the link between NAD<sup>+</sup>(H) depletion and cell death using a T-ALL cell model after induction of the primary effects of NAMPT inhibition, namely NAD<sup>+</sup>(H) and ATP depletion, while nearly preserving total cell viability. The functional consequences of NAD<sup>+</sup>(H) depletion upon FK866 treatment resulted in a marked inhibition of the three major pathways regulating the translation process and in a striking arrest of protein synthesis. Interestingly, FK866 efficacy in blocking protein synthesis was higher than all the other chemotherapeutics tested and even higher than the MTOR inhibitor rapamycin, suggesting that this is a crucial event in the cell response to FK866. This phenomenon is general because it was observed in primary leukemic samples, coming both from B-CLL and T-ALL patients, and in T-ALL derived cancer cell lines. Nicotinic acid rescue experiments, treatment with the FK866 analog CHS-828 and NAMPT genetic ablation showed that translation arrest was dependent on the shortage of ATP and NAD<sup>+</sup>(H) induced by the inhibition of the NAMPT catalytic function and not by unspecific FK866 effects. FK866 has been shown to have contrasting effects on AMPK. In neuronal cells FK866 decreased AMPK activation and was detrimental for neuronal survival [25], however in cancer cells that have a dysregulated metabolic demand, it has been observed the opposite. In prostate cancer cells, FK866 treatment reduced fatty acid and phospholipid synthesis, partly *via* AMPK activation [23]. FK866 induced activation of AMPK and subsequent decreased phosphorylation of 4EBP1 by MTOR has been observed in hepatocarcinoma cells. Given the importance of MTOR in sustaining cancer cell growth, this event was proposed as an effective mechanism to target cancer cells [23]. By evaluating the early molecular effects of FK866 treatment on protein synthesis, we observed the involvement of the same pathway but, in addition, we showed a protective role for AMPK and EIF2A. In our experimental conditions, the inactivation of MTOR by AMPK and consequent protein synthesis arrest had a protective effect conferring temporary resistance to the FK866-induced energetic stress. Additionally, we determined that AMPK-induced hyper-phosphorylation of EIF2A is regulated by the fluctuations of NAD availability at the intracellular level. This molecular mechanism, leading to inhibition of translation initiation, followed AMPK activation. In fact, genetic AMPK down-regulation of both

isoforms of the  $\alpha$  catalytic subunit rescued the FK866 induced hyper-phosphorylation of EIF2A. As a further confirmation, the same results were obtained by AMPK functional ablation using the inhibitor Compound C or by inactivation of its upstream regulator LKB1. Indeed, rescue of 4EBP1 phosphorylation levels was observed only after Compound C administration, suggesting that EIF2A is a preferential target of the AMPK signaling cascade, at least in the initial phase of cell response to FK866. Interestingly, in our cell model and at the doses we used, we did not observe Compound C-induced phosphorylation of EIF2A as recently reported in different cancer cells [41]. Our cell model resembles the AICAR-induced AMPK activation that leads to EIF2A phosphorylation in adipocytes, an event shown to be crucial for AMPK-induced apoptosis [42], and supports the idea that FK866 induced activation of the AMPK-EIF2A axis can be a novel pathway to be investigated to elucidate the pharmacology of FK866.

Many types of cancer, as sporadic lung, cervical, and endometrial cancers, carry LKB1 deficiency that can be exploited with metabolic drugs since these cells are unable to appropriately respond to metabolic stress [43]. Given the protective role of LKB1/AMPK pathway against FK866, our study suggests the utilization of FK866 as a metabolism-based cancer therapeutic to selectively target LKB1-deficient tumors. Indeed in cells lacking a functional LKB1 pathway, metabolic stress has been demonstrated to result in rapid apoptosis as the cells are unable to sense energetic stresses and activate mechanisms to restore energy homeostasis [44].

Previous studies have shown that inhibition of the MTOR/4EBP1 pathway in leukemia cells leads to a reduction in the levels of the anti-apoptotic protein MCL1, with important implications for chemosensitivity [45]. Down-regulation of MCL1 through inhibition of translation has been clearly associated with enhanced lethality in Jurkat cells [46]. Importantly, FK866 administration led to smooth death [40] *via* EIF2A-dependent MCL1 down-regulation consequent to translation arrest and simultaneous proteasome activation. Indeed, MCL1 intracellular levels were shown to be strictly dependent on the activation of EIF2A [47] and AMPK [48], and to the subsequent translation arrest. This could provide a molecular explanation for the anti-leukemic activity of NAMPT inhibitors. Notably, the ectopic expression of the non-phosphorylatable mutant EIF2A-S51A increased FK866 toxicity. Therefore the activation of the AMPK-EIF2A axis is essential for the tumor cell to adapt to the shortage of NAD<sup>+</sup>(H). For example, the increased expression level of BiP mRNA is a specific adaptive response observed in the integrated stress response (ISR) and translational repression [49]. The exacerbation of proteasome inhibition with bortezomib has been shown to potentiate FK866 efficacy through the activation of

the caspases' cascade [40]. Here we show the relevance of EIF2A activation in this mechanism. Additionally, the synergistic effect of FK866 with cyclosporine in leukemia cells has been ascribed to the activation of the UPR [50]. This suggests that the exacerbation of the UPR, which is dependent on EIF2A, can be thought as a relevant strategy to potentiate the effect of FK866 in conditions in which activation of the EIF2A-dependent UPR is desirable, i.e., diabetes, atherosclerosis, or neurodegenerative disorders [51]. Indeed, FK866 effects on translation resemble the ones induced by metformin, a well-known AMPK activator with antidiabetic and antitumoral properties [52, 53]. Finally, de-phosphorylation of EIF4E, never linked to NAMPT inhibitors or AMPK activation before, completes the general picture of a global inhibition of the translation process, even though the mechanism leading to upstream MNK activation has not been investigated yet.

## Conclusions

In conclusion, this work describes the activation of a complex signaling network in which the AMPK-EIF2A axis is responsible for the early cellular response to the metabolic stress produced by FK866. In an experimental condition in which catastrophic proteolytic cascades are not yet started but the energetic demand is high, EIF2A acts as an early master regulator of cell fate, blocking anabolic processes and, at the same time, modulating cell death and adaptive pathways. Therefore EIF2A-dependent processes, such as protein synthesis and UPR, acquire fundamental relevance in explaining the mechanism of action of NAMPT inhibitors.

## Additional files

**Additional file 1: Cell-cycle analysis and *Click-IT* detection of RNA and Protein synthesis.** A) Cell-cycle analysis with PI staining of the nuclei after 48 h of treatment. Overnight serum starvation is shown as a positive control of induced cell cycle synchronization in G0/G1 phase. Cell phase analysis was done with ModFit LT 3.2 software by using the Sync Wizard model (30000 cells/sample in biological duplicate). B) Jurkat cells were treated for 48 h with or without (Mock) the indicated concentration of FK866 or for 3 h with 5  $\mu$ M Actinomycin D, an RNA synthesis blocking agent, then subjected to *Click-it* biochemistry and flow-cytometry analyses including 7-AAD to identify living cells. C) Jurkat cells were treated for 48 h with or without (Mock) the indicated concentration of FK866 or for 3 h with 350  $\mu$ M Cycloheximide, as a positive control for protein synthesis inhibition, then stained as in B. In B and C. Experiments were carried out on two biological replicates (50000 events/sample). (PDF 1562 kb)

**Additional file 2: Luciferase assays.** A) Light units, normalized to protein concentration, of RLuc-cMyc 5'UTR IRES-FLuc reporter vector transduced in Jurkat cells with lentiviral particles after 48 h of treatment with or without (Mock) the indicated concentration of FK866. Two hour treatment with 250 nM of Torin 1 served as a positive control for IRES-dependent protein translation ( $p$ -value <0.05). B) Light units, normalized to protein concentration, of FLuc-HCV-RLuc and FLuc-CrPV-RLuc reporter vectors transduced in Jurkat cells with lentiviral particles. Cap-dependent translation (FLuc) was strongly reduced with 5 nM and 100 nM FK866

(48 h) in comparison to Mock condition ( $p$ -value <0.0001). RLuc signal is not shown because of its low level and its variability between technical and biological replicates. Cells transduced with the pHR-SIN-F-HCV-R were serum starved for 5 h as a positive control of IRES activation, as shown in the graph ( $p$ -value <0.05). In A and B data are represented as mean and SD of three independent experiments. (PDF 584 kb)

**Additional file 3: Effects of CHS-828 and chemotherapeutics on protein translation.** A) Jurkat cells were treated for 48 h with or without (Mock) the indicated concentration of CHS-828. Caspase 3/7 activity was quantified (using 5  $\mu$ M of Camptothecin for 4 h as a positive control of apoptosis) and relative ATP levels were determined and then normalized to the number of viable cells. The levels of total AMPK, p-AMPK, total EIF2A and p-EIF2A, total 4EBP1, p-4EBP1 were evaluated by WB. Histogram shows the densitometric analysis of p-AMPK and p-EIF2A (\* indicates  $p$ -value <0.05). Mean and SD of a biological triplicate. B) Jurkat cells were treated with the indicated concentration of drugs for 48 h and cell viability was measured by Cell Titer Glo. Data are represented as mean and SD of three independent experiments. C) *Click-it* chemistry based on the incorporation of an amino acid analog (AHA) was used to monitor protein synthesis. Jurkat cells were treated for 48 h with or without (Mock) the indicated concentration of FK866, Rapamycin (RAPA), Doxorubicin (DOXO), Cisplatin (CIS) and Dexamethasone (DEXA). The histogram quantifies the % of AHA positive cells (active protein-synthesizing cells) in the viable cell population. Flow-cytometry experiments were carried out on two biological replicates and statistics were based on acquisition of 20000 events/sample. D) Jurkat cells were treated as in C and the level of p-EIF2A and p-4EBP1 was evaluated. Histogram shows the densitometric analysis of p-EIF2A (\* indicates  $p$ -value <0.05). Mean and SD of a biological triplicate. E) Primary B-CLL cells were treated for 48 h with or without 30 nM FK866 in the presence or absence of 1 mM NA. Histogram shows the densitometric analysis of p-AMPK/AMPK. (PDF 691 kb)

**Additional file 4: Protective role of EIF2A.** A) WB analysis indicated the levels of AMPK, p-AMPK, p-EIF2A, p-4EBP1 in H460 cells expressing LKB1 (LKB1 WT) or transduced with an empty vector (pBABE) treated or not (Mock) with 100 nM FK866 for 48 h, left panel. H460 cells were treated with indicated concentration of FK866 for 48 h and cell viability as shown in dose-response curve was evaluated by MTT assay, right panel. Mean and SD of three biological replicates. B) Jurkat viability after 48 h of treatment with FK866 5nM in un-transfected (NTC) cells and transfected with EIF2A wild type, EIF2A-S51A, EIF2A-S51D (mean and SD of three experiments,  $p$ -value < 0.1). (PDF 274 kb)

## Abbreviations

4EBP1: Eukaryotic translation initiation factor 4E-binding protein 1; ACC: Acetyl-CoA carboxylase; AKT: v-akt murine thymoma viral oncogene homolog 1; AMPK: AMP-activated protein kinase; BCL-2: B-Cell lymphoma 2; B-CLL: B-cell chronic lymphocytic Leukemia; BiP: Glucose-regulated protein 78 kDa; EIF2A: Eukaryotic translation initiation factor 2A; EIF4E: Eukaryotic translation initiation factor 4E; EMT: Epithelial-mesenchymal transition; ERK: Mitogen-activated protein kinase; LKB1: Liver kinase B1; MCL1: Myeloid cell leukemia 1; MNK: MAP Kinase Interacting Serine/Threonine Kinase; MTOR: Mammalian target of rapamycin; NA: Nicotinic acid; NAD: Nicotinamide adenine dinucleotide; NAMPT: Nicotinamide phosphoribosyltransferase; T-ALL: T-cell acute lymphoblastic Leukemia; UPR: Unfolded protein response.

## Competing interests

Authors declare no competing interests.

## Authors' contributions

CZ and VGD carried out most of the experiments, participated in the study design and drafted the manuscript, AC cloned and produced viral vectors, BM, NT, DS, MC and IC helped with immunoassays and genetic experiments, AB, SI, AQ provided clinical samples and participated in the study design, AN and AP conceived the study, participated in its design and coordination and wrote the manuscript. All authors drafted, read and approved the final manuscript.

## Acknowledgements

We thank Dr V. Adami, High Throughput Screening Facility, and I. Pesce, Cell Analysis and Separation Facility, University of Trento, Italy, for helpful support;

Dr Sabatini DM for shscramble pLKO based vector provided through Addgene and Dr Root DE for pLKO.1 - TRC cloning vector. The pBABE-LKB1 vector was received from Dr. Lewis Cantley through Addgene.

#### Financial support

AP and AN thank the Italian Ministry of Health grant GR-2008-1135635 and FP7 project PANACREAS #256986. AN thanks AIRC Start-Up grant #6108, Compagnia di San Paolo, Fondazione Umberto Veronesi, Fondazione CARIGE, Università di Genova. AP thanks the CIBIO start-up grant, University of Trento.

#### Author details

<sup>1</sup>Laboratory of Genomic Screening, CIBIO, University of Trento, Trento, Italy.

<sup>2</sup>Laboratory of Molecular Virology, CIBIO, University of Trento, Trento, Italy.

<sup>3</sup>Department of Internal Medicine, University of Genoa, Genoa, Italy.

<sup>4</sup>Laboratory of Translational Networks, CIBIO, University of Trento, Trento, Italy. <sup>5</sup>Istituto Oncologico Veneto IOV-IRCCS, Padova, Italy.

Received: 15 April 2015 Accepted: 23 October 2015

Published online: 05 November 2015

#### References

- Kroemer G, Pouyssegur J. Tumor cell metabolism: cancer's Achilles' heel. *Cancer Cell*. 2008;13(6):472–82.
- Tan B, Young DA, Lu Z-H, Wang T, Meier TI, Shepard RL, et al. Pharmacological inhibition of nicotinamide phosphoribosyltransferase (NAMPT), an enzyme essential for NAD<sup>+</sup> biosynthesis, in human cancer cells: metabolic basis and potential clinical implications. *J Biol Chem*. 2013;288(5):3500–11.
- Revollo JR, Grimm AA, Imai S. The NAD biosynthesis pathway mediated by nicotinamide phosphoribosyltransferase regulates Sir2 activity in mammalian cells. *J Biol Chem*. 2004;279(49):50754–63.
- Skokowa J, Lan D, Thakur BK, Wang F, Gupta K, Cario G, et al. NAMPT is essential for the G-CSF-induced myeloid differentiation via a NAD<sup>+</sup>-sirtuin-1-dependent pathway. *Nat Med*. 2009;15(2):151–8.
- Xiao Y, Elkins K, Durieux JK, Lee L, Oeh J, Yang LX, et al. Dependence of Tumor Cell Lines and Patient-Derived Tumors on the NAD Salvage Pathway Renders Them Sensitive to NAMPT Inhibition with GNE-618. *Neoplasia*. 2013;15(10):1151–60.
- Soncini D, Caffa I, Zoppoli G, Cea M, Cagnetta A, Passalacqua M, et al. Nicotinamide phosphoribosyltransferase promotes epithelial-to-mesenchymal transition as a soluble factor independent of its enzymatic activity. *J Biol Chem*. 2014;289(49):34189–204.
- Wang B, Hasan MK, Alvarado E, Yuan H, Wu H, Chen WY. NAMPT overexpression in prostate cancer and its contribution to tumor cell survival and stress response. *Oncogene*. 2011;30(8):907–21.
- Nakajima TE, Yamada Y, Hamano T, Furuta K, Gotoda T, Katai H, et al. Adipocytokine levels in gastric cancer patients: resistin and visfatin as biomarkers of gastric cancer. *J Gastroenterol*. 2009;44(7):685–90.
- Montecucco F, Cea M, Cagnetta A, Damonte P, Nahimana A, Ballestrero A, et al. Nicotinamide phosphoribosyltransferase as a target in inflammation-related disorders. *Curr Top Med Chem*. 2013;13(23):2930–8.
- Bruzzone S, Fruscione F, Morando S, Ferrando T, Poggi A, Garuti A, et al. Catastrophic NAD<sup>+</sup> depletion in activated T lymphocytes through Nampt inhibition reduces demyelination and disability in EAE. *PLoS One*. 2009;4(11):e7897.
- Zoppoli G, Cea M, Soncini D, Fruscione F, Rudner J, Moran E, et al. Potent synergistic interaction between the Nampt inhibitor APO866 and the apoptosis activator TRAIL in human leukemia cells. *Exp Hematol*. 2010;38(11):979–88.
- Nahimana A, Attinger A, Aubry D, Greaney P, Ireson C, Thougard AV, et al. The NAD biosynthesis inhibitor APO866 has potent antitumor activity against hematologic malignancies. *Blood*. 2009;113(14):3276–86.
- Nencioni A, Cea M, Montecucco F, Longo VD, Patrone F, Carella AM, et al. Autophagy in blood cancers: biological role and therapeutic implications. *Haematologica*. 2013;98(9):1335–43.
- Wosikowski K, Mattern K, Schemanda I, Hasmann M, Rattel B, Löser R. WK175, a novel antitumor agent, decreases the intracellular nicotinamide adenine dinucleotide concentration and induces the apoptotic cascade in human leukemia cells. *Cancer Res*. 2002;62(4):1057–62.
- Christensen MK, Erichsen KD, Olesen UH, Tjørnelund J, Fristrup P, Thougard A, et al. Nicotinamide phosphoribosyltransferase inhibitors, design, preparation, and structure-activity relationship. *J Med Chem*. 2013;56(22):9071–88.
- Montecucco F, Cea M, Bauer I, Soncini D, Caffa I, Lasigliè D, et al. Nicotinamide phosphoribosyltransferase (NAMPT) inhibitors as therapeutics: rationales, controversies, clinical experience. *Curr Drug Targets*. 2013;14(6):637–43.
- Cerna D, Li H, Flaherty S, Takebe N, Coleman CN, Yoo SS. Inhibition of nicotinamide phosphoribosyltransferase (NAMPT) activity by small molecule GMX1778 regulates reactive oxygen species (ROS)-mediated cytotoxicity in a p53- and nicotinic acid phosphoribosyltransferase1 (NAPRT1)-dependent manner. *J Biol Chem*. 2012;287(26):22408–17.
- Del Nagro C, Xiao Y, Rangell L, Reichelt M, O'Brien T. Depletion of the Central Metabolite NAD Leads to Oncosis-mediated Cell Death. *J Biol Chem*. 2014;289(51):35182–92.
- Ginet V, Puyal J, Rummel C, Aubry D, Breton C, Cloux A-J, et al. A critical role of autophagy in antileukemia/lymphoma effects of APO866, an inhibitor of NAD biosynthesis. *Autophagy*. 2014;10(4):603–17.
- Settembre C, De Cegli R, Mansueto G, Saha PK, Vetrini F, Visvikis O, et al. TFEB controls cellular lipid metabolism through a starvation-induced autoregulatory loop. *Nat Cell Biol*. 2013;15(6):647–58.
- Cea M, Cagnetta A, Fulcinitti M, Tai Y-T, Hideshima T, Chauhan D, et al. Targeting NAD<sup>+</sup> salvage pathway induces autophagy in multiple myeloma cells via mTORC1 and extracellular signal-regulated kinase (ERK1/2) inhibition. *Blood*. 2012;120(17):3519–29.
- Hardie DG. The AMP-activated protein kinase pathway—new players upstream and downstream. *J Cell Sci*. 2004;117(Pt 23):5479–87.
- Bowlby SC, Thomas MJ, D'Agostino RB, Kridel SJ. Nicotinamide phosphoribosyl transferase (Nampt) is required for de novo lipogenesis in tumor cells. *PLoS One*. 2012;7(6):e40195.
- Schuster S, Penke M, Gorski T, Gebhardt R, Weiss TS, Kiess W, et al. FK866-induced NAMPT inhibition activates AMPK and downregulates mTOR signaling in hepatocarcinoma cells. *Biochem Biophys Res Commun*. 2015;458(2):334–40.
- Wang P, Xu T-Y, Guan Y-F, Tian W-W, Viollet B, Rui Y-C, et al. Nicotinamide phosphoribosyltransferase protects against ischemic stroke through SIRT1-dependent adenosine monophosphate-activated kinase pathway. *Ann Neurol*. 2011;69(2):360–74.
- Spriggs KA, Stoneley M, Bushell M, Willis AE. Re-programming of translation following cell stress allows IRES-mediated translation to predominate. *Biol Cell*. 2008;100(1):27–38.
- Agnusdei V, Minuzzo S, Frasson C, Grassi A, Axelrod F, Satyal S, et al. Therapeutic antibody targeting of Notch1 in T-acute lymphoblastic leukemia xenografts. *Leukemia*. 2013;28(2):278–88.
- D'Agostino VG, Adami V, Provenzani A. A novel high throughput biochemical assay to evaluate the HuR protein-RNA complex formation. *PLoS One*. 2013;8(8):e72426.
- Zufferey R, Nagy D, Mandel RJ, Naldini L, Trono D. Multiply attenuated lentiviral vector achieves efficient gene delivery in vivo. *Nat Biotechnol*. 1997;15(9):871–5.
- Sarbasov DD, Guertin DA, Ali SM, Sabatini DM. Phosphorylation and regulation of Akt/PKB by the rictor-mTOR complex. *Science*. 2005;307(5712):1098–101.
- Moffat J, Grueneberg DA, Yang X, Kim SY, Kloepfer AM, Hinkle G, et al. A lentiviral RNAi library for human and mouse genes applied to an arrayed viral high-content screen. *Cell*. 2006;124(6):1283–98.
- Sonenberg N, Hinnebusch AG. Regulation of translation initiation in eukaryotes: mechanisms and biological targets. *Cell Elsevier Inc*. 2009;136(4):731–45.
- Cea M, Cagnetta A, Patrone F, Nencioni A, Gobbi M, Anderson KC. Intracellular NAD<sup>+</sup> depletion induces autophagic death in multiple myeloma cells. *Autophagy*. 2013;9(3):410–2.
- Shi Y, Yan H, Frost P, Gera J, Lichtenstein A. Mammalian target of rapamycin inhibitors activate the AKT kinase in multiple myeloma cells by up-regulating the insulin-like growth factor receptor/insulin receptor substrate-1/ phosphatidylinositol 3-kinase cascade. *Mol Cancer Ther*. 2005;4(10):1533–40.
- Waskiewicz AJ, Flynn A, Proud CG, Cooper JA. Mitogen-activated protein kinases activate the serine/threonine kinases Mnk1 and Mnk2. *EMBO J*. 1997;16(8):1909–20.
- Krishnamoorthy T, Pavitt GD, Zhang F, Dever TE, Hinnebusch AG. Tight binding of the phosphorylated alpha subunit of initiation factor 2 (eIF2alpha) to the regulatory subunits of guanine nucleotide exchange

- factor eIF2B is required for inhibition of translation initiation. *Mol Cell Biol*. 2001;21(15):5018–30.
37. Zhang C-S, Jiang B, Li M, Zhu M, Peng Y, Zhang Y-L, et al. The Lysosomal v-ATPase-Ragulator Complex Is a Common Activator for AMPK and mTORC1, Acting as a Switch between Catabolism and Anabolism. *Cell Metab*. 2014;20(3):526–40.
  38. Liu X, Chhipa RR, Nakano I, Dasgupta B. The AMPK inhibitor compound C is a potent AMPK-independent anti glioma agent. *Mol Cancer Ther*. 2014;13(3):596–605.
  39. Wang S, Kaufman RJ. The impact of the unfolded protein response on human disease. *J Cell Biol*. 2012;197(7):857–67.
  40. Cagnetta A, Cea M, Calimeri T, Acharya C, Fulciniti M, Tai Y-T, et al. Intracellular NAD<sup>+</sup> depletion enhances bortezomib-induced anti-myeloma activity. *Blood*. 2013;122(7):1243–55.
  41. Dai RY, Zhao XF, Li JJ, Chen R, Luo ZL, Yu LX, et al. Implication of transcriptional repression in compound C-induced apoptosis in cancer cells. *Cell Death Dis*. 2013;4:e883.
  42. Dagon Y, Avraham Y, Berry EM. AMPK activation regulates apoptosis, adipogenesis, and lipolysis by eIF2alpha in adipocytes. *Biochem Biophys Res Commun*. 2006;340(1):43–7.
  43. Shackelford DB, Abt E, Gerken L, Vasquez DS, Seki A, Leblanc M, et al. LKB1 inactivation dictates therapeutic response of non-small cell lung cancer to the metabolism drug phenformin. *Cancer Cell*. 2013;23(2):143–58.
  44. Shaw RJ, Kosmatka M, Bardeesy N, Hurley RL, Witters LA, DePinho RA, et al. The tumor suppressor LKB1 kinase directly activates AMP-activated kinase and regulates apoptosis in response to energy stress. *Proc Natl Acad Sci U S A*. 2004;101(10):3329–35.
  45. Mills JR, Hippo Y, Robert F, Chen SMH, Malina A, Lin C-J, et al. mTORC1 promotes survival through translational control of Mcl-1. *Proc Natl Acad Sci U S A*. 2008;105(31):10853–8.
  46. Zhou T, Li G, Cao B, Liu L, Cheng Q, Kong H, et al. Downregulation of Mcl-1 through inhibition of translation contributes to benzyl isothiocyanate-induced cell cycle arrest and apoptosis in human leukemia cells. *Cell Death Dis*. 2013;4:e515.
  47. Fritsch RM, Schneider G, Saur D, Scheibel M, Schmid RM. Translational repression of MCL-1 couples stress-induced eIF2 alpha phosphorylation to mitochondrial apoptosis initiation. *J Biol Chem*. 2007;282(31):22551–62.
  48. Pradelli LA, Bénétteau M, Chauvin C, Jacquin MA, Marchetti S, Muñoz-Pinedo C, et al. Glycolysis inhibition sensitizes tumor cells to death receptors-induced apoptosis by AMP kinase activation leading to Mcl-1 block in translation. *Oncogene*. 2010;29(11):1641–52.
  49. Palam LR, Baird TD, Wek RC. Phosphorylation of eIF2 facilitates ribosomal bypass of an inhibitory upstream ORF to enhance CHOP translation. *J Biol Chem*. 2011;286(13):10939–49.
  50. Cagnetta A, Caffa I, Acharya C, Soncini D, Acharya P, Adamia S, et al. APO866 Increases Antitumor Activity of Cyclosporin-A by Inducing Mitochondrial and Endoplasmic Reticulum Stress in Leukemia Cells. *Clin Cancer Res*. 2015;21(17):3934–45.
  51. Fullwood MJ, Zhou W, Shenolikar S. Targeting phosphorylation of eukaryotic initiation factor-2a to treat human disease. *Prog Mol Biol Transl Sci*. 2012;106:75–106.
  52. Dowling RJO, Zakikhani M, Fantus IG, Pollak M, Sonenberg N. Metformin inhibits mammalian target of rapamycin-dependent translation initiation in breast cancer cells. *Cancer Res*. 2007;67(22):10804–12.
  53. Larsson O, Morita M, Topisirovic I, Alain T, Blouin M-J, Pollak M, et al. Distinct perturbation of the translome by the antidiabetic drug metformin. *Proc Natl Acad Sci U S A*. 2012;109(23):8977–82.

**Submit your next manuscript to BioMed Central  
and take full advantage of:**

- Convenient online submission
- Thorough peer review
- No space constraints or color figure charges
- Immediate publication on acceptance
- Inclusion in PubMed, CAS, Scopus and Google Scholar
- Research which is freely available for redistribution

Submit your manuscript at  
[www.biomedcentral.com/submit](http://www.biomedcentral.com/submit)



## APO866 Increases Antitumor Activity of Cyclosporin-A by Inducing Mitochondrial and Endoplasmic Reticulum Stress in Leukemia Cells

Antonia Cagnetta<sup>1,2</sup>, Irene Caffa<sup>1</sup>, Chirag Acharya<sup>2</sup>, Debora Soncini<sup>1</sup>, Prakrati Acharya<sup>3</sup>, Sophia Adamia<sup>2</sup>, Ivana Pierri<sup>1</sup>, Micaela Bergamaschi<sup>1</sup>, Anna Garuti<sup>1</sup>, Giulio Fraternali<sup>4</sup>, Luca Mastracci<sup>5</sup>, Alessandro Provenzani<sup>6</sup>, Chiara Zucal<sup>7</sup>, Gianluca Damonte<sup>7</sup>, Annalisa Salis<sup>7</sup>, Fabrizio Montecucco<sup>8,9</sup>, Franco Patrone<sup>1</sup>, Alberto Ballestrero<sup>1</sup>, Santina Bruzzone<sup>7</sup>, Marco Gobbi<sup>1</sup>, Alessio Nencioni<sup>1</sup>, and Michele Cea<sup>1,2</sup>

### Abstract

**Purpose:** The nicotinamide phosphoribosyltransferase (NAMPT) inhibitor, APO866, has been previously shown to have antileukemic activity in preclinical models, but its cytotoxicity in primary leukemia cells is frequently limited. The success of current antileukemic treatments is reduced by the occurrence of multidrug resistance, which, in turn, is mediated by membrane transport proteins, such as P-glycoprotein-1 (Pgp). Here, we evaluated the antileukemic effects of APO866 in combination with Pgp inhibitors and studied the mechanisms underlying the interaction between these two types of agents.

**Experimental Design:** The effects of APO866 with or without Pgp inhibitors were tested on the viability of leukemia cell lines, primary leukemia cells (AML,  $n = 6$ ; B-CLL,  $n = 19$ ), and healthy leukocytes. Intracellular nicotinamide adenine dinucleotide ( $NAD^+$ ) and ATP levels, mitochondrial transmembrane potential ( $\Delta\psi_m$ ), markers of

apoptosis and of endoplasmic reticulum (ER) stress were evaluated.

**Results:** The combination of APO866 with Pgp inhibitors resulted in a synergistic cytotoxic effect in leukemia cells, while sparing normal  $CD34^+$  progenitor cells and peripheral blood mononuclear cells. Combining Pgp inhibitors with APO866 led to increased intracellular APO866 levels, compounded  $NAD^+$  and ATP shortage, and induced  $\Delta\psi_m$  dissipation. Notably, APO866, Pgp inhibitors and, to a much higher extent, their combination induced ER stress and ER stress inhibition strongly reduced the activity of these treatments.

**Conclusions:** APO866 and Pgp inhibitors show a strong synergistic cooperation in leukemia cells, including acute myelogenous leukemia (AML) and B-cell chronic lymphocytic leukemia (B-CLL) samples. Further evaluations of the combination of these agents in clinical setting should be considered. *Clin Cancer Res*; 21(17); 3934–45. ©2015 AACR.

<sup>1</sup>Department of Hematology and Oncology, IRCCS AOU S. Martino-IST, Genoa, Italy. <sup>2</sup>Department of Medical Oncology, Dana-Farber Cancer Institute, Harvard Medical School, Boston, Massachusetts. <sup>3</sup>Mount Auburn Hospital, Harvard Medical School, Cambridge, Massachusetts. <sup>4</sup>Laboratories Department, Pathology Unit, IRCCS AOU S. Martino-IST, Genoa, Italy. <sup>5</sup>Department of Surgical and Diagnostic Sciences (DISC), Pathology Unit, IRCCS AOU S. Martino-IST, Genoa, Italy. <sup>6</sup>Center for Integrative Biology, University of Trento, Trento, Italy. <sup>7</sup>Department of Experimental Medicine, Section of Biochemistry, and CEBR, University of Genoa, Italy. <sup>8</sup>Division of Cardiology, Department of Internal Medicine, Foundation for Medical Researchers, University of Geneva, Geneva, Switzerland. <sup>9</sup>Department of Medical Specialties, University of Geneva, Geneva, Switzerland.

**Note:** Supplementary data for this article are available at Clinical Cancer Research Online (<http://clincancerres.aacrjournals.org/>).

A. Cagnetta, I. Caffa, C. Acharya, and D. Soncini share first authorship.

A. Nencioni and M. Cea share senior authorship.

**Corresponding Authors:** Michele Cea, University of Genoa, 16132 Genoa, Italy. Phone: +39-010-353-8628; Fax: +39-010-353-38701; E-mail: [michele.cea@unige.it](mailto:michele.cea@unige.it); and Alessio Nencioni, University of Genoa, 16132 Genoa, Italy. Phone: 39-010-353-8990; Fax: 39-010-353-7989; E-mail: [alessio.nencioni@unige.it](mailto:alessio.nencioni@unige.it)

**doi:** 10.1158/1078-0432.CCR-14-3023

©2015 American Association for Cancer Research.

### Introduction

Intracellular nicotinamide adenine dinucleotide ( $NAD^+$ ) is essential for several cellular processes, acting either as a coenzyme in redox reactions or as a substrate for  $NAD^+$ -degrading enzymes. Cancer cells are highly dependent on  $NAD^+$  to face increased metabolic demands and high proliferation rates (1). Tryptophan, nicotinic acid (NA), nicotinamide (NAM), and nicotinamide ribose are the main  $NAD^+$  precursors in mammals. Specifically,  $NAD^+$  production from NAM via nicotinamide phosphoribosyltransferase (NAMPT) appears to play a major role in lymphocytes and hematopoietic cells and to be further upregulated in leukemia cells, justifying their susceptibility to NAMPT inhibitors such as APO866 (formerly known as FK866 or WK175; refs. 2–9). On the basis of its promising preclinical activity, APO866 was proposed as novel drug for different hematologic malignancies (4, 7, 10, 11). Nevertheless, this agent exhibits variable and frequently limited cytotoxicity against primary leukemia cells, which limits its applicability as a single agent. In the attempt to obviate to such limitation, APO866 has been combined with TRAIL (12), DNA-damaging agents (daunorubicin, cisplatin, Ara-C, and melphalan; refs. 13, 14),

### Translational Relevance

The rate-limiting enzyme in nicotinamide adenine dinucleotide (NAD<sup>+</sup>) biosynthesis from nicotinamide, NAMPT (nicotinamide phosphoribosyltransferase), regulates growth and metastatic potential of tumor cells. Leukemic cells show a higher NAD<sup>+</sup> turnover rate than normal cells, suggesting that NAD<sup>+</sup> biosynthesis could be critically required in hematologic malignancies, too. Here, we show that the NAMPT inhibitor APO866 is active, but only achieves a partial cell killing in primary leukemia cells. Inhibition of P-glycoprotein 1 (Pgp), which is one of the key factors mediating multidrug resistance, is shown to potentiate the cytotoxic effects of APO866 in leukemia cells, but not in healthy leukocytes and hematopoietic progenitor cells, by increasing intracellular APO866 concentration and thereby exacerbating ATP shortage and endoplasmic reticulum stress. Our data indicate a possible, new, safe, and widely applicable approach for treating hematologic malignancies.

ionizing radiations (15), rituximab (16), and proteasome inhibitors (17), frequently achieving remarkable anticancer effects.

Multidrug resistance (MDR) limits the benefit of different types of anticancer agents (18). Its etiology is multifactorial, but overexpression of membrane transport proteins, such as 170-kDa P-glycoprotein-1 (Pgp), represents a leading cause (19). By extruding drugs across the plasma membrane, Pgp reduces their intracellular concentration and, thus, their efficacy (20–25). Consistent with this biologic function, high levels of Pgp are frequently observed in hematologic (lymphomas, multiple myeloma, and leukemia; refs. 26, 27), as well as in solid (neuroblastoma and soft tissue sarcoma) tumors (28) and Pgp overexpression has been frequently associated with a poor prognosis. Several natural and synthetic Pgp inhibitors have been identified, including drugs in clinical use, such as calcium channel blockers (verapamil and nifedipine), indole alkaloids (reserpine), steroids (progesterone and tamoxifen) and the immunosuppressive agents cyclosporin A and rapamycin (29). A recent clinical study evaluated PSC-833 (valsopodar), a second-generation Pgp inhibitor, in combination with chemotherapy in patients with acute myelogenous leukemia (AML; ref. 30). Disappointingly, this trial failed to show any clinical advantage from the use of the Pgp inhibitor, suggesting that the clinical settings and the anticancer treatments that are going to benefit the most from the use of Pgp inhibitors may still have to be identified.

Here, we demonstrate that Pgp inhibitors, such as cyclosporin A (CsA), verapamil, and PGP-4008, synergistically increase the antileukemic activity of APO866. This effect is shown to reflect an increased intracellular concentration of APO866, which, in turn, increases its ability to block growth- and survival-promoting pathways in leukemia cells.

## Materials and Methods

### Cell lines and reagents

The leukemia (OCI/AML2, OCI/AML3, HL-60, HEL, KG1a, SET1, MV4-11, MEC.1, MEC.2, and LAMA-84 imatinib sensitive

or resistant) multiple myeloma (RPMI-8226 and Dox40) and lymphoma (Daudi, U937, Raji, and SU-DHL1) cell lines were provided by collaborators or purchased from ATCC or DSMZ (Braunschweig, Germany). All cell lines were grown in RPMI-1640-based medium supplemented with 10% FBS (GIBCO; Life Technologies), 2  $\mu$ mol/L L-glutamine, 100 U/mL penicillin, and 100  $\mu$ g/mL streptomycin (GIBCO; Life Technologies). Nilotinib was supplied by Novartis and was stored at 10 mmol/L in DMSO at  $-20^{\circ}$ C. CsA, verapamil, melphalan, doxorubicin, fludarabine, and velcade were obtained from the pharmacy of the S. Martino Hospital in Genoa, Italy. PGP-4008 was purchased from Alexis Biochemicals (Plymouth Meeting). Tetramethylrhodamine ethyl ester (TMRE), 4-PBA, NAM, and NA were obtained from Sigma-Aldrich (Sigma-Aldrich Italia). APO866 was generously provided by the NIMH Chemical Synthesis and Drug Supply Program.

### Primary cell isolation from patient samples

Following written consent obtainment, peripheral blood samples were obtained from a cohort of 25 patients (19 B-CLL and 6 AML) and healthy donors ( $n = 3$ ) at the Department of Internal Medicine of the University of Genova (Genova, Italy), according to the Declaration of Helsinki. The clinical and laboratory features of B-cell chronic lymphocytic leukemia (B-CLL) and AML patients are summarized in Tables 1 and 2, respectively. For B-CLL cell isolation, peripheral blood mononuclear cells (PBMC) were isolated by density gradient centrifugation on Ficoll-Hypaque (Biotest). The B-CLL phenotype of the obtained cell preparations was confirmed by immunostaining with anti-CD19, anti-CD5, and anti-CD23 (Immunotech), followed by the flow cytometric analysis. The purity of the isolated B-CLL cells was typically >85%. AML blasts were isolated by adding a 6% dextran solution (Fresenius Kabi) to the blood specimens at a ratio of 4:5, followed by a 1-hour incubation at room temperature. Thereafter, the leukocytes-enriched supernatants were transferred to a 50 mL conical centrifuge tube and centrifuged at  $300 \times g$  for 10 minutes. Residual red blood cells were lysed by suspending the cell pellets in 4 mL 0.2% NaCl for 30 seconds followed by addition of 4 mL 1.6% NaCl and immediate centrifugation at  $300 \times g$  for 10 minutes. Normal PBMCs were isolated from healthy donor blood samples by density gradient centrifugation on Ficoll-Hypaque. Cells were either used immediately for viability assays or for mRNA isolation, or stored at  $-80^{\circ}$ C in medium containing 20% FBS and 10% DMSO. CD34<sup>+</sup> peripheral blood precursor cells (PBPC) were obtained from the excess PBPC concentrates (1–2 mL) of G-CSF-mobilized patients undergoing autologous PBPC transplantation ( $n = 3$ ), after obtaining informed consent according to the Declaration of Helsinki. CD34<sup>+</sup> cells were purified using the CD34 MicroBead Kit from Miltenyi Biotec (Bergisch Gladbach) according to the manufacturer's instructions. Using this method, CD34<sup>+</sup> cells were typically >80% pure and >80% viable as detected by propidium iodide (PI) staining and flow cytometry (see below).

### Viability assays

A total of  $2 \times 10^5$  cells per well (primary leukemia cells, PBMCs and PBPCs) or  $5 \times 10^4$  cells per well (OCI/AML3 and MEC.1) were plated in 96-well plates in a final volume of 200  $\mu$ L in the presence or absence of the indicated stimuli. Dead cells were quantified

Cagnetta et al.

**Table 1.** Clinical and laboratory features of B-CLL patients

Patient no.	Sex	Age, y	Cytogenetics	RAI stage	IgV <sub>H</sub>	Zap70	CD38
#1*	M	71	Nor	RAI 0	Mutated	Neg	Neg
#2*	F	67	13q-	RAI IV	Mutated	Pos	Pos
#3*	F	68	Nor	RAI IV	Mutated	Neg	Neg
#4	M	74	17p-	RAI 0	Unmutated	Pos	Neg
#5	M	76	Nor	RAI II	Mutated	Neg	Neg
#6	M	65	ND	RAI IV	Mutated	Neg	Neg
#7	M	66	17p-	RAI II	Mutated	Pos	Pos
#8*	M	58	Nor	RAI II	Mutated	Neg	Neg
#9*	M	79	13q-,17p-	RAI 0	Unmutated	Pos	Pos
#10	M	72	Nor	RAI IV	Unmutated	Pos	Pos
#11*	F	67	ND	RAI 0	Mutated	Neg	Neg
#12	M	56	17p-	RAI 0	Mutated	Pos	Pos
#13	M	77	12 +	RAI II	Mutated	Neg	Neg
#14	M	75	ND	RAI III	Unmutated	Pos	Neg
#15*	M	73	13q-,11q-	RAI IV	Unmutated	Neg	Pos
#16	M	67	Nor	RAI 0	Mutated	Neg	Neg
#17	M	65	ND	RAI II	Mutated	Pos	Pos
#18	M	77	12+	RAI IV	Mutated	Pos	Neg
#19*	F	75	ND	RAI II	ND	ND	ND

Abbreviations: ND, not determined; Nor, normal; +, trisomy; \*, chemo-naïve patient.

96 hours later by PI staining (2 µg/mL) and flow cytometry (FACS Calibur; Becton Dickinson). Specific death was calculated as follows: [(% experimental death – % spontaneous death)/(100 – % spontaneous death)] × 100. For Annexin-V/PI staining 3 × 10<sup>6</sup> leukemic cells were plated in 1 mL medium in 24-well plates in the presence of the indicated stimuli and for the indicated amounts of time. Afterwards, cells were washed, stained with Annexin-V-FITC (Becton Dickinson) and PI and analyzed by flow cytometry. For the detection of hypodiploid cell nuclei, cell pellets were suspended in a buffer containing 0.1% sodium citrate, 0.1% Triton-X 100, and 50 µg/mL PI. Thereafter, cells were analyzed by flow cytometry.

#### Mitochondrial transmembrane potential ( $\Delta\psi_m$ ) determination

$\Delta\psi_m$  was determined as previously described (4, 17). Briefly, cells were harvested, washed and incubated in the presence of 50 nmol/L TMRE in regular RPMI-based medium for 15' at 37°C. Thereafter, cells were analyzed by flow cytometry.

#### Immunoblotting

Whole-cell lysates and cell fractions were prepared as previously described (4, 17). Protein concentrations were determined by Bradford assay (Bio-Rad) and 10 to 50 µg proteins were subjected to SDS-PAGE, transferred to polyvinylidene difluoride membranes, and detected with the following antibodies: anti-NAMPT (Bethyl Laboratories, Inc.), anti-BIP, -IRE1 $\alpha$ , -ubiquitin, -CHOP, -MDR1/ABC1 (Cell Signaling Technology), anti- $\gamma$ -tubulin (mouse monoclonal; Sigma Aldrich) and anti-

nucleolin (Santa Cruz Biotechnology). Standard enhanced chemiluminescence (ECL by Thermo Fisher Scientific) was used for protein bands detection.

#### Determination of NAD<sup>+</sup> and ATP levels

Intracellular NAD(H) content was determined with an NAD(H) Quantification Kit by BioVision following the instructions of the manufacturer. Intracellular ATP content was determined with Cell titer Glo Luminescent Cell Viability Assay (Promega). NAD<sup>+</sup> and ATP values were normalized to the number of viable cells as determined with Trypan Blue (Lonza).

#### Intracellular APO866 measurement

A total of 20 × 10<sup>6</sup> primary B-CLL cells were plated in 6-well plates and treated for 24 hours with 3 nmol/L APO866 in presence or absence of CsA 0.3 µmol/L. Thereafter, cells were harvested and lysed in water. The extracted material was analyzed on an Agilent 1100 capillary chromatography system, equipped with a diode array detector and coupled to a mass spectrometer Agilent 1100 series LC/MSD Trap, equipped with an orthogonal geometry electrospray ion source and an ion-trap analyzer. HPLC separation was performed on a Waters Atlantis TM dC18 column (150 × 1 mm; particle size, 3 µm) at a flow rate of 30 µl/min; eluent A was 0.1% formic acid in water, eluent B was acetonitrile containing 0.1% formic acid, and the applied gradient was as follows: during the first 5 minutes eluent B was maintained at 5%. Subsequently, between 5 and 35 minutes, eluent B was progressively increased to 100%. Detection wavelength was set at 220 and 260 nm. MS spectra were acquired in positive ion mode in the m/z range, 100 to 400. APO866 concentration values were normalized to a protein concentration.

#### Immunohistochemistry

Sections of bone marrow (BM) samples from patients diagnosed with hematologic malignancies at the IRCCS AOU San Martino-IST were stained with anti-NAMPT (clone H-300; sc-67020; Santa Cruz Biotechnology; ref. 31). IHC was performed using the Ventana BenchMark XT automated immunostainer. Tissue sections were deparaffinized and rehydrated. After antigen

**Table 2.** Clinical and laboratory features of AML patients

Patient nr.	Sex	Age	Sample source	FAB Stage	% Blasts
#20	M	53	PB	M4	95
#21	F	50	PB	M1	78
#22	M	80	BM	M0/M1	90
#23	M	78	PB	Secondary	80
#24	M	79	PB	Secondary	70
#25	F	79	PB	M4	80

Abbreviations: BM, bone marrow; PB, peripheral blood.

retrieval, sections were incubated with primary antibodies at a dilution of 1:200 and 3,3'-diaminobenzidine (DAB) was used as a chromogen. Sections were counterstained with May-Grünwald-Giemsa.

#### RNA interference

RNAi was performed with an ON-TARGET PLUS SMART pool targeting ABCB1 (GE Dharmacon). A nontargeting scrambled negative control siRNA was used as negative control (GE Dharmacon). Briefly, OCI/AML3 and MEC-1 cells were transiently transfected with MDR-1 siRNA with the Amaxa technology (V-solution with X-001 or U-013 program, respectively).

#### Statistical analyses

Each experiment was repeated at least three times. Statistical analyses were performed with GraphPad Prism software 6 using one-way ANOVA for multiple group comparison or the unpaired *t* test for two-group comparison. *P* values below 0.05 were considered significant. Expression levels of NAMPT in human cancer cell lines were obtained from datasets collected in OncoPrint portals at <http://www.oncoPrint.org> (Barretina Cell Line dataset). Copy-number data for the human 7q22.3 locus (where NAMPT maps) in tumor cell lines was downloaded from the publicly available database (<http://www.broadinstitute.org/cgle>). Next, data were analyzed using the Integrative Genomics Viewer (IGV) analysis software. Expression levels of NAMPT in different hematologic tumors, were obtained from publicly available Gene Expression Omnibus (GEO) datasets (accession numbers GSE12417 for AML; GSE4475 for DLBCL and GSE22762 for CLL). Differences in median-centered transcript levels between different groups of samples were evaluated by the unpaired Student *t* test. Drug synergism was analyzed by isobologram analysis using the CalcuSyn Version 2.0 software program (Biosoft). A combination index (CI) less than 1.0 indicates synergism; CI = 1, additive effect; and CI > 1, no significant combination effect (32).

## Results

### NAMPT is overexpressed and has adverse prognostic relevance in hematologic malignancies

We first investigated the relevance of NAMPT in hematologic malignancies by characterizing its expression in a wide range of cell lines and patient samples. In line with previously published data (4, 7, 12, 17, 33), an analysis of the Cancer Cell Line Encyclopedia database (34) revealed higher NAMPT expression levels in hematologic malignancies (including lymphomas, leukemias, and multiple myeloma) compared with cancer cell lines of epithelial origin (Fig. 1A). An array-based comparative genomic hybridization analysis of the same dataset showed focal amplification of the NAMPT locus (mapping on 7q22.3) and NAMPT transcript levels were found to correlate with the DNA copy number, particularly in cell lines derived from hematologic malignancies (Pearson value = 0.391; *P* = 0.002; Supplementary Fig. S1A and S1B). These findings, supported by the strong NAMPT expression in leukemia cell lines (Fig. 1B) and by our previous study of NAMPT's role in multiple myeloma (4, 17, 35), prompted us to further investigate the role of this enzyme in leukemogenesis. Using IHC, we were able to confirm that BM biopsies from newly diagnosed AML and B-CLL patients exhibit significantly increased NAMPT levels than samples obtained from

healthy donors (Fig. 1C). We also retrospectively analyzed the prognostic relevance of baseline NAMPT expression by interrogating microarray datasets of AML, DLBCL, and B-CLL patients. As shown in Fig. 1D, high NAMPT expression in hematologic malignancies was significantly associated with poor overall survival (OS). Thus, altogether, these data supported the notion that NAMPT plays an important role in the pathophysiology of hematologic malignancies and that it represents an attractive therapeutic target (11, 16, 34, 36).

### Pgp inhibitors synergistically cooperate with APO866 to the killing of human leukemia cells

The variability of APO866 antitumor effects prompted us to search for drugs that, when combined with this NAMPT inhibitor would enhance its efficacy (12, 14, 16, 17, 37). To this end, we screened several agents that are widely used in hematology, monitoring their effects on viability of primary leukemia cells (either as single agents or in combination with APO866). As shown in Fig. 2A, CsA was readily identified as one of the best sensitizers of primary B-CLL cells to the activity of APO866. CsA is an immunosuppressant whose mechanism of action entails the obstruction of calcineurin and, thereby, inhibition of NF-AT (nuclear factor of activated T cells) (38–40). However, when treating primary B-CLL cells with FK506 (tacrolimus), an unrelated calcineurin inhibitor, we found that this agent failed to enhance APO866 activity (Supplementary Fig. S2), suggesting that the potentiation effect observed with CsA may reflect an alternative mode of action of the latter. In addition to inhibiting calcineurin, CsA is also a well-known Pgp inhibitor (41–43). Thus, we reasoned that Pgp inhibition may be the mechanism underlying CsA-mediated enhancement of APO866 antileukemic activity and tested other, unrelated Pgp inhibitors in combination with APO866 to see whether they would recreate the effects of CsA. Indeed, both verapamil and PGP-4008 strongly enhanced APO866 activity in two leukemia cell lines (OCI/AML3—AML and MEC.1—B-CLL; Fig. 2B and C) and in primary leukemia cells from a cohort of patient that included cases of AML (*n* = 6) and B-CLL (*n* = 19; Fig. 2C and Tables 1–3).

Consistent with the hypothesis that APO866 may be a Pgp substrate, using HPLC/MS, we were able to show that both CsA and PGP-4008 increase APO866 intracellular levels in primary B-CLL cells (Fig. 2D and Supplementary Fig. S3). Finally, additional evidence in support of the notion that APO866 antileukemic activity is regulated by Pgp activity was obtained in RNAi experiments and in studies with Pgp-overexpressing cell lines. In a first set of experiments, the leukemia cell lines OCI-AML3 and MEC1 were transfected with Pgp siRNA and Pgp silencing was verified by WB 2 days after transfection (Fig. 3A, upper insets). As shown in Fig. 3A (lower insets), Pgp depletion significantly enhanced leukemia cell death upon APO866 treatment vs. control (non-targeting siRNA). Notably, the addition of CsA in leukemia cells in which Pgp was previously silenced further enhanced APO866 activity, suggesting that reducing Pgp protein levels by RNAi may be used to further increase the efficacy of pharmacologic Pgp inhibitors. Subsequently, Doxo40 (44) and LAMA84-r (45), two well-characterized Pgp-overexpressing cell lines, were compared with their parental cell lines (RPMI8226 and LAMA84, respectively) in terms of susceptibility to APO866, CsA, and their combination. As predicted, cells overexpressing Pgp were found to be more resistant to APO866 than the non-Pgp-overexpressing cells

Cagnetta et al.

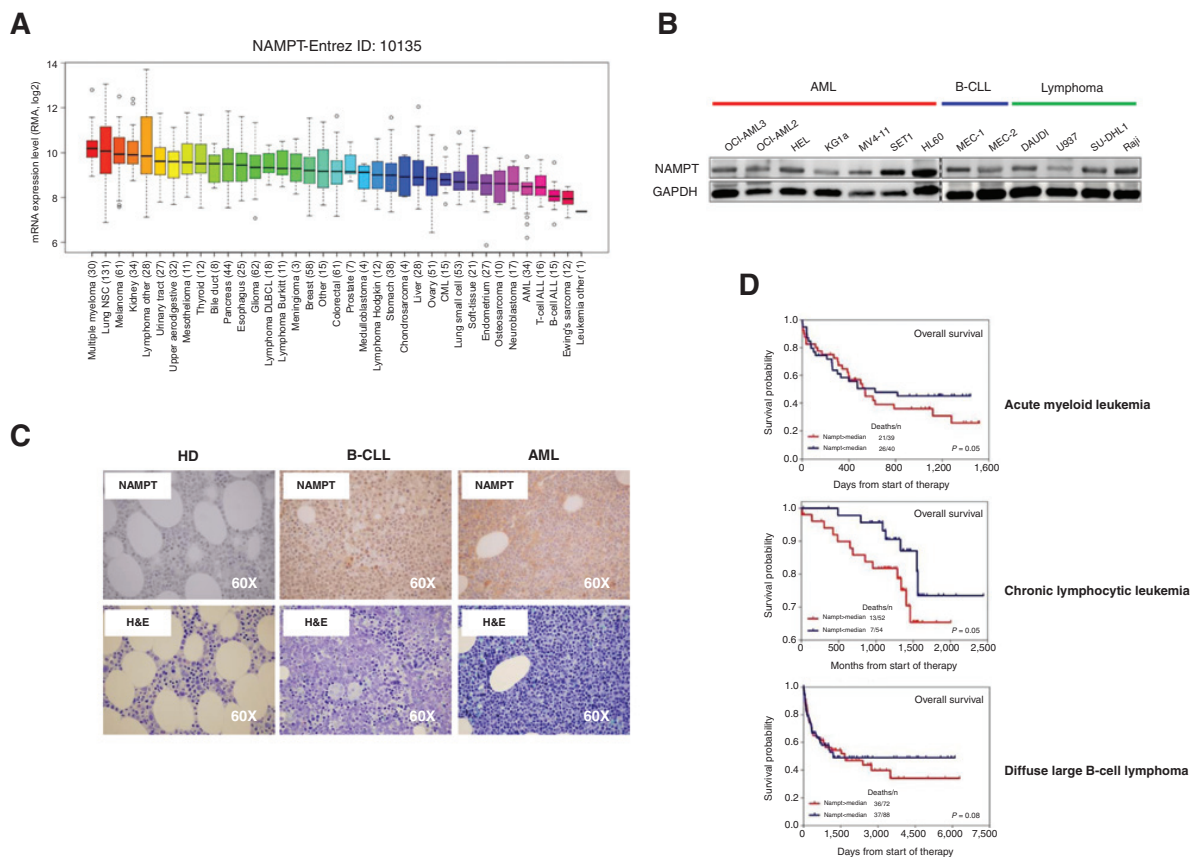


**Figure 1.** NAMPT expression and its prognostic relevance in hematologic malignancies. A, NAMPT mRNA expression in solid tumors and hematologic cancers across lines included in the Cancer Cell Line Encyclopedia (Oncomine at <http://www.oncomine.org>; Barretina Cell Line dataset). In the box plots, the middle bars represent the median value, the boxes encompass the values from the lower to the upper quartile (25th–75th percentile), and the whiskers encompass the 25th percentile minus 1.5 times the interquartile range and the 75th percentile plus 1.5 times the interquartile range. B, whole-cell lysates from AML (OCI-AML3, OCI-AML2, HEL, KG1a, MV4-11, SET1, and HL60), B-CLL (Mec.1 and Mec.2), and lymphoma (DAUDI, U937, SU-DHL1 and Raji) cell lines were analyzed for NAMPT expression. Glyceraldehyde 3-phosphate dehydrogenase (GAPDH) was used as loading control. C, IHC analysis on three representative BM specimens derived from healthy donors (HD), AML, and B-CLL affected patients, show NAMPT expression (positive cells are brown) and hematoxylin and eosin (H&E); magnification,  $\times 60$ . D, Kaplan-Meier plots showing prognostic relevance of NAMPT expression on OS of AML ( $n = 79$ ; GSE12417; ref. 56), chronic lymphocytic leukemia ( $n = 148$ ; GSE22762; ref. 57), and diffuse large B-cell lymphoma ( $n = 396$ ; GSE4475; ref. 58) patients. Medians  $\pm$  SD are presented. The group of patients with higher SIRT6 expression (red line) had shorter OS than patients with lower SIRT6 expression (blue line; log-rank test).

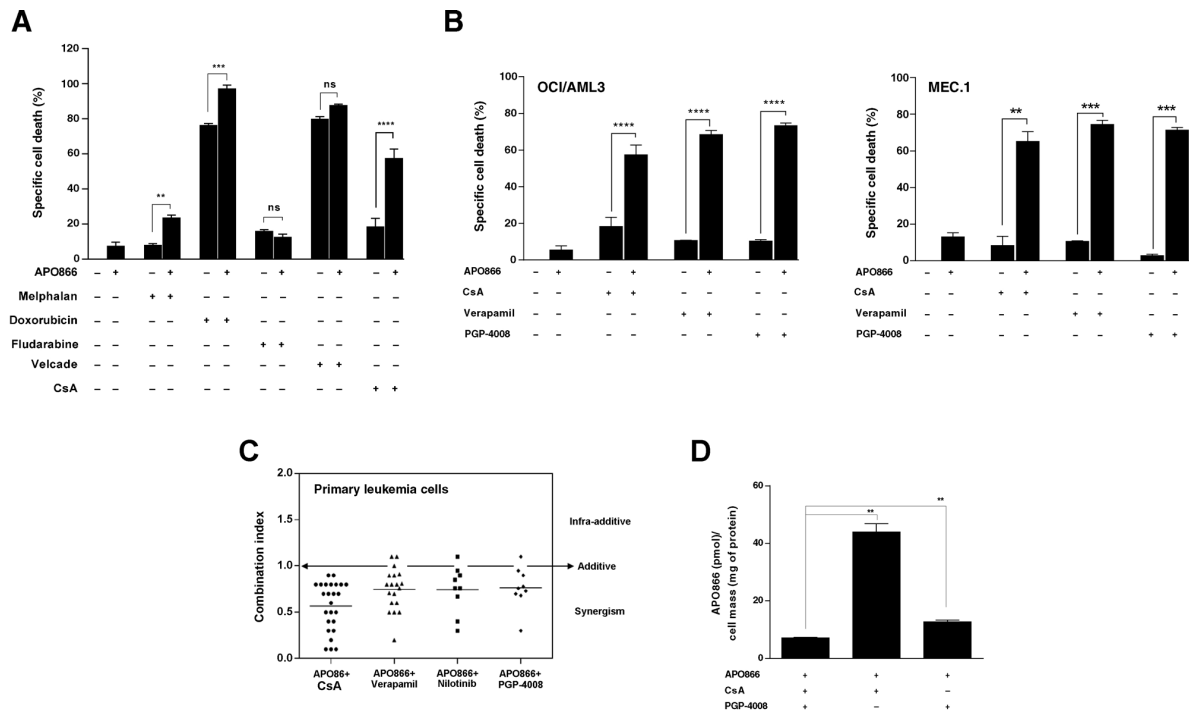
(Fig. 3B). Therefore, collectively, these findings are consistent with the hypothesis that APO866 is a substrate of Pgp and that APO866 activity can be with Pgp inhibitors, including CsA.

Finally, we assessed whether combining APO866 with Pgp inhibitors would result in an increased cytotoxicity in healthy PBMC and PBPC, too. However, neither APO866 nor Pgp inhibitors or their combination induced cell death in these cells, suggesting that these treatments could have a favorable therapeutic index *in vivo*, too (Supplementary Fig. S5A and S5B).

**CsA enhances NAD<sup>+</sup> shortage,  $\Delta\psi_m$  loss and apoptosis triggered by APO866**

It is well established that APO866-mediated cytotoxicity largely relies on the depletion of intracellular NAD<sup>+</sup> stores, which, in turn, ultimately leads to ATP shortage (2, 36, 46). Using a cycling enzymatic assay, we monitored the metabolic

changes occurring in primary leukemia cells (AML and B-CLL), as well as in leukemia cell lines, following their exposure to APO866, Pgp inhibitors, and their combinations. In line with our previous studies, APO866 treatment alone consistently reduced intracellular NAD<sup>+</sup> content, as well as ATP, in cell lines and in primary leukemia cells (Fig. 4A and B and Supplementary Fig. S6). Interestingly, Pgp inhibitors alone were found to also slightly reduce both NAD<sup>+</sup> and ATP. However, in response to a treatment with combined APO866 and Pgp inhibitors, both NAD<sup>+</sup> and ATP depletion were exacerbated. To gain further insight into the mechanism of cell death occurring in response to combined APO866 and Pgp inhibitors, we monitored  $\Delta\psi_m$  and the occurrence of apoptosis (by PI/Annexin-V staining), as well as of hypodiploid cell nuclei, in leukemia cells over time. With this combined approach, we were able to show that APO866 causes  $\Delta\psi_m$  dissipation, an

**Figure 2.**

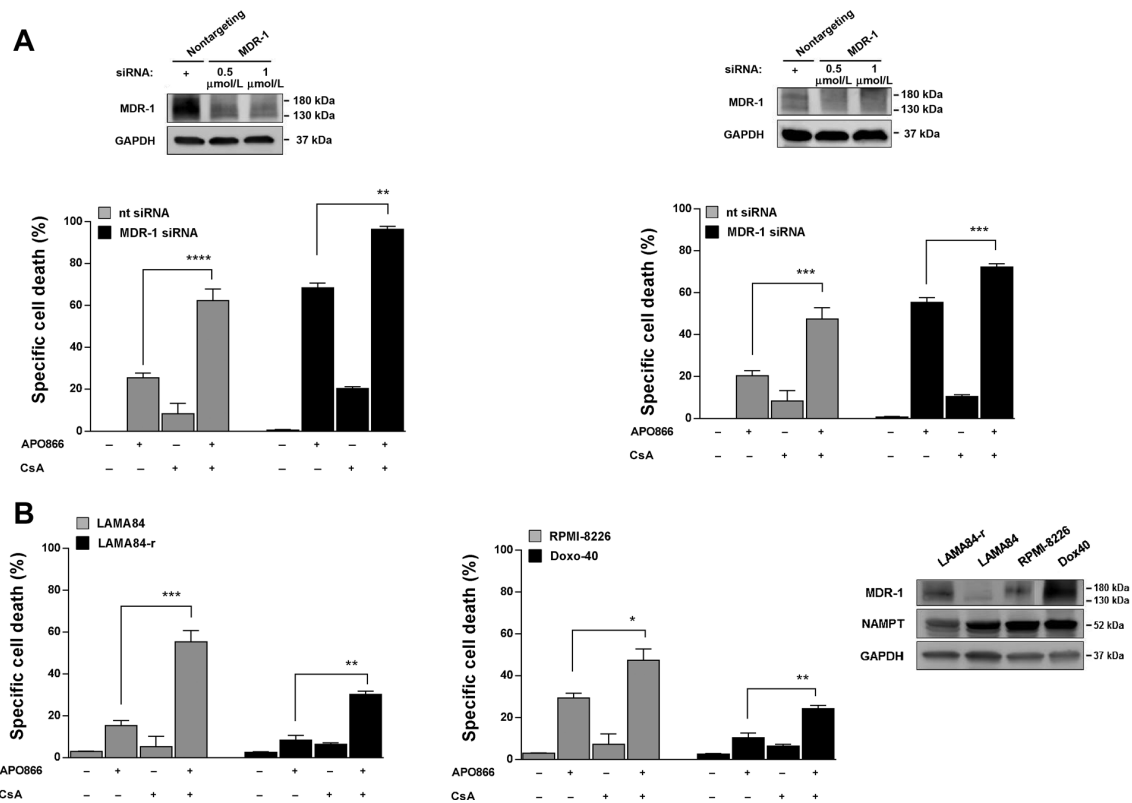
NAMPT inhibition triggers synergistic antileukemia effect with CsA. A,  $2.5 \times 10^4$  primary B-CLL cells were incubated in 96-well plates in the presence or absence of 3 nmol/L APO866 and different antileukemia drugs (0.5  $\mu$ mol/L melphalan, 0.3  $\mu$ mol/L doxorubicin, 5  $\mu$ mol/L fludarabine, 0.01  $\mu$ mol/L velcade, and 1  $\mu$ mol/L CsA) or their combination. Cell death was assessed 96 hours later by PI staining and flow cytometry. Results are means of triplicates  $\pm$  SD; ns, not significant; \*\*,  $P = 0.01$ ; \*\*\*,  $P = 0.002$ ; \*\*\*\*,  $P < 0.0001$ . B,  $2.5 \times 10^4$  OCI/AML3 (left) or Mec.1 (right) cells were plated in 96-well plates and treated with or without increasing doses of APO866 (3 nmol/L) for 48 hours, and then vehicle or Pgp modulators (10  $\mu$ mol/L verapamil, 1  $\mu$ mol/L CsA, and 10  $\mu$ mol/L PGP-4008) were added for further 48 hours. Viability was assessed using PI staining and FACS analysis. Data, means of triplicate  $\pm$  SD ( $n = 3$ ; \*\*,  $P = 0.02$ , \*\*\*,  $0.001 < P < 0.003$ , \*\*\*\*,  $P < 0.0001$ ). C, primary leukemic cells from 25 patients (19 B-CLL and 6 AML) were plated in 96-well plates and incubated with 3 nmol/L APO866 and various Pgp modulators (verapamil, Nilotinib, or PGP-4008). Cell death was assessed 96 hours later by PI staining and flow cytometry. Results are means of triplicates  $\pm$  SD. CI values  $< 1$ , = 1 and  $> 1$  mean indicate synergistic, additive or infra-additive effect, respectively. D,  $2 \times 10^7$  primary B-CLL cells per well were plated in 6-well plates and treated for 24 hours with 3 nmol/L APO866 in presence or absence of CsA 1  $\mu$ mol/L. Thereafter, cells were harvested and lysed in water. The extracted material was then analyzed by mass spectrometry. APO866 concentration in each extract was normalized to protein concentration.

apoptotic cell phenotype (AnnexinV<sup>+</sup>/PI<sup>-</sup> or AnnexinV<sup>+</sup>/PI<sup>+</sup>), as well as a strong increase in hypodiploid (apoptotic) cell nuclei in primary B-CLL cells (Fig. 5A–C). Taken as single agents, Pgp inhibitors (CsA, PGP-4008 and nilotinib) were much less effective than APO866. However, adding a Pgp inhibitor to APO866 consistently led to a much more pronounced  $\Delta\psi_m$  loss and apoptotic phenotype. Because previous studies showed autophagy to be frequently associated with APO866-induced leukemia cell death (4, 11, 16, 17), we also investigated whether an aberrant activation of the autophagic machinery would also be involved in the cooperation between APO866 and Pgp inhibitors. However, addition of a Pgp inhibitor failed to increase the expression of LC3B-II (a marker of autophagy activation) above the levels detected with APO866 alone (data not shown). In addition, autophagy inhibition with 3-methyl adenine (3-MA) failed to protect leukemia cells from APO866 in combination with Pgp inhibitors (data not shown). Therefore, these data essentially rule out a major role of autophagy in the observed synergistic effects between APO866 and Pgp inhibitors.

#### Evidence for an involvement of ER stress and UPR in leukemia cells sensitization to APO866 by Pgp inhibitors

Previous studies by our groups showed that APO866 negatively affect endoplasmic reticulum (ER) physiology in susceptible cells. In addition, recent studies have also linked the anticancer activity of Pgp inhibitors (including CsA and verapamil) to the induction of ER stress and of a terminal unfolded protein response. Thus, because ER stress is a main trigger for apoptotic responses, we assessed its potential relevance in the antileukemic effects of APO866, Pgp inhibitors and their combination (13, 47–51). ER stress inhibition with the chemical chaperone 4-phenyl butyric acid (4-PBA; ref. 52) significantly reduced the cytotoxic effects of APO866, CsA, and of the two combined agents in OCI/AML3 and MEC.1 cells, as well as in primary B-CLL cells (Fig. 6A). An analysis of ER stress-related markers was also performed. As predicted, in cells that were cotreated with APO866 and CsA a stronger increase in IRE1 $\alpha$ , C/EBP-homologous protein (CHOP) and BIP levels as compared with the single-agent treatments was observed (Fig. 6B and Supplementary Fig. S7). A marked increase in the

Cagnetta et al.

**Figure 3.**

Modulation of P-glycoprotein (Pgp) activity affects APO866 sensitivity in leukemia cells. A, OCI-AML3 (left) and MEC.1 (right) were transfected using different concentrations of ON-TARGET PLUS SMART pool targeting MDR-1 or nontargeting negative control siRNA (nt siRNA). Twenty-four hours after transfection, leukemia cells were treated with 3 nmol/L APO866 in the presence or absence of 1 μmol/L CsA. Cell lysates were obtained 48 hours after transfection and subjected to Western blot analysis to confirm decrease in MDR1 protein expression. GAPDH was used as loading control. Cell death was assessed 72 hours later by PI staining and flow cytometry. B,  $2.5 \times 10^4$  LAMA84r (left) or Doxo40 (right) cells, in parallel with their parental cell lines (LAMA84 and RPMI8226, respectively), were plated in 96-well plates and treated with or without increasing doses of APO866 (3 nmol/L) for 48 hours. Then, vehicle or CsA (1 μmol/L) were added for further 48 hours. Viability was assessed using PI staining and FACS analysis. A and B, data, means of triplicate  $\pm$  SD ( $n = 3$ ; \*,  $P = 0.05$ ; \*\*,  $0.003 < P < 0.002$ ; \*\*\*,  $0.001 < P < 0.0003$ ; \*\*\*\*,  $P < 0.0001$ ).

molecular chaperone BIP was also detected in primary B-CLL cells treated with APO866 and CsA (Fig. 6C). Finally, a considerable accumulation of misfolded proteins, detected as a smear of high-molecular weight adducts (Fig. 6B) in response to combined CsA and APO866 was also documented, whereas a weaker smear, previously identified as made of polyubiquitinated proteins (53), was observed in response to APO866 alone. Thus, overall, these findings indicate a novel role for ER stress and unfolded protein accumulation in the antileukemic activity of APO866 and of its combination with Pgp inhibitors.

#### Nicotinamide and nicotinic acid completely abolish activity of cotreatment in leukemia cells

The Preiss Handler pathway (2, 8) for  $NAD^+$  biosynthesis sees the conversion of nicotinic acid to nicotinic acid mononucleotide (NaMN) by the enzyme Nicotinic Acid Phosphoribosyl Transferase (NAPRT1). NaMN is subsequently converted to  $NAD^+$  by an additional enzymatic reaction. In NAPRT1-proficient cells, NA addition is typically sufficient to rescue the cytotoxic activity of APO866, allowing to verify that APO866-induced

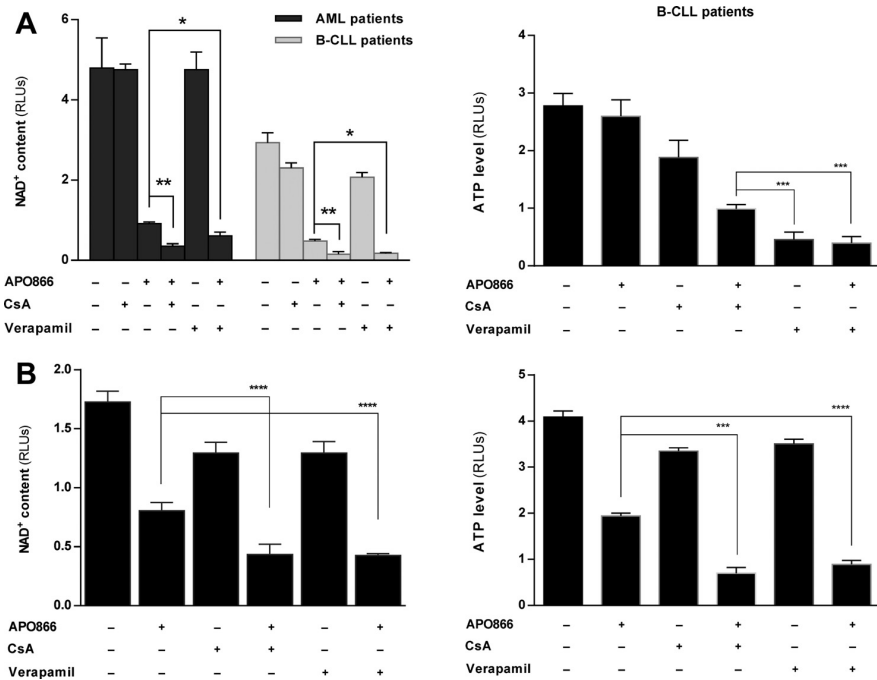
cell death is indeed mediated by reduced  $NAD^+$  availability (54, 55). On the basis of these premises, we first determined *NAPRT1* expression in primary leukemia cells by Q-PCR and essentially found that *NAPRT1* was ubiquitously expressed. Thereafter, we investigated the specific role of  $NAD^+$  depletion in the observed synergism (between APO866 and Pgp inhibitors) by rescuing  $NAD^+$  biosynthesis with NA supplementation. Consistent with our previous findings (37), NA supplementation completely abrogated the antileukemic activity of APO866, both as a single agent and in combination with CsA (Supplementary Fig. S8A and S8B), confirming the role of  $NAD^+$  depletion in the activity of these antileukemic treatments. Interestingly, no protection from APO866, CsA, or their combination was conferred to leukemia cells by tryptophan supplementation, essentially ruling out a major role for the *de novo*  $NAD^+$  biosynthetic pathway in this type of cancer (data not shown).

#### Discussion

Here, we show that the antileukemic activity of the  $NAD^+$ -lowering agent APO866 is strongly enhanced by

**Figure 4.**

Pgp modulators treatment combined with APO866 enhances NAD<sup>+</sup> and ATP depletion produced by APO866. A, 2 × 10<sup>5</sup> primary leukemic (AML and B-CLL) cells per well were plated in 6-well plates and incubated with 3 nmol/L APO866, 1 μmol/L CsA, and 6 μmol/L Verapamil alone or in combination. After 24 hours (left) or 48 hours (right) later, cells were harvested and NAD<sup>+</sup> or ATP levels were determined in cell extracts. B, 1 × 10<sup>5</sup> Mec.1 cells per well were plated in 6-well plates and incubated with or without 3 nmol/L APO866 and Pgp modulators (10 μmol/L Verapamil, 1 μmol/L CsA). After 24 hours (left) or 48 hours (right) later, cells were harvested and intracellular NAD (H)<sup>+</sup> and ATP levels were evaluated and compared with those in control cells. A and B, means ± SD of at least three independent experiments are shown; \*, 0.05 < P < 0.03; \*\*, 0.004 < P < 0.002; \*\*\*, 0.001 < P < 0.0009; \*\*\*\*, P < 0.0001.



combining it with Pgp inhibitors. The latter are shown to increase APO866 intracellular concentration, exacerbating APO866's effects on cellular energetics. In addition, a key role for ER stress in the anticancer activity of APO866 and of its combination with Pgp inhibitors is demonstrated for the first time.

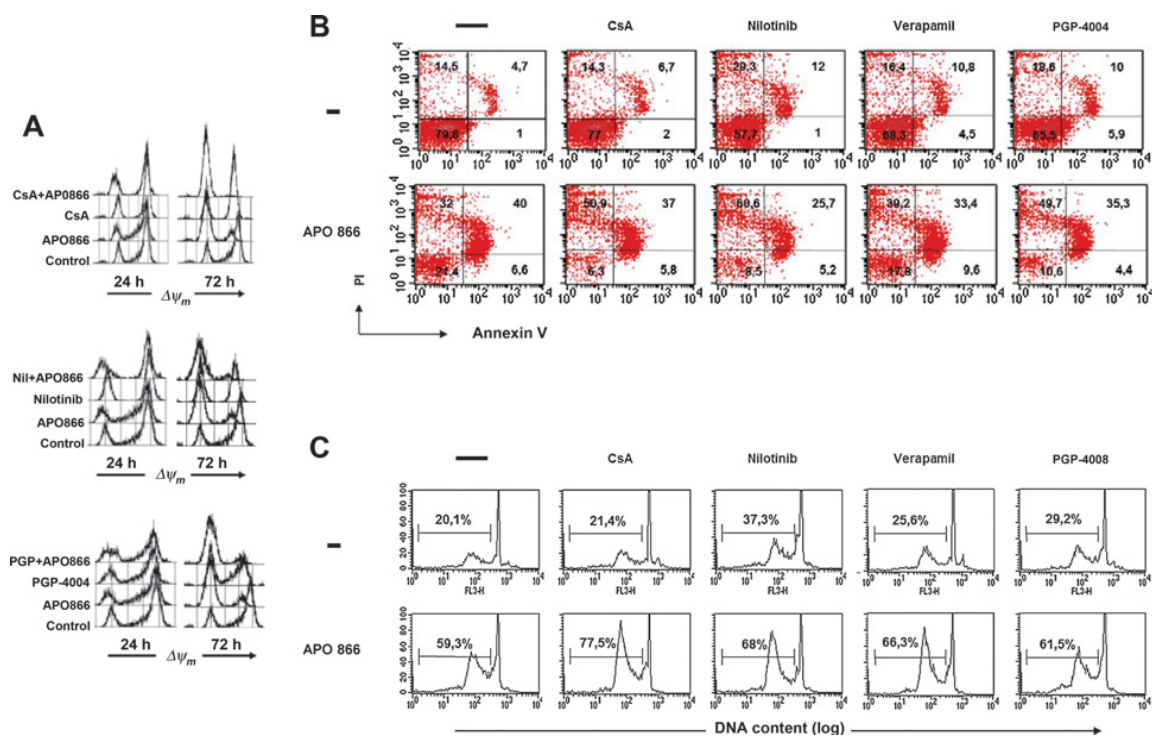
We first documented that high levels of NAMPT are expressed in several types of hematologic malignancies and demonstrated the prognostic relevance of this protein. Next, in the attempt to identify agents that, when combined with APO866, would enhance its antileukemic activity, we discovered CsA as

**Table 3.** Synergistic interactions between APO866 and efflux pump inhibitors in primary leukemia cell

Patient nr.	CsA (1 μmol/L)	Verapamil (6 μmol/L)	AP0866 (10 nmol/L)	CsA+AP0866	Verapamil+AP0866
#1	2.7	ND	5	67.56 (0.1)	ND
#2	1.8	ND	43.5	94.24 (0.4)	ND
#3	5.58	ND	1.13	51.33 (0.1)	ND
#4	3.42	ND	1.41	44.44 (0.1)	ND
#5	6.13	8.8	46.43	75.51 (0.7)	67.35 (0.8)
#6	17.55	2.19	43.11	86.77 (0.7)	73.73 (0.6)
#7	0.9	26	24	84 (0.3)	84 (0.6)
#8	9	ND	5.6	35.7 (0.4)	ND
#9	21.1	ND	4.7	89.8 (0.3)	ND
#10	14.6	ND	35.3	99.35 (0.5)	ND
#11	35.8	9.5	27.72	83.78 (0.7)	76.5 (0.5)
#12	35.7	ND	0.25	73.3 (0.5)	ND
#13	27.6	32.7	24.7	63.2 (0.8)	59.2 (0.9)
#14	41	10.9	30.3	80 (0.8)	55.6 (0.7)
#15	27.6	32.74	24.7	73.9 (0.7)	69.23 (0.8)
#16	5.6	6	46.9	95.4(0.5)	95.1 (0.5)
#17	20.4	13.9	54.9	84.8 (0.8)	85.05 (0.8)
#18	6.6	ND	3.8	42.44 (0.2)	ND
#19	21.25	13.9	54	84.81 (0.8)	85.05 (0.79)
#20	56.7	ND	37.6	95.1 (0.9)	ND
#21	40.5	ND	24.7	73.5 (0.8)	ND
#22	15	ND	7.46	30.31 (0.8)	ND
#23	23.4	27.6	37.8	68.63 (0.8)	66.45 (0.9)
#24	21	ND	34	87.5 (0.6)	ND
#25	43.4	7.6	37.8	84.5 (0.9)	81.9 (0.5)

NOTE: Primary B-CLL (#1-17) or AML (#18-25) cells were plated in 96-well plates and stimulated with 1 μmol/L CsA, 6 μmol/L verapamil, and 3 nmol/L APO866 alone or their combinations. Specific cell death was detected four days later by PI staining and flow cytometry. CIs are indicated in parentheses. Abbreviation: ND, not determined.

Cagnetta et al.

**Figure 5.**

The antileukemic effect of APO866 plus CsA occurs via apoptosis. A,  $3 \times 10^6$  primary B-CLL cells per well were plated in 6-well plates and incubated for 72 hours with 3 nmol/L APO866 and different Pgp modulators alone or their combination.  $\Delta\psi_m$  was monitored at the indicated time points by TMRE staining and flow cytometry. B and C,  $1 \times 10^6$  primary B-CLL cells per well were plated in 6-well plates and treated for 48 hours with or without 3 nmol/L APO866 and Pgp modulators (1  $\mu$ mol/L CsA, 10  $\mu$ mol/L Verapamil, 10 nmol/L Nilotinib, or 10 nmol/L PGP-4008). Thereafter, cells were harvested, washed, and used for Annexin-V/PI staining and flow cytometry (B), or for flow cytometric quantification of hypodiploid cell nuclei (C). The results are means  $\pm$  SD of three separate experiments.

a highly effective potentiator. Notably, the combination of CsA with APO866, whereas highly active in different types of leukemias, was found to spare healthy PBMCs and PBPC, suggesting that this novel regimen should have a favorable therapeutic index in patients, too.

At the molecular level, the ability of CsA to boost APO866 activity is shown to reflect its function as a Pgp inhibitor, instead of as a calcineurin inhibitor. Consistent with this notion, CsA and other Pgp inhibitors increase intracellular APO866 levels, thereby enhancing APO866-induced NAD<sup>+</sup> depletion,  $\Delta\psi_m$  loss, and ATP shortage (Supplementary Fig. S8C). Activation of the apoptosis machinery is one of the downstream events leading to leukemia cell death in response to combined APO866 and Pgp inhibitors, as detected by Annexin-V/PI staining and by the occurrence of hypodiploid cell nuclei. In addition, we show here for the first time that APO866 and, to a higher extent, its combination with Pgp inhibitors induce ER stress and that this type of response plays a role in the anticancer activity of these agents. Notably, this type of cell death appears to be distinct from the autophagic cell death that was previously observed with single-agent APO866 treatment (11, 16). The lack of effect of autophagy inhibition on the cell demise that occurs in response to APO866 plus CsA could reflect the fact that, by strongly increasing the intracellular levels of APO866 and, consequent-

ly, its metabolic effects (i.e., NAD<sup>+</sup> and ATP shortage), CsA leads to a shift in the cell death programs activated by the NAMPT inhibitor, preferentially activating apoptosis and ER stress (51).

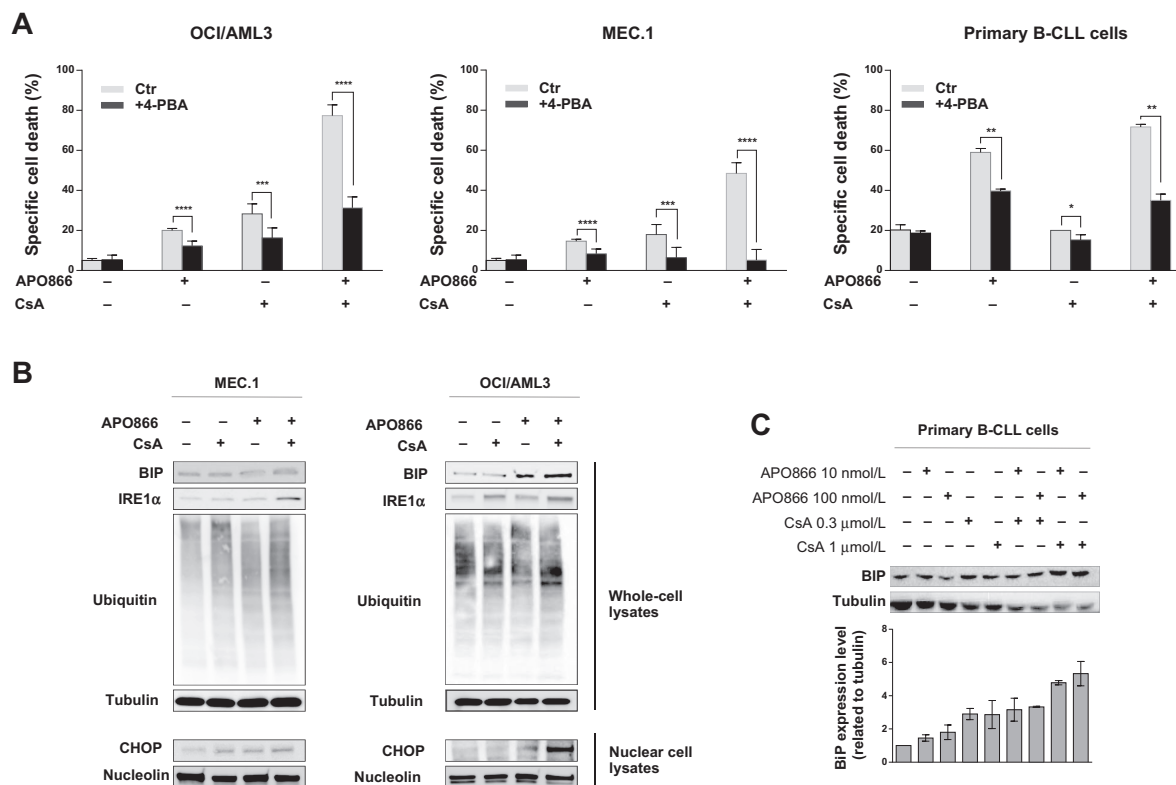
In conclusion, our data indicate that APO866 is a *bona fide* Pgp substrate and that combining this agent with Pgp inhibitors (including CsA) strongly potentiates its cytotoxic activity on leukemia, but not on healthy cells. We demonstrate a key role for ER stress in the observed synergistic interaction between APO866 and Pgp inhibitors. Our data provide the biologic rationale for combining Pgp inhibitors with APO866 in leukemia patients.

#### Disclosure of Potential Conflicts of Interest

No potential conflicts of interest were disclosed.

#### Authors' Contributions

Conception and design: A. Cagnetta, M. Gobbi, A. Nencioni, M. Cea  
Development of methodology: A. Cagnetta, C. Acharya, D. Soncini, P. Acharya, M. Cea  
Acquisition of data (provided animals, acquired and managed patients, provided facilities, etc.): I. Caffa, C. Acharya, D. Soncini, P. Acharya, I. Pierri, M. Bergamaschi, G. Fraternali, L. Mastracci, C. Zucal, A. Salis, A. Nencioni, M. Cea

**Figure 6.**

CsA plus APO866 antileukemic effect is mediated by ER stress-dependent UPR signaling. A,  $1 \times 10^6$  OCI/AML3, Mec.1 or primary B-CLL cells per well were plated in 96-well plates and preincubated for 2 hours with or without 4-phenyl butyric acid (4-PBA). Thereafter, leukemia cells were treated with APO866 (3 nmol/L) for 48 hours; CsA (1 μmol/L) was then added for additional 48 hours followed by cell death analysis using PI staining and FACS analysis. Data, mean  $\pm$  SD of triplicate samples (\*,  $0.05 < P < 0.01$ ; \*\*,  $0.008 < P < 0.002$ ; \*\*\*,  $0.0006 < P < 0.0002$ ; \*\*\*\*,  $P < 0.0001$ ). B, OCI/AML3 or Mec.1 cells were pretreated with or without a low dose of APO866 (3 nmol/L) for 24 hours, and then CsA (1 μmol/L) was added for additional 24 hours. Cells were then harvested, and cell lysates were subjected to immunoblot analysis using anti-BIP, anti-IRE1α, anti-ubiquitin, anti-CHOP, anti-tubulin, or anti-nucleolin antibodies. C, B-CLL primary cells were treated with APO866 (10–100 nmol/L), CsA (0.3–1 μmol/L), or combined therapy for 48 hours. Cell lysates were subjected to Western blot analysis, using anti-BIP and anti-tubulin Abs. Blots shown are representative of three independent experiments. Relative expression was calculated by taking the ratio of the densitometry signal for BIP to tubulin in each sample using the ImageJ software (1.37v; NIH, <http://rsb.info.nih.gov/ij/>; bottom).

**Analysis and interpretation of data (e.g., statistical analysis, biostatistics, computational analysis):** A. Cagnetta, C. Acharya, D. Soncini, P. Acharya, G. Fraternali, G. Damonte, S. Bruzzone, A. Nencioni, M. Cea  
**Writing, review, and/or revision of the manuscript:** A. Cagnetta, S. Adamia, A. Provenzani, G. Damonte, F. Montecucco, F. Patrone, A. Nencioni, M. Cea  
**Administrative, technical, or material support (i.e., reporting or organizing data, constructing databases):** A. Garuti, M. Cea  
**Study supervision:** F. Patrone, A. Ballestrero, M. Gobbi, A. Nencioni, M. Cea  
**Other (technical support in performing and evaluation of immunohistochemical reactions):** L. Mastracci  
**Other (accepted the final version of the article):** F. Montecucco

## Acknowledgments

The authors thank the NIMH Chemical Synthesis and Drug Supply Program for generously providing APO866 for this study.

## References

- Belenky P, Bogan KL, Brenner C. NAD<sup>+</sup> metabolism in health and disease. *Trends Biochem Sci* 2007;32:12–9.
- Hasmann M, Schemainda I. FK866, a highly specific noncompetitive inhibitor of nicotinamide phosphoribosyltransferase, represents a novel

## Grant Support

This work was supported in part by the Associazione Italiana per la Ricerca sul Cancro (#6108; to A. Nencioni); by the Italian Ministry of Health grant GR-2008-1135635 (to A. Nencioni); by the Compagnia di San Paolo (R.O.L. 689; to A. Nencioni); by the Fondazione Umberto Veronesi (to A. Nencioni); by the Associazione Cristina Bassi (to A. Cagnetta) and by the American Italian Cancer Foundation (to M. Cea). In addition, the research leading to these results has received funding from the European Community's Seventh Framework Program [FP7-2007-2013] under grant agreement n° HEALTH-F2-2013-256986 (Panacreas).

The costs of publication of this article were defrayed in part by the payment of page charges. This article must therefore be hereby marked *advertisement* in accordance with 18 U.S.C. Section 1734 solely to indicate this fact.

Received November 20, 2014; revised April 20, 2015; accepted April 26, 2015; published OnlineFirst May 11, 2015.

Cagnetta et al.

- mechanism for induction of tumor cell apoptosis. *Cancer Res* 2003;63:7436–42.
3. Revollo JR, Grimm AA, Imai S. The regulation of nicotinamide adenine dinucleotide biosynthesis by NAMPT/PBEF/visfatin in mammals. *Curr Opin Gastroenterol* 2007;23:164–70.
  4. Cea M, Cagnetta A, Fulciniti M, Tai YT, Hideshima T, Chauhan D, et al. Targeting NAD<sup>+</sup> salvage pathway induces autophagy in multiple myeloma cells via mTORC1 and extracellular signal-regulated kinase (ERK1/2) inhibition. *Blood* 2012;120:3519–29.
  5. Bi TQ, Che XM, Liao XH, Zhang DJ, Long HL, Li HJ, et al. Overexpression of NAMPT in gastric cancer and chemopotentiating effects of the NAMPT inhibitor FK866 in combination with fluorouracil. *Oncol Rep* 2011;26:1251–7.
  6. Wang B, Hasan MK, Alvarado E, Yuan H, Wu H, Chen WY. NAMPT overexpression in prostate cancer and its contribution to tumor cell survival and stress response. *Oncogene* 2011;30:907–21.
  7. Gehrke I, Bouchard ED, Beiggi S, Poepl AG, Johnston JB, Gibson SB, et al. On-target effect of FK866, a nicotinamide phosphoribosyl transferase inhibitor, by apoptosis-mediated death in chronic lymphocytic leukemia cells. *Clin Cancer Res* 2014;20:4861–72.
  8. Bogan KL, Brenner C. Nicotinic acid, nicotinamide, and nicotinamide riboside: a molecular evaluation of NAD<sup>+</sup> precursor vitamins in human nutrition. *Annu Rev Nutr* 2008;28:115–30.
  9. Khan JA, Tao X, Tong L. Molecular basis for the inhibition of human NMPRTase, a novel target for anticancer agents. *Nat Struct Mol Biol* 2006;13:582–8.
  10. Cea M, Zoppoli G, Bruzzone S, Fruscione F, Moran E, Garuti A, et al. APO866 activity in hematologic malignancies: a preclinical *in vitro* study. *Blood* 2009;113:6035–7.
  11. Nahimana A, Attinger A, Aubry D, Greaney P, Ireson C, Thougard AV, et al. The NAD biosynthesis inhibitor APO866 has potent antitumor activity against hematologic malignancies. *Blood* 2009;113:3276–86.
  12. Zoppoli G, Cea M, Soncini D, Fruscione F, Rudner J, Moran E, et al. Potent synergistic interaction between the NAMPT inhibitor APO866 and the apoptosis activator TRAIL in human leukemia cells. *Exp Hematol* 2010;38:979–88.
  13. Chan M, Gravel M, Bramoulle A, Bridon G, Avizonis D, Shore GC, et al. Synergy between the NAMPT inhibitor GMX1777(8) and pemetrexed in non-small cell lung cancer cells is mediated by PARP activation and enhanced NAD consumption. *Cancer Res* 2014;74:5948–54.
  14. Pogrebniak A, Schemainda I, Azzam K, Pelka-Fleischer R, Nussler V, Hasmann M. Chemopotentiating effects of a novel NAD biosynthesis inhibitor, FK866, in combination with antineoplastic agents. *Eur J Med Res* 2006;11:313–21.
  15. Rongvaux A, Galli M, Denanglaire S, Van Gool F, Dreze PL, Szpirer C, et al. Nicotinamide phosphoribosyl transferase/pre-B cell colony-enhancing factor/visfatin is required for lymphocyte development and cellular resistance to genotoxic stress. *J Immunol* 2008;181:4685–95.
  16. Ginet V, Puyal J, Rummel C, Aubry D, Breton C, Cloux AJ, et al. A critical role of autophagy in antileukemia/lymphoma effects of APO866, an inhibitor of NAD biosynthesis. *Autophagy* 2014;10:603–17.
  17. Cagnetta A, Cea M, Calimeri T, Acharya C, Fulciniti M, Tai YT, et al. Intracellular NAD(+) depletion enhances bortezomib-induced anti-myeloma activity. *Blood* 2013;122:1243–55.
  18. Hennessy M, Spiers JP. A primer on the mechanics of P-glycoprotein the multidrug transporter. *Pharmacol Res* 2007;55:1–15.
  19. Gottesman MM, Pastan I. Biochemistry of multidrug resistance mediated by the multidrug transporter. *Annu Rev Biochem* 1993;62:385–427.
  20. Sugawara I. Expression and functions of P-glycoprotein (mdr1 gene product) in normal and malignant tissues. *Acta Pathol Jpn* 1990;40:545–53.
  21. Leith CP, Kopecky KJ, Chen IM, Eijdens L, Slovak ML, McConnell TS, et al. Frequency and clinical significance of the expression of the multidrug resistance proteins MDR1/P-glycoprotein, MRP1, and LRP in acute myeloid leukemia: a Southwest Oncology Group Study. *Blood* 1999;94:1086–99.
  22. Mahadevan D, List AF. Targeting the multidrug resistance-1 transporter in AML: molecular regulation and therapeutic strategies. *Blood* 2004;104:1940–51.
  23. Gerrard G, Payne E, Baker RJ, Jones DT, Potter M, Prentice HG, et al. Clinical effects and P-glycoprotein inhibition in patients with acute myeloid leukemia treated with zosuquidar trihydrochloride, daunorubicin, and cytarabine. *Haematologica* 2004;89:782–90.
  24. Abraham J, Edgerly M, Wilson R, Chen C, Rutt A, Bakke S, et al. A phase I study of the P-glycoprotein antagonist tariquidar in combination with vinorelbine. *Clin Cancer Res* 2009;15:3574–82.
  25. Steinbach D, Legrand O. ABC transporters and drug resistance in leukemia: was Pgp nothing but the first head of the Hydra? *Leukemia* 2007;21:1172–6.
  26. Malayeri R, Filipits M, Suchomel RW, Zochbauer S, Lechner K, Pirker R. Multidrug resistance in leukemias and its reversal. *Leuk Lymphoma* 1996;23:451–8.
  27. Ross DD, Wooten PJ, Sridhara R, Ordonez JV, Lee EJ, Schiffer CA. Enhancement of daunorubicin accumulation, retention, and cytotoxicity by verapamil or cyclosporin A in blast cells from patients with previously untreated acute myeloid leukemia. *Blood* 1993;82:1288–99.
  28. Di Nicolantonio F, Mercer SJ, Knight LA, Gabriel FG, Whitehouse PA, Sharma S, et al. Cancer cell adaptation to chemotherapy. *BMC Cancer* 2005;5:78.
  29. Watanabe T, Tsuge H, Oh-Hara T, Naito M, Tsuruo T. Comparative study on reversal efficacy of SDZ PSC 833, cyclosporin A and verapamil on multidrug resistance *in vitro* and *in vivo*. *Acta Oncol* 1995;34:235–41.
  30. Kolitz JE, George SL, Marcucci G, Vij R, Powell BL, Allen SL, et al. P-glycoprotein inhibition using valsopodar (PSC-833) does not improve outcomes for patients younger than age 60 years with newly diagnosed acute myeloid leukemia: cancer and leukemia group B study 19808. *Blood* 2010;116:1413–21.
  31. Soncini D, Caffa I, Zoppoli G, Cea M, Cagnetta A, Passalacqua M, et al. Nicotinamide phosphoribosyltransferase promotes epithelial-to-mesenchymal transition as a soluble factor independent of its enzymatic activity. *J Biol Chem* 2014;289:34189–204.
  32. Chou TC, Talalay P. Quantitative analysis of dose-effect relationships: the combined effects of multiple drugs or enzyme inhibitors. *Adv Enzyme Regul* 1984;22:27–55.
  33. Skokowa J, Lan D, Thakur BK, Wang F, Gupta K, Cario G, et al. NAMPT is essential for the G-CSF-induced myeloid differentiation via a NAD(+)–sirtuin-1-dependent pathway. *Nat Med* 2009;15:151–8.
  34. Barretina J, Caponigro G, Stransky N, Venkatesan K, Margolin AA, Kim S, et al. The Cancer Cell Line Encyclopedia enables predictive modelling of anticancer drug sensitivity. *Nature* 2012;483:603–7.
  35. Cea M, Cagnetta A, Patrone F, Nencioni A, Gobbi M, Anderson KC. Intracellular NAD(+) depletion induces autophagic death in multiple myeloma cells. *Autophagy* 2013;9:410–2.
  36. Bruzzone S, Fruscione F, Morando S, Ferrando T, Poggi A, Garuti A, et al. Catastrophic NAD<sup>+</sup> depletion in activated T lymphocytes through NAMPT inhibition reduces demyelination and disability in EAE. *PLoS ONE* 2009;4:e7897.
  37. Cea M, Soncini D, Fruscione F, Raffaghello L, Garuti A, Emionite L, et al. Synergistic interactions between HDAC and sirtuin inhibitors in human leukemia cells. *PLoS ONE* 2011;6:e22739.
  38. Powles RL, Clink HM, Spence D, Morgenstern G, Watson JG, Selby PJ, et al. Cyclosporin A to prevent graft-versus-host disease in man after allogeneic bone-marrow transplantation. *Lancet* 1980;1:327–9.
  39. Wang P, Heitman J. The cyclophilins. *Genome Biol* 2005;6:226.
  40. Clipstone NA, Crabtree GR. Identification of calcineurin as a key signalling enzyme in T-lymphocyte activation. *Nature* 1992;357:695–7.
  41. Hall AG, Cattan AR. Drug resistance mechanisms in leukaemia. *Baillieres Clin Haematol* 1991;4:655–81.
  42. Verweij J, Herweijer H, Oosterom R, van der Burg ME, Planting AS, Seynaeve C, et al. A phase II study of epidoxorubicin in colorectal cancer and the use of cyclosporin-A in an attempt to reverse multidrug resistance. *Br J Cancer* 1991;64:361–4.
  43. Fridborg H, Jonsson B, Nygren P, Csoka K, Nilsson K, Oberg G, et al. Activity of cyclosporins as resistance modifiers in primary cultures of human haematological and solid tumours. *Br J Cancer* 1994;70:11–7.
  44. Dalton WS, Salmon SE. Drug resistance in myeloma: mechanisms and approaches to circumvention. *Hematol Oncol Clin North Am* 1992;6:383–93.
  45. Mahon FX, Deininger MW, Schultheis B, Chabrol J, Reiffers J, Goldman JM, et al. Selection and characterization of BCR-ABL positive cell lines with

- differential sensitivity to the tyrosine kinase inhibitor STI571: diverse mechanisms of resistance. *Blood* 2000;96:1070–9.
46. Yang H, Yang T, Baur JA, Perez E, Matsui T, Carmona JJ, et al. Nutrient-sensitive mitochondrial NAD<sup>+</sup> levels dictate cell survival. *Cell* 2007;130:1095–107.
  47. Wang M, Kaufman RJ. The impact of the endoplasmic reticulum protein-folding environment on cancer development. *Nat Rev Cancer* 2014;14:581–97.
  48. Todd DJ, Lee AH, Glimcher LH. The endoplasmic reticulum stress response in immunity and autoimmunity. *Nat Rev Immunol* 2008;8:663–74.
  49. Yoshida H. ER stress and diseases. *FEBS J* 2007;274:630–58.
  50. Dantuma NP, Lindsten K. Stressing the ubiquitin-proteasome system. *Cardiovasc Res* 2010;85:263–71.
  51. Ciechomska IA, Gabrusiewicz K, Szczepankiewicz AA, Kaminska B. Endoplasmic reticulum stress triggers autophagy in malignant glioma cells undergoing cyclosporin a-induced cell death. *Oncogene* 2013;32:1518–29.
  52. Koh IU, Lim JH, Joe MK, Kim WH, Jung MH, Yoon JB, et al. AdipoR2 is transcriptionally regulated by ER stress-inducible ATF3 in HepG2 human hepatocyte cells. *FEBS J* 2010;277:2304–17.
  53. Lam YA, Pickart CM, Alban A, Landon M, Jamieson C, Ramage R, et al. Inhibition of the ubiquitin-proteasome system in Alzheimer's disease. *Proc Natl Acad Sci U S A* 2000;97:9902–6.
  54. Watson M, Roulston A, Belec L, Billot X, Marcellus R, Bedard D, et al. The small molecule GMX1778 is a potent inhibitor of NAD<sup>+</sup> biosynthesis: strategy for enhanced therapy in nicotinic acid phosphoribosyltransferase 1-deficient tumors. *Mol Cell Biol* 2009;29:5872–88.
  55. Wosikowski K, Mattern K, Schemainda I, Hasmann M, Rattel B, Loser R. WK175, a novel antitumor agent, decreases the intracellular nicotinamide adenine dinucleotide concentration and induces the apoptotic cascade in human leukemia cells. *Cancer Res* 2002;62:1057–62.
  56. Metzeler KH, Hummel M, Bloomfield CD, Spiekermann K, Braess J, Sauerland MC, et al. An 86-probe-set gene-expression signature predicts survival in cytogenetically normal acute myeloid leukemia. *Blood* 2008;112:4193–201.
  57. Herold T, Jurinovic V, Metzeler KH, Boulesteix AL, Bergmann M, Seiler T, et al. An eight-gene expression signature for the prediction of survival and time to treatment in chronic lymphocytic leukemia. *Leukemia* 2011;25:1639–45.
  58. Hummel M, Bentink S, Berger H, Klapper W, Wessendorf S, Barth TF, et al. A biologic definition of Burkitt's lymphoma from transcriptional and genomic profiling. *N Engl J Med* 2006;354:2419–30.



## ACKNOWLEDGEMENTS

At the end of this 4-year experience, I wish to thank various people for their fundamental contribution to my PhD. Firstly, I would like to express my deep gratitude to my research tutor Dr. Alessandro Provenzani, who gave me the opportunity to join his Laboratory of Genomic Screening and to be involved in this challenging project. He has encouraged me throughout these years with his enthusiasm and with his useful and constructive critiques.

My grateful thanks are also extended to my advisor Dr. Vito D'Agostino, for teaching me a lot with his patient and professional guidance, his valuable support and his sincere friendship.

The Centre for Integrative Biology (CIBIO) of the University of Trento offered me the possibility to work in a young, highly dynamic, and stimulating research environment. I would also like to express my very great appreciation for the training provided by the International PhD program I was enrolled in, headed by Dr. Paolo Macchi. Daily assistance provided by Betty Balduin was greatly appreciated.

I wish to acknowledge the help provided by internal and external collaborators. Valuable technical support on this project came from CIBIO Core Facilities. In particular, advices and support given by Valentina Adami, Pamela Gatto and Michael Pancher (High Throughput Screening Core Facility) have been a great help. Dr. Toma Tebaldi (Laboratory of Translational Genomics) provided me with very valuable assistance with the bioinformatic analysis of the project. Antonio Casini (Laboratory of Molecular Virology) helped me in applying viral vector-based techniques to the research.

The research was funded by the Italian Ministry of Health and was in collaboration with the University of Genoa. A special thanks goes to Dr. Alessio Nencioni's group, in particular to Irene Caffa, and Dr. Michele Cea.

My thanks are extended to our collaborators Dr. Stefano Indraccolo from the University of Padua and Dr. Nadia Raffaelli from the University of Ancona.

I spent an amazing period abroad in Dr. Olli Kallioniemi's Lab (FIMM, Helsinki, Finland). I wish to thank Dr. Päivi Östling and Mariliina Arjama and all the PhD

students for their kind help (Dishaben Malani, Susanne Hultsch, Poojitha Ojamies, Khalid Saeed).

I am particularly grateful to the members of the Provenzani Lab, Rosa, Nat, Preet and Isabelle (and former members Barbara, Ilaria and Elisa), who shared with me good and bad times and have always helped me. Thank you all for the happy and enjoyable atmosphere in the Lab. I also wish to acknowledge the help provided by the students who were involved in the project: Elena, Laura, Alice, Pietro, Alessia, Simone and Elisa. They joined this research with a lot of enthusiasm.

Finally, I wish to thank my family for their complete support and encouragement throughout my study. A deep thanks goes to the people who love me and have always believed in me: grazie mille.

*“Io sto cercando, sto cercando qualcosa:  
l'immagine è offuscata, ma c'è. Qualcuno può indicarmi cos'è?  
Temo che possa svanire, temo di perderla prima d'averla toccata.”*

*“I am looking, I am looking for something:  
the image is bleary, but it is there. Can someone show me what is it?  
I fear it could disappear, I fear it will be lost before I can touch it.”*

*Valeria Lauria*